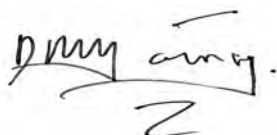**FACULTY OF SCIENCE AND AGRICULTURE DECLARATION 1: PLAGIARISM**

I, Paul Michael Young, declare that:

1. The research reported in this thesis is my original research, except where otherwise indicated.

2. This thesis has not been submitted for any degree or examination at any other university.

3. This thesis does not contain other persons' data, pictures, graphs or other information, unless specifically acknowledged as being sourced from other persons.

4. This thesis does not contain other persons' writing, unless specifically acknowledged as being sourced from other researchers. Where other written sources have been quoted, then:

    a. Their words have been re-written but the general information attributed to them has been referenced.

    b. Where their exact words have been used, then their writing has been placed in italics and inside quotation marks, and referenced.

5. This thesis does not contain text, graphics or tables copied and pasted from the Internet, unless specifically acknowledged, and the source being detailed in the thesis and in the References sections.

Signed

……………………………………………………………………………………………………

Paul Michael Young

October 2009

An integrated marine GIS bathymetric dataset

for

KwaZulu-Natal

Paul Michael Young

School of Geological Sciences

Faculty of Science and Agriculture

University of KwaZulu-Natal

(Westville Campus)

Submitted for the partial fulfilment of the academic requirements for the degree of Master of Science

As the candidate's supervisor, I agree to the submission of this thesis.

..……………………………………………………………………………………………………

Dr. Ron Uken

October 2009

ABSTRACT

Bathymetry forms the basis for studies in marine geology, biology and oceanography and is essential for the Extended Continental Shelf Claim (ECSC), a legal framework established by the United Nations (UN) to encourage a nation's governance and management of its marine resources. This research provides the first digital, integrated, Geographical Information System (GIS) based bathymetric dataset for KwaZulu-Natal that combines near-shore and deep-water datasets for use in marine sciences.

A total of 32 datasets acquired using a range of techniques and instruments between 1911 and 2006 were considered. Twenty nine of these were near-shore datasets with data densities varying from 6 to 57 406 points per km^2. Of these, 15 were acquired by the Council for Geoscience (CGS), 9 by the South African Navy and 5 by the African Coelacanth Ecosystem Programme (ACEP). Two of the remaining 3 deep-water datasets were grids acquired digitally for this work, while the third was a digitised contour dataset. The 2003 General Bathymetric Chart of the Oceans (GEBCO) grid is based on digitised point and contour data with a point every 1 852 m, while the 1997 Smith and Sandwell grid is based on predicted satellite altimetry data with a point every 3 704. The third deep-water dataset was digitised from a northern Natal Valley bathymetric contour map developed in 1978 and has data densities varying from 0.02 to 1 point per km^2.

Datasets were prioritised in the following descending order of quality defined by the available metadata: multi-beam echo-sounder-derived datasets, followed by single-beam echo-sounder-derived datasets and lastly lead line datasets. The digitised northern Natal Valley bathymetric contour dataset after Dingle et al. (1978) was considered authoritative for the deep-water areas, while the 2-minute interval Smith and Sandwell satellite derived bathymetry dataset was integrated south of 31° S where no other dataset coverage existed.

Availability of good metadata describing bathymetric dataset positioning and depth measuring instruments were essential. Where good metadata did exist, interrogation, integration and quality control were straightforward. However, where the year of acquisition and depth measuring instrument type were the only available metadata, information about positioning and depth measuring instruments were inferred. The digitised northern Natal Valley bathymetric contour dataset offered the best deep-water coverage and was derived from heterogeneous point datasets about which no metadata was available. Metadata for the Smith and Sandwell satellite derived bathymetric dataset suggested limited ship track data control for the study

area, while it was known to contain noise caused by an unquantified, rough sea state.

The integration process was successful but noticeable artefacts were recognised. Concentric contour artefacts were present where the digitised northern Natal Valley bathymetric contour dataset and the South African Navy Admiralty Fair Chart 34 dataset were integrated. Regional conjoined arc-like contour artefacts north of 31° S as well as bumpy seafloor textures south of 31° S in the deep water areas were also found. In addition, artefacts were discovered in one of the multi-beam datasets, normally associated with good high-resolution data coverage.

Intuitive, user-friendly, Geographical Information System (GIS) software and mapping software were used to aid visual interrogation of the final contour dataset and the contour editing capabilities in ESRI ® ArcGIS ® were used to edit concentric contour and conjoined arc-like contour artefacts north of 31° S. GIS software was further used as a visual filter to remove the regional bumpy seafloor texture south of 31° S, caused by noise in the satellite altimetry dataset. An edited point dataset component south of 31° S was re-interpolated and the resultant grid re-mosaiced with the original final grid north of 31° S, yielding an improved final contour dataset.

The 1:3 000 000 scale final contour dataset resolved regional features such as the Thukela Cone, the Thukela and 29° 25' Canyons along with a broad un-named valley, termed here as the Maputaland Valley, which drains the Maputaland Canyons. Near-shore areas of the continental shelf were also resolved at higher scales of up to 1:45 000. Obvious data gaps emerged with five areas prioritised for the acquisition of new digital data as part of a systematic mapping programme to improve the dataset.

Powerful, cost-effective computer hardware and cost-effective, intuitive, user-friendly computer software driven by ongoing technological advances made this work possible. These technology advances continue to improve bathymetric data acquisition, positioning and processing methods as well as improving data interpolation and map development.

The usefulness of this digital, integrated, marine GIS contour dataset has been demonstrated by the interest of KwaZulu-Natal based organisations such as the University of KwaZulu-Natal (UKZN), the Oceanographic Research Institute (ORI), Ezemvelo KwaZulu-Natal Wildlife (EKZNW) and Umgeni Water along with the Cape Town based Marine and Coastal Management (MCM) and the Pretoria based Council for Scientific and Industrial Research (CSIR). Establishing this dataset as a base map for a KwaZulu-Natal 3D marine cadastre to add other GIS data must be encouraged to improve collaboration, promote research and

improve ocean governance in KwaZulu-Natal, after which this type of 3D marine cadastre should be extended to include the whole of South Africa.

ACKNOWLEDGEMENTS

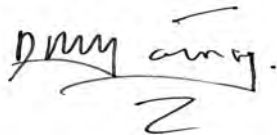This work is dedicated to our daughter Tamara Melissa.

PREFACE

This work was carried out under the research collaboration of the Durban Marine Geoscience Unit consisting of the Council for Geoscience and the School of Geological Sciences of the University of KwaZulu-Natal as stakeholders. Academic supervision was provided by Dr. Ron Uken in the School of Geological Sciences at the University of KwaZulu-Natal.

The project was fully funded by the Council for Geoscience as a statutory project (ST-2008-0964) and the dissertation was completed between November 2007 and December 2008 while in the employ of The Council for Geoscience.

This dissertation is submitted for the fulfilment of the academic requirements for the degree of Master of Science in the School of Geological Sciences, University of KwaZulu-Natal.

It represents original work by the author, except where duly acknowledged, and has not been submitted in any form for a degree at any other tertiary institution.

Signed

Paul Michael Young

October 2009

ALPHABETICAL LIST OF ACRONYMS USED

AABW: Antarctic Bottom Water

ACEP: African Coelacanth Ecosystem Programme

AFC: Admiralty Fair Chart

ANN: Artificial Neural Network

AUV: Autonomous Underwater Vehicle

CARIS: Canadian hydrographic software company

LOTS: Law Of The Sea – *LOTS ® is software developed by CARIS ® for Extended Continental Shelf Claim (ECSC) work – i.e.: CARIS ® LOTS ®*

CD Port: Chart Datum Port – *a tidal datum*

CGS: Council for Geoscience – *formerly the Geological Survey of South Africa*

CUBE: Combined Uncertainty Bathymetry Estimator

dB: Decibel or $^{1/10}$ of a bel (B) – *a dimensionless logarithmic ratio*

DBDB2: Digital Database 2-minute

DBDB5: Digital Database 5-minute

DBDBV: Digital Database Variable Resolution

DBMS: Database Management System

DECCA: Named after the Decca Record Company – *a low frequency marine radio navigation system*

DEM: Digital Elevation Model

DGPS: Differential GPS – *a more accurate version of GPS*

DTM: Digital Terrain Model

ECSC: Extended continental shelf Claim

EKZNW: Ezemvelo KwaZulu-Natal Wildlife – *formally the Natal Parks Board*

ETOPO2: Earth Topography 2-minute Grid Dataset

ETOPO5: Earth Topography 5-minute Grid Dataset

ERS: European Remote Sensing Satellite

EEZ: Exclusive Economic Zone – *200 Nautical miles*

FC: Fair Chart

GB: Gigabyte – *1024 or 2^{10} megabytes (MB)*

GDA: GEBCO Digital Atlas

GEBCO: General Bathymetric Chart of the Oceans

GEODAS: Geophysical Data System

GEOSAT: Geodetic Satellite

GHz: Gigahertz – *A million hertz*

GIS: Geographical Information System

GLONASS: Global Orbiting Navigation Satellite System – *developed by the USSR/Russia*

GMT: Generic Mapping Tools (software) or Greenwich Mean Time (central meridian)

GPS: Global Positioning System – *developed by the United States of America*

GSLWP: Greater St. Lucia Wetland Park – *Now the iSimangaliso Wetland Park*

GUI: Graphic User Interface – *descriptive term for the user-friendly windows-like interface presented to a user by modern Microsoft ® Windows ®, Apple ®, Linux ® and Unix ® operating systems that has replaced the command line interface in older Microsoft ® DOS ®, Linux ® and Unix ® operating systems*

Hz: Hertz – *Unit of frequency measurement*

IHO: International Hydrographic Organisation

INR: Institute of Natural Resources

ITRF: International Terrestrial Reference Frame

kHz: Kilohertz – *A thousand hertz*

KB: Kilobyte – *1024 or 2^{10} bytes (B) and not 1000 or 10^{3} bytes*

MB: Megabyte – *1024 or 2^{10} kilobytes (KB)*

MBES: Multi-beam echo-sounder

MCM: Marine and Coastal Management – *Formally the Sea Fisheries Research Institute*

MESH: Mapping European Seabed Habitats

MGS: Marine Geosolutions

MGU: Marine Geoscience Unit – joint *research collaboration between the Durban Marine Unit of the CGS and the UKZN. A similar, now dissolved research collaboration existed between the Cape Town Marine Unit of the CGS and the UCT*

MPA: Marine Protected Area

MSL: Mean Sea Level – *a tidal datum*

MSK: Minimum Shift Key – *a type of differential GPS system*

NADW: North Atlantic Deep Water

NN: Neural Network

NRF: National Research Foundation

NOAA: National Oceanographic and Atmospheric Administration

NPA: National Ports Authority

NRF: National Research Foundation

ORI: Oceanographic Research Institute

PC: Personal Computer

RADAR: Radio Detection and Ranging

RDBMS: Relational Database Management System

RTCM: Radio Technical Commission for Maritime Services

RTK: Real Time Kinematic – *a type of differential GPS system*

RV: Research Vessel

SANHO: South African Navy Hydrographic Office

SASS: Sonar Array Sounding System

SBES: Single-beam echo-sounder

SCAR: Scientific Committee on Antarctic Research

SQL: Structured Query Language

SSS: Side-scan Sonar

TM: Transverse Mercator

TIN: Triangulated Irregular Network – *a GIS term*

UCT: University of Cape Town

UKZN: University of KwaZulu-Natal – *formerly the University of Natal*

UNCLOS: United Nations Convention on Law of the Sea

USGS: United States Geological Survey

UTM: Universal Transverse Mercator

WGS84: World Geodetic System of 1984 – *a standard ellipsoid and a geocentric datum*

WVS: World Vector Shoreline

LIST OF FIGURES

LIST OF TABLES

CONTENTS

1   INTRODUCTION

1.1 Background

The Durban-based Marine Geoscience Unit (MGU) is a research collaboration started in the 1990's between the former Geological Survey of South Africa (now the Council for Geoscience) and the former University of Natal (now the University of KwaZulu-Natal). Marine geological mapping in South Africa is the statutory mandate of the MGU. This integrated bathymetric contour dataset research was initiated in 2001 to develop a single, integrated user-friendly, bathymetric dataset of the continental shelf and deeper ocean of KwaZulu-Natal marine environment as part of the MGU's mandate. This was needed for marine research as well as to identify data gaps and inaccuracies. The proven usefulness of Geographical Information Systems (GIS) as a tool in marine sciences to store, manipulate, interrogate and edit spatially diverse geographical scientific data (Scott, 2006) led to its use for this work. Built-in database management and a user friendly visual interface allows spatial scientific data to be accumulated, displayed and interrogated to aid research and such applications as decision making, training and data improvement.

1.2 Aims

The aims of this work were to convert near-shore and deep-water bathymetric datasets of varying vintage and accuracy into a GIS format. This was to facilitate their processing and correction to integrate into one useful dataset for generating the first integrated digital GIS regional bathymetric contour map of the KwaZulu-Natal marine environment at a scale of 1:3 000 000. This completed map was to include deep-water and selected near-shore continental shelf areas, to provide a tool for marine science and ocean governance. Dissemination of this marine GIS data, via the Council for Geoscience (CGS) GeoPortal to public, research, educational and commercial organisations is also proposed.

1.3 Bathymetric data

The oceans remain relatively unmapped when compared to studies on land and some of the other planets such as Mars and Venus. Ship acquired bathymetry, although slow and weather dependant produces the most accurate and detailed seafloor depth measurements of the Earth. It has been estimated that mapping the Earths oceans using modern multi-beam systems, with 100 m horizontal resolution and an appropriate survey line spacing, would require 125 ship-years (Sandwell and Smith, 2000) with Sandwell et al., (2006) having

estimated, more recently that mapping all worldwide areas shallower than 500 m could take 750 ship-years. This is because multi-beam echo-sounder swath width is proportional to the depth being surveyed.

Worldwide bathymetric coverage of the oceans is presently derived from two main regional scale sources, the Smith and Sandwell bathymetric dataset, predicted from satellite altimetry and the General Bathymetric Chart of the Oceans (GEBCO) derived from digitised contour maps and ship track data. The satellite altimetry dataset is based on a 2-minute grid, whereas the GEBCO dataset uses a 1-minute grid.

Both ship acquired and satellite predicted bathymetric measurements are prone to errors. These occur during the acquisition phase, by virtue of sea conditions and weather, as well as acquisition equipment and operator errors. Software limitations and operator bias also introduce errors during data processing.

Datasets used in this work were acquired either digitally or digitised from analogue paper charts by the Marine Geoscience Unit personnel or through data exchange agreements with other organisations. Regional deep-water bathymetric data in this work were digitised from the Marine Geoscience Unit's authoritative contour map of the northern Natal Valley after Dingle et al. (1978) and supplemented by the freely available Smith and Sandwell and GEBCO deep-water datasets. All three of these datasets have shallow water coverage limitations which were addressed by the inclusion of the Marine Geoscience Unit's better quality near-shore datasets.

Bathymetry is essential for understanding the marine environment and needs to be continually updated and improved; a need identified by the then directors of the MGU who initiated this work. This work has since led to interest from a number of marine institutions. These include: the Schools of Geological, and Life and Environmental Sciences at University of KwaZulu-Natal (UKZN); Ezemvelo KwaZulu-Natal Wildlife (EKZNW), for their Systematic Conservation Programme; the Oceanographic Research Institute (ORI) for their reef habitat and prawn monitoring programmes; and the ongoing African Coelacanth Ecosystem Programme (ACEP). In addition a proposed desalination plant in KwaZulu-Natal by Umgeni Water has directed interest to this dataset. Cape Town based Marine and Coastal Management (MCM) and, most recently, the Pretoria based Council for Scientific and Industrial Research (CSIR) have also indicated interest in this work.

1.4 Study area

The study area in (Figure 1.1) covers approximately 350 000 km^2, extending from 27° S to 33° S and seawards of the KwaZulu-Natal coastline to 36° E. This area includes most of the 200 nautical mile Exclusive Economic Zone (EEZ), as well as the 3 and 6 nautical mile zones, the 12 nautical mile Territorial Waters and the 24 nautical mile Contiguous Zone (United Nations Editorial Committee, 2009) for KwaZulu-Natal.
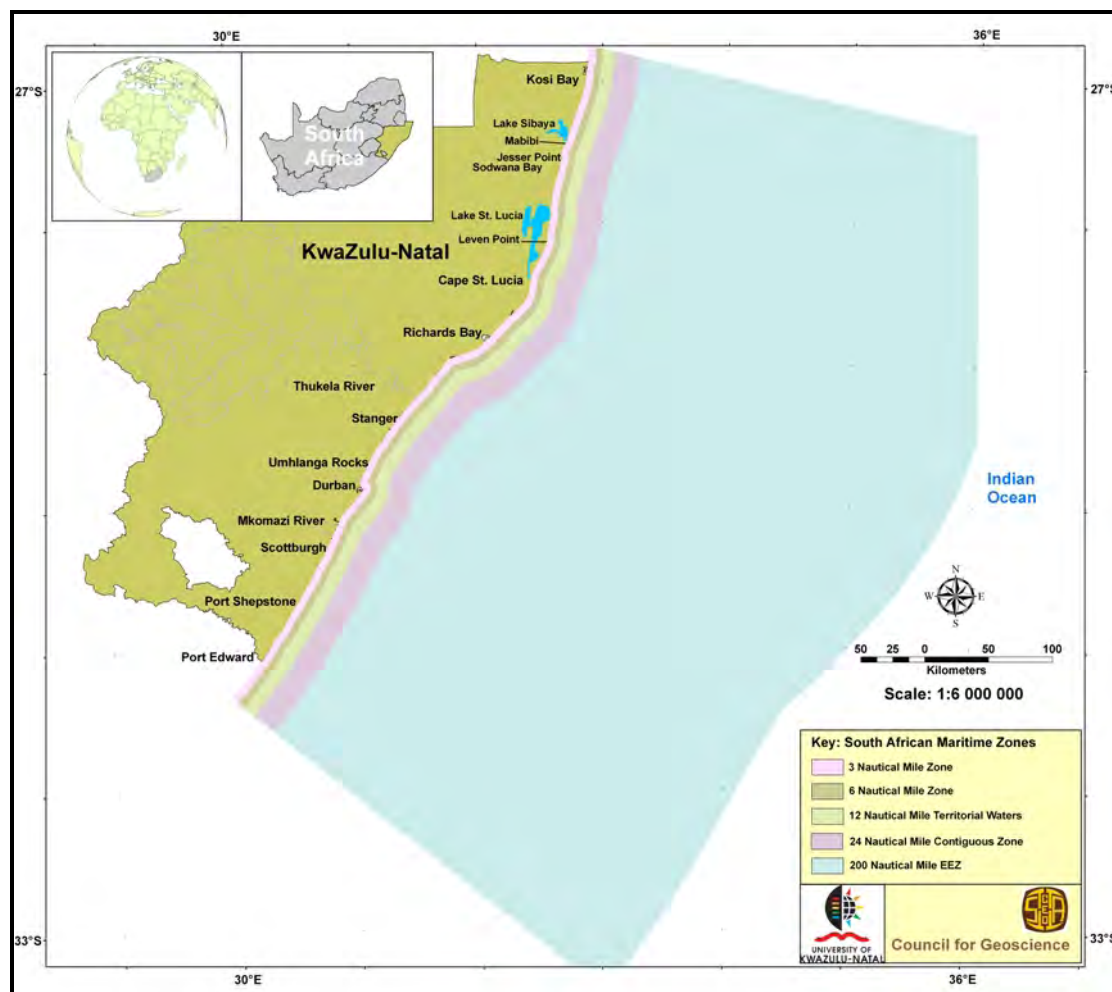
Figure 1.1. The study area in UTM Zone 36 S, extending from the coastline out to 36° E between 27° S and 33° S, including most of the South African 200 nautical mile Exclusive Economic Zone (EEZ) for the KwaZulu-Natal province. Also shown are the 3, 6, 12 and 24 nautical mile maritime zones.

1.5 Regional physiography

Dingle et al. (1978) recognised six physiographic provinces within the study area. These

include the continental shelf, the continental slope and rise, the Thukela Cone, the Mozambique Ridge and the deep ocean basin (Figure 1.2). The Transkei Basin and its shallower continuation, the Natal Valley, as well as the western part of the Mozambique Ridge (Martin, 1984; Martin and Flemming, 1988) form the main undersea features of the study area (Figure 1.2). Development of these features is related to the break-up of Gondwana and the subsequent expansion of the Indian Ocean in the Jurassic and Early Cretaceous periods (Martin and Flemming, 1988).

1.5.1   Durban to Cape St. Lucia

Between Durban and Cape St. Lucia (Area 2) the continental shelf is considerably wider than to the north and south (Areas 1 and 3, Figure 1.2) (Martin and Flemming, 1988). Continental shelf widths of up to 45 km are also narrower than that of the world average of 74 km (Shepard, 1963). Continental shelf gradients average 1:320 or 0.18^o in the south, whereas the narrower, steeper northern continental shelf gradients average 1:120 or 0.48^o (Goodlad, 1978). From Durban to the Thukela River mouth a steep, narrow near-shore section exists (Moir, 1974) with shelf gradients of 1:430 or 0.13^o found off the Thukela River mouth (Goodlad, 1978). Maximum gradients of 1:60 or 1° are also found with a depth of 100 m marking the poorly defined, sediment draped shelf break (Moir, 1974; Goodlad, 1986). Continental slope gradients vary from 1:26 or 2.2^o east of the Thukela River mouth up to 1:14 or 4.1^o off Cape St. Lucia (Moir, 1974). These gradients are less than those of the world average of 1:13 or 4.4^o (Moir, 1974; Martin and Flemming, 1988). In addition, the shelf break depth of between 100 m and 112 m is shallower than the world average of 132 m (Table 1.1) (Martin and Flemming, 1988).

Table 1.1. The average gradients, maximum gradients, shelf widths and shelf break depths for areas 1 to 4 in figure 1.2 of the continental shelf and continental slope (Goodlad, 1986).

Area	Average Gradient	Maximum Gradient	Shelf Width (km)	Shelf Break (m)
continental shelf				
Area 1	1:120 or 0.48^o	1:80 or 0.72^o	10 to 12	100
Area 2	1:320 or 0.18^o	1:120 or 0.48^o	4.5 to 45	100
Area 3	1:60 or 0.95^o	1:40 or 1.43^o	5	60 to 100
* World Average	1:500 or 0.12^o	–	73	130
continental slope				
Area 4	1:14 or 4.1^o	1:8 or 7.13^o	–	–
* World Average	1:13 or 4.4^o	–	–	–
* ***Data after Shepard (1963)***				

Figure 1.2. The northern Natal physiographic provinces after Dingle et al. (1978). The continental shelf (1 – 3), continental slope and rise (4), Thukela Cone (5 - 11), Central Terrace (12), Mozambique Ridge (13), Deep ocean basin (14 – 16). The bathymetric contours of the northern Natal Valley after Dingle et al. (1978) are overlaid as an georeferenced raster image.

1.5.2 Cape St. Lucia to Kosi Bay

Area 3 in figure 1.2 has continental shelf widths of between 2 km and 4 km and a shelf break depth of 65 m (Ramsay and Miller, 2006) contrasting with the world average shelf width of 74 km and shelf break depth of 132 m (Martin and Flemming, 1988). The continental shelf north of Jesser Point has gradients varying from 1:57 or 1° to 1:23 or 2.5^o, while the poorly defined continental shelf break south of Jesser Point has an average gradient of 1:44 or 1.3^o (Ramsay, 1996). The upper continental slope has gradients varying from 1:82 or 0.7^o, south of Jesser Point to 1:20 or 2.9^o north-east of Jesser Point. Sydow (1988) however, noticed that the upper continental slope off Jesser Point could be divided into a lower, moderately dipping 3° surface and an upper steeper 8.6^o surface.

A total of 23 submarine canyons, six mature-phase and 17 youthful-phase, were identified on northern KwaZulu-Natal continental shelf, confined to five distinct blocks stretching from Leven Point in the south to Mabibi in the north (Ramsay and Miller, 2006; Green and Uken, 2008). Canyon depths range from 29 m to 838 m within the dataset areas (Green and Uken, 2008).

1.5.3 Durban to southern KwaZulu-Natal border

Area 1 in figure 1.2 has continental shelf widths of between 10 km and 12 km with a well defined continental shelf break depth at approximately 100 m (Goodlad, 1986). Martin and Flemming (1988) reported a continental shelf break depth of 80 m to 90 m south of 30° 20' S. Continental shelf gradients average 1:120 or 0.48^o (Moir, 1974; Goodlad, 1986) and appear fairly uniform (Goodlad, 1978). Locally, continental shelf gradients of up to 1:80 or 0.7^o, have been reported in the area (Goodlad, 1986). Continental slope gradients in area 4 of figure 1.2 vary from 1:14 or 4.1^o up to 1:8 or 7.1^o (Goodlad, 1986; Martin and Flemming, 1988). The former value compares favourably to the Shepard (1963) world average value of 1:13 or 4.3^o. South of approximately 30° 40' S, narrow V-shaped canyons are found with the Mzumbe River Canyon, halfway between Port Shepstone and Scottburgh, attaining relief of 350 m (Goodlad, 1986). The continental slope in area 4 is poorly developed (Hobday, 1982) and is transitional into the deep ocean basin at a depth of 2 920 m (Goodlad, 1986).

1.5.4 Thukela Cone

The Thukela Cone is a triangular-shaped marginal plateau that extends seaward for approximately 220 km south-east of the Thukela River mouth (Martin and Flemming, 1988).

Defined by areas 5 to 11 in figure 1.2, it dominates the middle of the Natal Valley and is bounded by the deep ocean basin to the south and east while to the north-east it is bounded by a wide valley, separating it from the Central Terrace (Goodlad, 1986), discussed in section 1.5.5. Average and maximum gradients for the Thukela Cone are listed in table 1.2.

Table 1.2. The average and maximum gradient dimensions for the areas 5 to 10 in figure 1.2 of the Thukela Cone (Goodlad, 1986).

Area	Average Gradient	Maximum Gradient
Area 5	1:33 or 1.7^o	1:15 or 3.81^o
Area 6	1:27 or 2.12^o	1:17 or 3.37^o
Area 7	1:125 or 0.46^o	1:40 or 1.43^o
Area 8	1:80 or 0.7^o	1:40 or 1.43^o
Area 9 Axis	1:53 or 1.1^o	1:26 or 2.2^o
Area 9 Wall	1:8 or 7.13^o	1:4 or 14.04^o
Area 10 Axis	1:130 or 0.44^o	–
Area 10 Wall	1:70 or 0.82^o	1:36 or 1.59^o

The Thukela Cone upper slope, is bounded by the shelf break at a depth of approximately 100 m and the 1 500 m isobath (Goodlad, 1986). Upper slope gradients of approximately 1:15 or 3.81^o occur in water depths between 200 m and 700 m, while gradients of approximately 1:36 or 1.59^o occur in water depths below 700 m (Goodlad, 1986). Bang (1968) identified short, steep sided canyons, dissecting the upper continental slope but not the continental shelf.

The southern boundary of the Thukela Cone is an east-west orientated, smooth-faced slope of steep gradients between 1:27 or 2.12^o and 1:17 or 3.37^o (Goodlad, 1986). The deep ocean basin breaks the slope of the southern margin, at approximately 2 920 m (Moir, 1974). The less steep eastern margin, has a complex surface relief with gradients that vary between 1:160 or 0.36^o and 1:40 or 1.43^o (Goodlad, 1986). The northeastern margin has smoother, steeper slopes averaging 1:85 or 0.67^o (Goodlad, 1986). The eastern margin forms a stepped terraced slope, extending to the deep ocean basin at approximately 2 800 m near the cone apex (Goodlad, 1986). In the north, the northeastern margin of the cone is abutted by the deep ocean basin at 2 480 m (Goodlad, 1978).

Area 11 in figure 1.2 defines the apex of the Thukela Cone. It consists of dome-shaped mounds with relief of between 60 m and 120 m, subdued towards the marginal areas of the cone apex and the deep ocean basin (Goodlad, 1986).

The Thukela Cone is dissected by two large canyons, the Thukela and the 29° 25' S Canyons (Areas 9 and 10 in Figure 1.2). The Thukela Canyon, dissects the upper slope, and the

southern boundary, whereas, the 29° 25' S Canyon has less relief and dissects the eastern and the northeastern margins (Goodlad, 1986; Martin and Flemming, 1988).

Thukela Canyon

The Thukela Canyon originates 50 km offshore of the Thukela River mouth, extending from the north-west to south-east (Moir, 1974; Goodlad, 1986; Martin and Flemming, 1988). It is 120 km long and deeply incises the southern margin of the Thukela Cone originating in a water depth of 500 m as a 20 m deep valley deepening to a maximum axial relief of 800 m midway along its length (Goodlad, 1986). Canyon wall gradients are in the order of 1:8 or 7.13^o with floor widths of between 500 m and 20 km. Tributary canyons are found along the canyon's sinuous profile (Goodlad, 1986). A stepped axial decent with gradients of between 1:150 or 0.38^o and 1:26 or 2.2^o occurs as the axis deflects eastwards from its origin towards the Natal Valley (Goodlad, 1986).

The 29 ^{o} 25 ' S Canyon

The 29° 25' S Canyon dissects the Thukela Cone and starts as a small 20 m deep valley (Martin and Flemming, 1988) deepening to 250 m while becoming a 50 km wide, shallow valley at a depth of 1 400 m (Goodlad, 1986). Both the 1:130 or 0.44^o axial gradients and the 1:70 or 0.82^o side wall gradients are less steep than those of the Thukela Canyon and tributaries occur, especially on the northern side wall (Goodlad, 1986). The canyon emerges from the Thukela Cone at 2 320 m, and as in the case of the Thukela Canyon, deflection is to the left when looking down-canyon (Goodlad, 1986).

1.5.5 Central Terrace

The Central or Tongaland Terrace is one of two main terraces in the region which, in Mozambique, is wide with convex slopes (Martin, 1984; Goodlad, 1986). Slope gradients vary between 1:400 or 0.14^o and 1:300 or 0.19^o and extend from between 1 300 m and 1 600 m to between 1 840 m and 2 000 m depths (Martin, 1984; Goodlad, 1986). The central axis trends more north north-west to south south-east as it progresses southwards, with two convex axes curving south-eastwards (Martin, 1984; Goodlad, 1986). Two prominent valleys flank the Central Terrace, with the first, to the east, separating it from the Mozambique Ridge, while the second, to the west, separates it from the continental margin and the Thukela Cone (Martin, 1978; Goodlad, 1986).

To the south, the steep, straight southern margin is transitional into the deep ocean basin at 2 400 m, with gradients of approximately 1:30 or 1.9^o (Goodlad, 1978).

1.5.6 Mozambique Ridge

The sediment draped Mozambique Ridge, (Area 13 in Figure 1.2), marks the eastern boundary of the Natal Valley. The smooth western margin has gradients of between 1:100 or 0.57^o and 1:25 or 2.29^o and rises to a high relief in excess of 800 m (Goodlad, 1986). In the vicinity of 29° S the slope is more rugged and incised with steep ridges and mounds with amplitudes of some 140 m and gradients of 1:10 or 5.7^o (Goodlad, 1986). At approximately 30° S the ridge is indented by a wide deep valley adjacent to a 250 m deep saddle on the crest, whereas the ridge edge is somewhat steeper to the south with local gradients of approximately 1:25 or 2.29^o (Goodlad, 1978). A sharp, western edge discontinuity at a depth of approximately 2 700 m marks the transition into the deep ocean basin (Goodlad, 1986).

1.5.7 Deep ocean basin

The deep ocean basin is subdivided into three sections (Areas 14, 15 and 16, Figure 1.2). The first section, the eastern deep ocean basin (Area 14) is a south trending crest of sediment with gentle slopes of 1:750 or 0.08^o to 1:500 or 0.11^o with steeper flanks (Goodlad, 1986). A wide sedimentary moat of 5 km to 20 km width and between 20 m and 60 m relief is found along the base of the Mozambique Ridge (Goodlad, 1986). Gradient values for the deep ocean basin are given in table 1.3.

Table 1.3. The average and maximum gradient dimensions for areas 14, 15 and 16 in figure 1.2 of the deep ocean basin (Goodlad, 1986).

Area	Average Gradient	Maximum Gradient
Area 14	1:500 or 0.11^o	1:250 or 0.23^o
Area 15	1:200 or 0.29^o	–
Area 16	1:600 or 0.1^o	1:200 or 0.3^o

The second section (Area 15), between the Thukela Cone and the eastern deep ocean basin has gradients of 1:200 or 0.29^o and the third section (Area 16), is defined by a smooth seafloor with gradients of approximately 1:600 or 0.1^o (Goodlad, 1986). Towards the Thukela Cone and the continental margin, gradients increase to approximately 1:200 or 0.29^o (Goodlad, 1986). Isobaths deflect southwards, south of the Thukela Canyon mouth, delineating a possible depositional fan (Goodlad, 1986). At approximately 33° 30' S and 33° 45' E, the Thukela Cone foot, a large dissected lobe of sediment, possibly a slumped mass, exists on the flat ocean basin floor, while a series of closed depressions line the base of the western continental slope in this area (Goodlad, 1986).

1.6   Regional oceanography

Acoustic measurements of depth depend on temperature, salinity and hydrostatic pressure (water depth) implying that oceanic structure is essential for accurate depth measurements. Surface circulation in the study area is dominated by the Agulhas Current System penetrating to depths of 2 500 m, while the deep circulation is dominated by the North Atlantic Deep Water (NADW) rising as shallow as 2 400 m (Goodlad, 1986).

Routes 1, 2 and 3 in figure 1.3 show the surface circulation of the Mozambique, Agulhas and the Mozambique Ridge Currents respectively as mentioned in the works of Martin (1984) and Goodlad (1986). The dominant surface current, the Agulhas Current is a western boundary, geostrophic current. This current type results from the Coriolis Effect caused by the Earth's rotation, producing the current's deflection which, in turn is balanced by the effect of the pressure gradient force causing the current flow (Kennet, 1982). A comprehensive review of the Agulhas Current is given by (Lutjeharms, 2006) where it is indicated that whereas knowledge of its effects have been known since 1497, the first early scientific research was only carried out as late as 1935. Subsequently its importance as a western boundary current in the Indian Ocean has been established with disagreements about its origin still existing today. Lutjeharms (2006) also asserts that little good hydrographic data are available to verify the ocean structure and flow patterns developed by the numerical models for the South West Indian Ocean.

Johnson and Damuth (1979), Kolla et al. (1980) and Westall (1984) confirmed a deep northward flowing western boundary current within the South West Indian Ocean, with two layers of water originating in high latitudes, the North Atlantic Deep water (NADW) and the Antarctic Bottom Water (AABW). AABW is restricted to abyssal depths below 4 000 m, not reaching the study area (Figure 1.4), while NADW does circulate in the South West Indian Ocean reaching the study area (Figure 1.4). According to Lutjeharms (2006) NADW flows eastwards and northwards into the South West Indian Ocean (Figure 1.4) between 3 200 m and 2 500 m flowing northwards in the Natal Valley below the Agulhas Current. The current follows the continental slope and Thukela Cone margins as a Coriolis-reinforced boundary current below 2 400 m, and on moving northwards up the shallower Central Terrace deflects southwards along the western Mozambique Ridge exiting into the Transkei Basin (Goodlad, 1986).
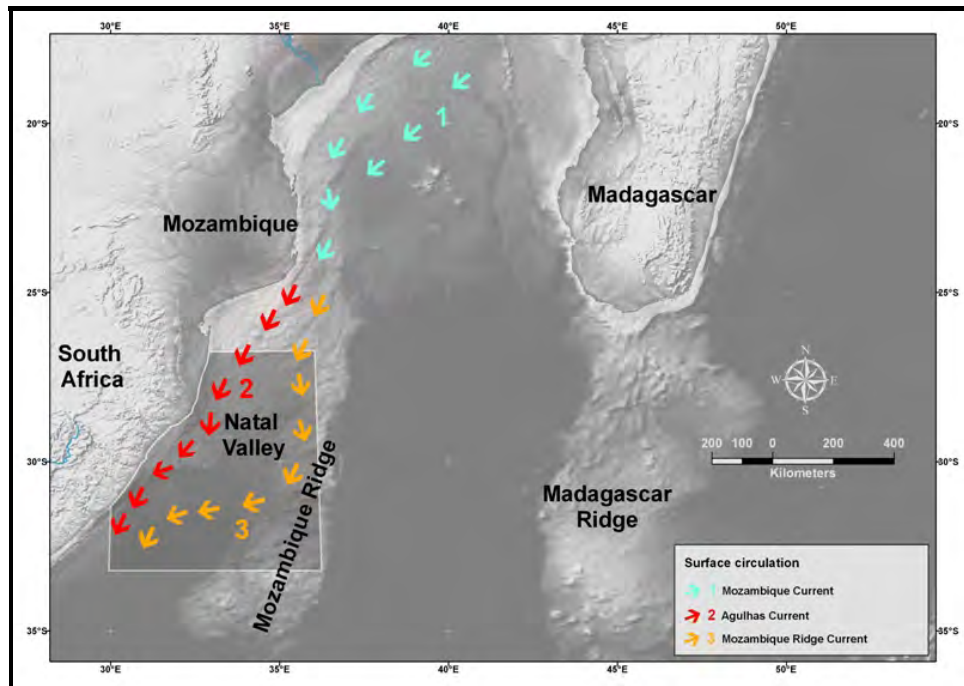
Figure 1.3. The surface circulation of the South West Indian Ocean showing the Mozambique, Agulhas and Mozambique Ridge Currents after Goodlad (1986). The study area is also outlined. Background image map source: ESRI.
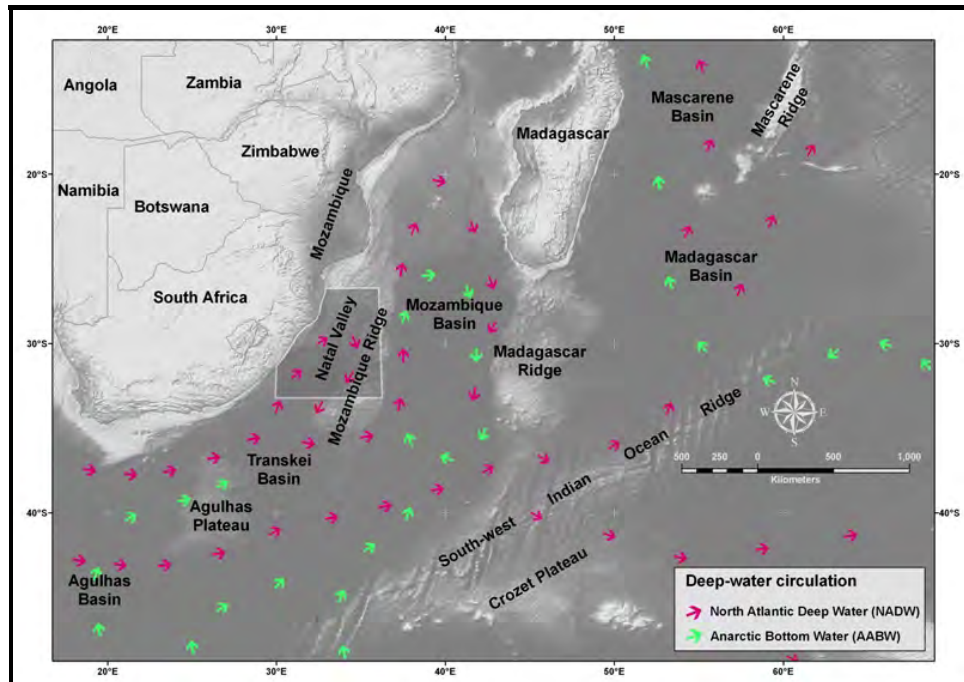
Figure 1.4. Regional deep oceanic circulation in the South West Indian Ocean after Goodlad (1986). Oceanographic data from Le Pichon (1960) Wyrtki et al. (1971) Kolla et al. (1976; 1980) and Johnson and Damuth (1979). The study area is also outlined. Background image map source: ESRI.

1.7 Regional weather and climate

Climate determines sea surface and subsurface conditions, influencing ship acquired bathymetric data acquisition quality. The sea surface is also the geoid, orbiting satellites use to determine their altitude and from which bathymetry is then predicted. Sea conditions (roughness) thus influences the quality of orbiting satellite predicted bathymetric measurement and ship acquired bathymetric data.

1.7.1 Circulation affecting study area

The predominantly dry South African climate is caused by anticyclonic (high pressure) circulation except for the near-surface low pressure circulation in summer (Preston-Whyte and Tyson, 2004). The southwestern Cape has wetter winters, whereas the remainder of southern Africa has a sub-tropical summer rainfall (Preston-Whyte and Tyson, 2004).

Dry stable weather can give way to temperate disturbances such as cold fronts, more common in winter from June to August with winds having a southerly and westerly component causing high winds and large swells. Summer months are dominated by winds having a northerly and easterly component also capable of causing rough seas. The windiest months of the year are August to September. The optimum data acquisition window in the study area is from January to May during which the sea conditions are calmest and April and May were the months during which most data acquisition for this project occurred (Table 1.4).

Table 1.4. The months during which data acquisition was historically undertaken. It can be seen that April and May were the favoured months for data acquisition.

Near-shore dataset	Acquisition month (s)
East Coast Canyon datasets	March and April
NRF Block A, B and C datasets	May
NRF Kosi Bay dataset	April
NRF Island Rock dataset	April
NRF Sodwana Bay dataset	February
Leven Point to Gobey's Point dataset	May and September
Ntabende Hill dataset	March, April, May, July and September
Red Sands dataset	March, April, May, July and September
Richards Bay continental shelf dataset	April and May
Durban Bight dataset	April and May
Durban outer shelf dataset	May
Blood Reef dataset	April and May
Aliwal Shoal dataset	March and June

2   DATASET ACQUISITION, POSITIONING AND PROCESSING

2.1   Introduction

Safe travel at sea requires maps and navigation charts demarcating sailable areas and hazards. The oldest known navigation chart is the Carte Pisante thought to have been drawn at the end of the 13th century on animal skin in Genoa. This was followed by marine charts known as portolans depicting wind direction to assist in the plotting of a ships course. In 1584 the publication of 45 nautical charts covering the European coasts from Norway to the Straits of Gibraltar was a milestone in marine navigational charting. These charts included: the ability to recognise features landwards of the coastline to aid positioning at sea; symbols for buoys and landmarks such as church spires; and the reduction of depth soundings to a vertical datum at half tide. After World War One the International Hydrographic Office (IHO) was established in Monaco (where it remains today) to regulate the standardization of marine bathymetric charts. In South Africa, the South African Navy is the custodian of all national bathymetric data relating to maritime safety and navigation. All MGU acquired data is stored in the MGU digital database. It was from this that the KwaZulu-Natal bathymetric datasets for this work were sourced and then subdivided according to depth measuring instrument used (Figure 2.1 and Appendix 3B) and navigational instrument used (Figure 2.2 and Appendix 3C).

2.2   Depth measuring instruments

The depth measuring instruments (Appendix 3B) used in the acquisition of the sounding datasets used in this study included:

- Lead lines,

- Acoustic instruments such as single- and multi-beam echo-sounders and the boomer and

- Satellite altimeters

The lead line is the oldest instrument then the electronic single-beam echo-sounder, then the electronic multi-beam echo-sounder (Guy, 2000; International Hydrographic Organisation (IHO), 2005b) and electronic satellite altimeter.

Figure 2.1. Areas representing the coverage extent of near-shore datasets. The four colours indicate the four different depth measuring instruments used to acquire the dataset.

Figure 2.2. Areas representing the coverage extent of near-shore datasets. The four colours indicate the four different positioning measuring instruments used to acquire the dataset.

2.2.1   Lead lines

Guy (2000) provides a detailed account of the lead line depth measuring technique. Typically, a lead line was lowered to the seabed to measure depth, usually in fathoms (1.83 m or 6 feet), either mechanically or by hand depending on water depth. Positioning was done while the vessel was stationary using horizontal sextant angles for further offshore positions or triangulation for near-shore positioning. Generally, depth surveying was done while underway and to counter tidal and wave effects, the lead line was dropped ahead of the measurement point. This ensured that it was vertical when making seabed contact after which it was recovered and the process repeated. This continuous acquisition method was only effective down to a 20 m depth. It was used mostly at a 15 m measurement interval with a plot scale of 1:6 250 but also up to a 45 m interval at a scale of 1:50 000. The disadvantage of this method was that stationary measurements deeper than 20 m could not be done because of interval restrictions and thus deeper surveys were done using random stationary soundings. Dense lead line soundings were thus limited to shallow water measurements until the introduction of the mechanised Sommerville Sounding Gear (Figure 2.3) which increased the continuous measurement of depths to 165 m. All South African Navy Admiralty Fair Charts made use of the lead line method for bathymetric acquisition (Guy, 2000) and as noted in appendix 3B, 3 datasets used in this work, Admiralty Fair Charts (AFC's) 18, 19 and 34 made use of this method.
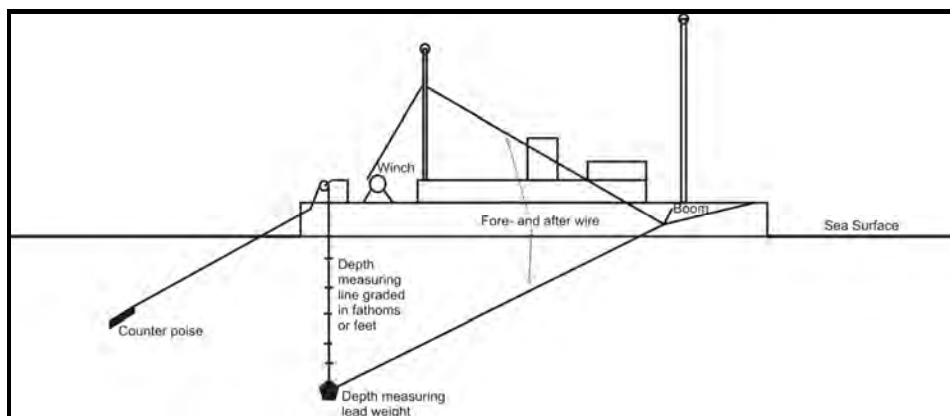
Figure 2.3. A typical Mechanical Somerville Sounding Gear system after Guy (2000). The winch was able to raise and lower the depth measuring line and weight via a boom attachment on the ship's bow while the vessel was underway. The stern towed counter poise offered resistance against the winch for controlling the lead line and weight accent and decent. Depths were measured in feet or fathoms graded on the depth measuring line.

2.2.1   Acoustic instruments

Acoustic instruments included in the acquisition of datasets used for this work include single-beam and multi-beam echo-sounders. Single beam echo-sounders were either of the analogue or the more modern digital types. Analogue types print out bathymetric records on paper charts during data acquisition while digital echo-sounders store the acquired bathymetric data. Multi-beam echo-sounders used for the dataset acquisition in this work were of the digital type. In all, 26 datasets used in this work made use of acoustic instruments (Appendix 3B).

Generation of an acoustic pulse

Beam-width of an ultrasonic pulse generated by an echo-sounder transducer is noted by IHO (2005b) and Jones (1999) as the width in degrees of the transmitted beam at its 3 dB or half power point. This beam-width is dependant on the transducer size, shape and frequency of the transmitted pulse and is parallel to the transducer face while the transducer axis is perpendicular to both its face and its aperture window (International Hydrographic Organisation (IHO), 2005b; Le Bas and Huvenne, 2008). A shape-dependant, conically formed beam is then steered through the water, insonifying a hyperbolic shaped footprint area of the seafloor to measure water depth. The capability of beam steering, either side of the transducer axis can change the size and shape of the insonified footprint, with Le Bas and Huvenne (2008) noting that the range on the one hand and resolution and operational frequency capabilities on the other hand of an echo-sounder are in opposition. Thus higher-resolution mapping requires a higher frequency device operating closer to the seabed.

Echo-sounders make use of either electro-restrictive or piezo-electric transducers at higher frequencies above 10 kHz or magneto-restrictive transducers at lower frequencies to generate sound pulses for the measurement of water depth (Jones, 1999; International Hydrographic Organisation (IHO), 2005b). Deep water measurements require lower frequency transducers operating at between 10 kHz and 15 kHz with slower output pulse rise times, higher power output, lower horizontal resolution and wider beam-widths of approximately 30°, whereas shallow water survey work requires transducers that operate at higher frequencies of 30 kHz to 210 kHz, with faster output pulse rise times, lower power output, higher horizontal resolution and narrower beam-widths of approximately 10° (Jones, 1999). Measured travel time precisions of 1 in 15 000 for emitted pulses can be obtained with beam-widths between 1° and 40° (Jones, 1999).

The two-way travel-time (twt) of this ultrasonic pulse is important. This time is halved and multiplied by the mean sound velocity for the water whose depth is being measured to yield water depth, as indicated by the equation:

$$Depth = \tfrac{1}{2}\,V_w\,t$$

Where V_w is the velocity of sound in sea water in ms^{-1} and t is the two-way travel time in seconds. Sound velocity in sea water can be between 1 400 ms^{-1} and 1 600 ms^{-1}, but averages 1 500 ms^{-1}. An acoustic signal is dependant on characteristics of the water whose depth is being measured and it will undergo spreading and absorption based on these properties (Le Bas and Huvenne, 2008). Sound velocity is temperature dependant (Figure 2.4a), increasing at 3 $ms^{-1}.^{\circ}C^{-1}$; salinity dependant (Figure 2.4b), increasing at 1.3 $ms^{-1}.‰^{-1}$ and hydrostatic pressure, or depth dependant (Figure 2.4c), increasing at 1.8 ms^{-1} for every 100 m depth increase (Jones, 1999). These characteristics were found to vary with different oceanic areas, but established trends in the variables led to the creation of standard tables of these variables for the different ocean areas to predict the sound velocity for bathymetric measurements to be done easily and quickly (Jones, 1999).

However, the complexity of the Agulhas Current and the oceanographic structure of South West Indian Ocean asserted by Lutjeharms (2006) along with the mention of minimal good hydrographic data to verify the numerical models in existence make such standardised tables unreliable for predicting sound velocities in the study area. This in turn may have lead to bathymetric measurement inaccuracies in the older datasets, especially where little descriptive metadata were available.

Transducer height below the water level and the tidal variations are also taken into account to yield the corrected water depth to a levelling (tidal) datum, such as Mean Sea Level (MSL) as used in this work. Tidal corrections are essential for accurate shallow water bathymetric measurements (Le Bas and Huvenne, 2008).
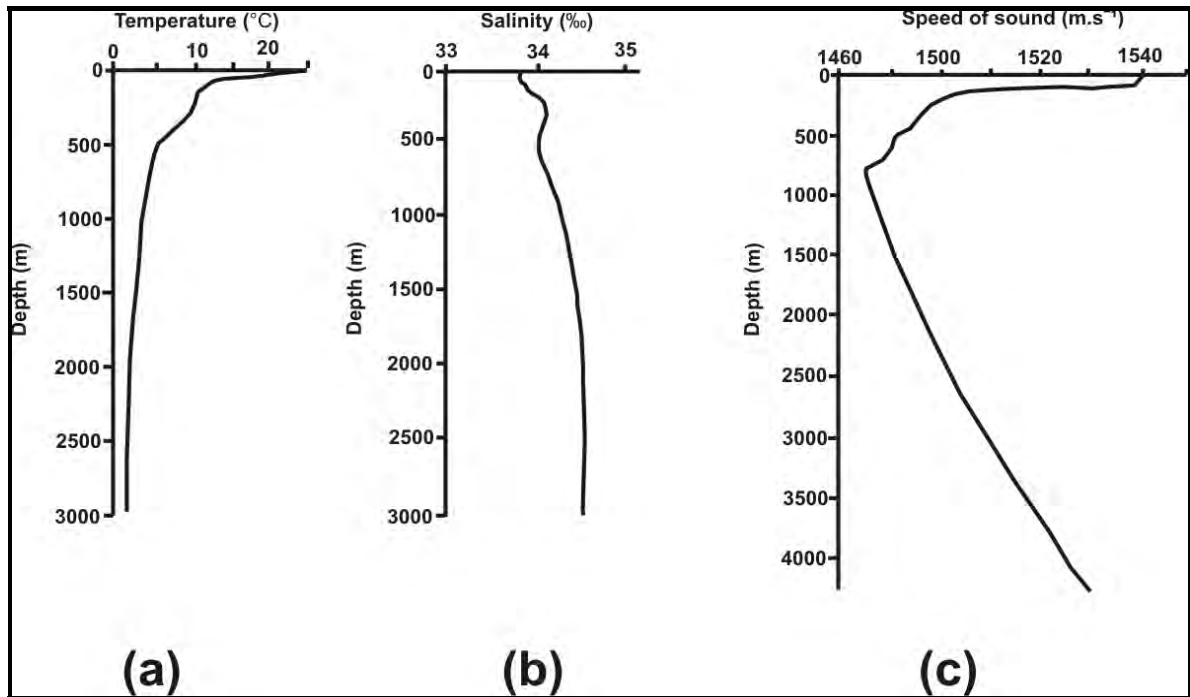
Figure 2.4. The variation of (a) temperature with depth, (b) salinity with depth and (c) the sound velocity with depth for an area in the central Pacific at 39°N, 146°W. The velocity of sound decreases to a minimum at a depth of 650 m (Jones, 1999).

Single-beam echo-sounders

Single-beam echo-sounders were introduced in the 1920's and data acquisition was considerably faster and of a higher density than that acquired by a lead line (Guy, 2000). High precision sound velocity and depth measurement, combined with digital measurement techniques found in more modern devices make them more accurate than older analogue devices. Of the datasets used in this work, 21 were acquired using single-beam echo-sounders of which 14 made use of digital single-beam echo-sounders while 7 made use of analogue single-beam echo-sounders (Appendix 3B).

The 14 MGU digitally acquired single-beam echo-sounder datasets used either a RESON ® Navisound 210 ® with a beam-width of 9° or an Odom ® EchoTrac 3100 ® with a 10° beam-width (Appendix 3B). Both are narrow-beam echo-sounders however, as noted by IHO (2005b) these devices can now have beam-widths of 2° to 5° for high-resolution mapping. One MGU dataset used an analogue SIMRAD ® EK 120 ® single-beam echo-sounder (Appendix 3B).

Metadata revealed that the 6 South African Navy Fair Chart datasets used in this work used single-beam echo-sounders for acquisition with their year of acquisition, leading to the assumption that an analogue as opposed to a digital device was used (Appendix 3B).

A block diagram showing the construction of a typical echo-sounder is shown in figure 2.5. Normally the transmitting and receiving elements (Figure 2.5) are combined into one transducer with the device mounted inside the ships hull or in the water outside the ships hull.
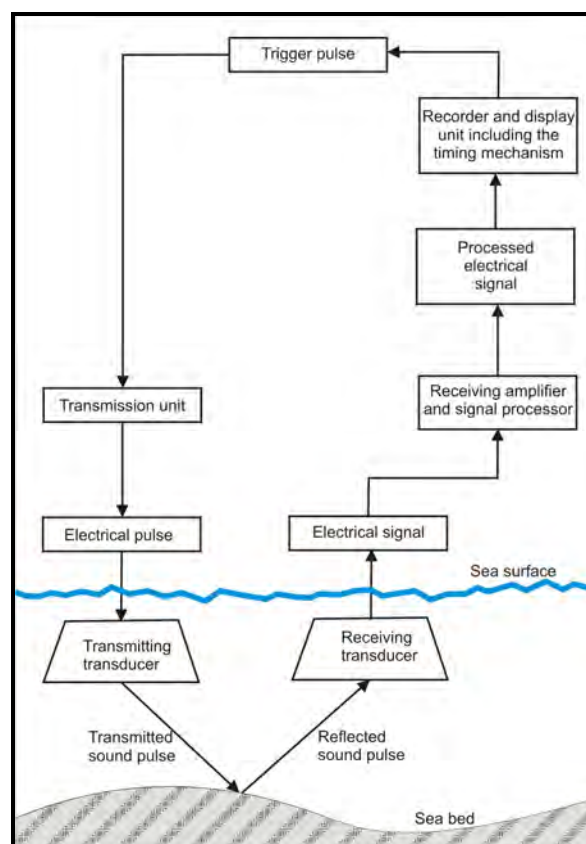
Figure 2.5: The components of an echo-sounder after McQuillin and Ardus (1977). The transmitting and receiving transducer are often combined into one device. All blocks above the sea surface in the diagram are part of the echo-sounder processing electronics aboard the vessel.

Multi-beam echo-sounders

Multi-beam echo-sounders consist of many individual echo-sounder transducers organised in a swath across the ships beam to map areas of the sea floor directly beneath the vessel and laterally while the ship is underway during a survey, thus providing higher acquisition data densities than that of single-beam echo-sounders (Jones, 1999; Brown and Blondel, 2008; Preston, 2008). As noted by Vasquez (2007) the many simultaneously transmitting and receiving transducers with narrow beam-widths are coupled with precise positional control and differential GPS, in this way improving system accuracy and seafloor object resolution but also adding to its complexity. Figure 2.6 shows how these multiple transmitted beams are received to image the seafloor. In this example, twenty magneto-restrictive 12 kHz transducers, each with a 2.67^o longitudinal size by 2.67^o latitudinal size (beam-width), span a total of 54° (20 elements by 2.67^o each) as in figure 2.6a. Forty fore- and aft-directed hydrophones receive the incoming signals and produce 16 beams. This beam-forming process, performed on the received beams is achieved by vector summation (Jones, 1999; Preston, 2008) as in figure 2.6b. Each return beam corresponds to a 2.67^o wide area insonified by the incident pulse with this 2.67^o wide area extending fore and aft by an angle of 20° normal to the transmitter axis (Jones, 1999). Overlapping transmitted and received beams results in the processed acoustic signals as shown in figure 2.6c. It is possible to map an area of 2 to 14 times the water depth, and whereas narrower beam angles will improve seafloor object resolution, allowing for the detection of smaller features, seafloor coverage is simultaneously decreased (Vasquez, 2007).

To measure the uncorrected water depth, the measured distance d to the seafloor is given by the equation:

$$d = r.cos\Theta$$

Where Θ is the stabilised beam angle (2.67^o in above example) and r is the slant range based on the mass centre of the beam array (distance shown by dotted lines in figure 2.6b).

The horizontal cross-track distance h is given by the equation:

$$h = (V_w/1500) \, r.sin\Theta$$

Where Θ is the stabilised beam angle, r is the slant range and V_w is the mean vertical sound velocity in sea water.
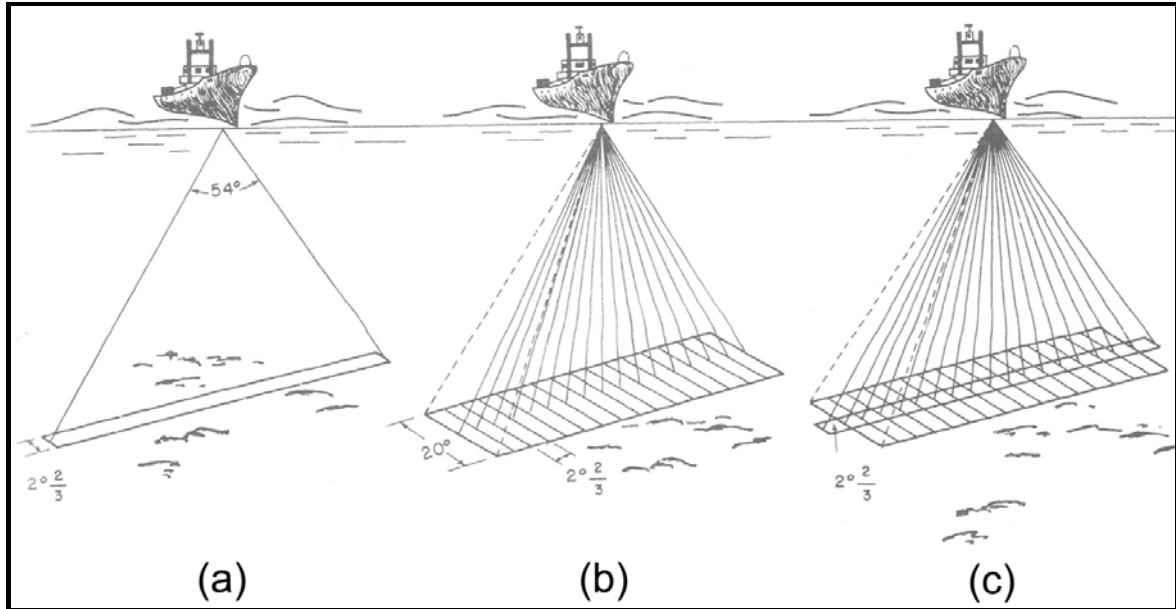
Figure 2.6. The principle of operation of a multi-beam echo-sounder. (a) The instantaneous seafloor area insonified by the transmitter is 20 x 2.67° = 54° across the ships beam and 2.67° normal to the ship hull. (b) Forty fore- and aft-directed hydrophone receivers produce 16 receiving beams of 2.67° by vector summation which extend fore-and aft of the ship by 20° normal to the transmitter axis. (c) Combination of (a) and (b) showing received acoustic energy from 16 square zones of 2.67° on the seafloor (Jones, 1999).

The cross-track distance, stabilised beam angle and water depth being measured determines the minimum resolvable horizontal resolution of features on the seabed (Jones, 1999; Hughes Clarke, 2005). The depth values measured are used as an electronic control signal to track the beams and these are stored with the cross-track distances, navigational information and recorded backscatter signals as metadata for real-time processing and contouring (Jones, 1999).

Deeper water systems operate at lower frequencies of 12 kHz to 15 kHz – the STN ATLAS Hydrosweep DS-2, a 15 kHz deep water system with 59 beams gives a swath width of 3.5 times water depth and a total swath angle of 120° (Jones, 1999). Shallow water systems operate at higher frequencies of 45 kHz such as the Echos XDM system (Jones, 1999). The MGU has a flexible, dual frequency RESON SeaBat 7125 operating 512 focused 0.5° x 1° beams at 400 kHz allowing 200 m water depth measurements or 256 focused 1° x 2° beams at 200 kHz allowing 500 m water depth measurements in both cases with a swath angle of 128° and a depth resolution of 5 mm (RESON Inc., 2006a).

As noted in appendix 3B, the 5 ACEP multi-beam datasets were acquired with a RESON ® 8111 ® 100 kHz system with 101 different 1.5^o by 1.5^o beams producing a 150° bathymetric swath of up to 7.4 times the water depth (RESON Inc., 2006b).

The improved seafloor mapping capability possible by the modern multi-beam echo-sounder results in high data volumes and processing intricacies (Guy, 2000; International Hydrographic Organisation (IHO), 2005b). Calder and Smith (2003) have predicted that modern shallow water multi-beam echo-sounder systems are capable of collecting in excess of 30 million data points per hour with deeper water collection systems having collection volumes of 2 orders of magnitude lower. High data collection density by multi-beam systems and their system complexity results in their increased susceptibility to system malfunctions and thus data collection errors and resultant artefact generation compared to single-beam systems. Jones (1999) notes that errors can result from incorrect bottom returns causing artefacts such as mound like features, while Vasquez (2007) also reports that artefacts from sea-bottom mistracking are more likely to occur in areas of complex rough seafloor and variable topographic areas. In addition, precise control of a multi-beam survey vessels pitch, roll and yaw is essential, along with tidal corrections and the precise location of all instruments (DGPS antenna, multi-beam instrument and motion reference unit) relative to one another is essential to reduce the possibility of errors (Hughes Clarke, 2003b; Vasquez, 2007). In addition, Hughes Clarke et al. (1996) describes the process of calibrating the multi-beam system known as the patch test, which is essential and must be accurate to ensure that acquired data are accurate and can be processed correctly.

Multi-beam data processing is more time consuming than single-beam and lead line data processing. Also as noted by Le Bas and Huvenne (2008) most of a multi-beam survey expense budget is generally consumed by its acquisition with little budget left for processing and interpretation, both of which they note are more time consuming and also important. Processing is often interactive with operator based processing in a subjective manner or it can be semi-automated with the use of custom standardised filters speeding up processing, with Hughes Clarke et al. (1996) Huvenne et al. (2007) and Le Bas and Huvenne (2008) noting that careful processing is essential to produce clear, accurate seafloor interpretation. One of the most well known and most useful of these filters is the Combined Uncertainty Bathymetry Estimator or CUBE and in areas of rough seafloor and steep topography its default

configuration is not recommended (Vasquez, 2007). In addition, survey area and multi-beam echo-sounder acquisition system knowledge is essential (Vasquez, 2007; Le Bas and Huvenne, 2008). The density of raw anisotropic multi-beam data requires it to be filtered during processing. This process creates a grid matrix and interpolates a bathymetric value at each grid node, so reducing the dataset size and making it isotropic. The acquisition data densities, the precision of multi-beam system, the time consuming data processing and system's mapping resolution can lead to the generation of artefacts being mapped, requiring filtering, whereas the lower data acquisition density of single-beam or lead line systems will not present such errors. However as noted by Greene et al. (1999), Kostylev et al. (2001) and Le Gonidec et al (2003) their superior high-density data collection capabilities and ability to accurately interpret the seafloor make them important, useful tools for seafloor mapping.

2.2.2   Satellite altimeters

The Smith and Sandwell version 8.2 global bathymetric dataset is predicted from satellite altimeter, derived gravitational anomaly measurements. This measurement principle is illustrated in figure 2.7. Gravitational attraction between the sea surface and the undersea topography results in undersea topographic features superimposed on the sea surface.

Two years of ERS-1 and four and a half years of GEOSAT satellite data were used to construct a global Mercator projected longitude and latitude gravity grid with precision of 2-minute longitudinal cells (Sandwell and Smith, 2000; Sandwell et al., 2006). The latitude cells were not of a 2-minute precision but cosine of the latitude multiplied by 2-minutes because of the increasing distance separation of latitude values in a polar direction of a Mercator projection (Sandwell and Smith, 2000). A method, known as Nettleton's Method (Appendix 2A), was used to create the global grid. The following along-track satellite derived sea surface slope data were used by Smith and Sandwell:

- High accuracy data from sixteen ERS-1 satellite repeat cycles along 35-day repeat tracks and 66 GEOSAT repeat cycles along 17-day repeat tracks (Sandwell and Smith, 2000).

- High density 1.5-year GEOSAT and 1-year ERS-1 Geodetic Satellite Missions (Sandwell and Smith, 2000; Sandwell et al., 2006).

Pulse limited radars aboard these satellites measure their heights above the closest sea surface point. Precise, concurrent global tracking and orbit dynamic calculations then

independently calculate heights above the ellipsoid. The height difference is equal to the sea surface or geoidal height (Sandwell and Smith, 2000; Sandwell et al., 2006) as shown in figure 2.7. Sea surface slope is derived by considering errors such as tropospheric and ionospheric effects on signal measurement, electromagnetic bias, ocean variability, mean ocean currents, tidal effects and sea surface slope (sea roughness). Sea surface slope was found to be the major contributor to errors at shorter wavelengths. A marine gravity grid with an accuracy of between 3 and 7 mGal was constructed from which topography was estimated (Sandwell and Smith, 2000).

Undersea topographic prediction was found to be most accurate between bandwidths of 20 km to 200 km. Bandwidths longer than 200 km were constrained by ship sounding data while those shorter than 20 km were constrained by multi-beam bathymetry where available. Worldwide predicted bathymetric accuracy was uncertain because of the lack of global ship track data to verify its accuracy (Sandwell and Smith, 2000). However, Goodwille (2004) suggests vertical accuracies of the single-beam bathymetric data components of the Smith and Sandwell dataset to be approximately 5 m in deep water when operated by a skilled operator, whereas the multi-beam bathymetric data components are considered to have vertical accuracies of 0.5 % of the water depth.
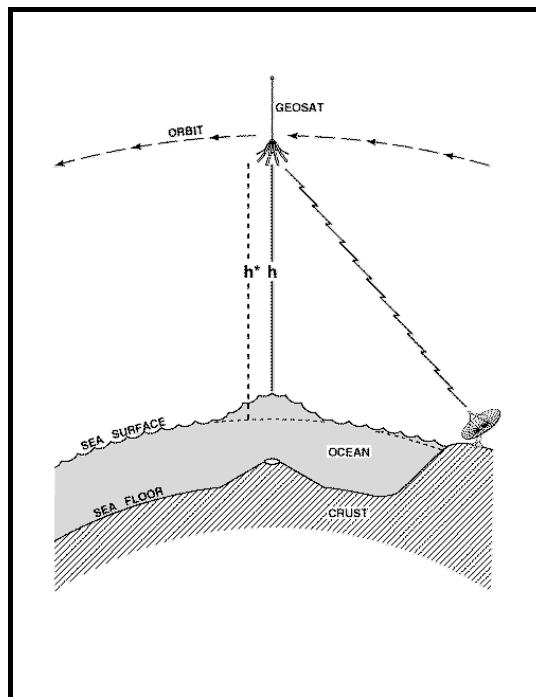
Figure 2.7. Calculating the satellite altitudes above the sea surface (h) and ellipsoid

(h*) to determine geoidal or sea surface height (Sandwell and Smith, 2000).

Sea roughness has a major influence on the accuracy of the shorter wavelength gravity field derived from satellite altimetry, affecting shorter wavelength bathymetric estimation (Sandwell and Smith, 2000). Wave heights of more than 6 m result in unreliable topographic prediction (Smith and Sandwell, 1997; Sandwell and Smith, 2000). However, wave height is generally less than 2 m, significantly more than the 20 mm sea surface height requirement for topographic determination. Electronic signal noise generated by a 2 m sea surface height would make the measurement of a 7 km feature the best resolution achievable. Sea roughness noise is improved by averaging 1 000 measurement pulses per second between the orbital height of 800 km and the sea surface. During this time the satellite travels a distance of 7 km with the noise signal reduced from between 1.5 m and 2 m down to approximately 0.05 m (Sandwell and Smith, 2000). Areas of high sedimentation also make the predicted bathymetry less accurate as the topography can be buried (Smith and Sandwell, 1997). The obvious advantages of this method are rapid acquisition, easy large scale coverage and potential repeat acquisition of data resulting in dataset improvement over time.

2.3 Navigational instruments

Data positioning depends on good navigational instrument precision and measurement repeatability in a known co-ordinate system. Digital electronic positioning achieves these requirements more accurately than analogue positioning as well as facilitating easy navigational data storage. The USA's Navstar GPS and Russia's GLONASS are both electronic digital satellite-based navigational technologies that are most commonly used. Navigational positioning instruments or methods used for the dataset collection in this study have included:

- Sextant- and triangulation based navigation

- Terrestrial radio based navigation

- Satellite based navigation

2.3.1   Sextant, marine chronometer and triangulation based navigation

Sextants and triangulation are the oldest navigation methods that apply to the datasets used for this work. Furthermore, Guy (2000) notes specifically that all the South African Navy Admiralty Fair Charts (AFC's) made use of these methods and appendix 3C indicates this to be true for AFC's 18, 19 and 34 acquired from 1911 to 1925. Sextants whose accuracies were between 370 m to 2.8 km, were used for celestial navigation by measuring angles between an observer and celestial bodies while marine chronometers, with accuracies known to be down to about 400 m allowed longitude to be derived from the time indicated. A sky almanac provided co-ordinates for known observed celestial objects from which latitude was then calculated (Bennet, 2007).

Celestial navigation was the only available method for offshore navigation where no land marks were observable. All countries have within their territorial boundaries fixed trigonometric beacons of known position (Figure 2.8a) forming networks of triangles. These are used to triangulate the vessel position, where known beacons are visible (A to D, Figure 2.8b). Angles are computed between points to create triangles with each triangle having one common side as shown in figure 2.8. Baselines of known length and azimuth (bearing) were set up to achieve an initial scale. However, scale errors tended to accumulate so additional baselines were required at suitable intervals depending on the accuracy requirements of the survey. Scale accuracy was proportional to the number of accurately measured baselines. In addition, azimuth measurements of one side of the triangle network were needed to determine the orientation of the network. Once again, orientation accuracy was proportional to the number of determined azimuth measurements along one side of the network (International Hydrographic Organisation (IHO), 2005a). The intersection points of lines forming the triangles were where bathymetric measurements or marker buoys could be deployed. Admiralty Fair Charts (AFC's) 18, 19 and 34 made use of these positioning methods (Appendix 3C).
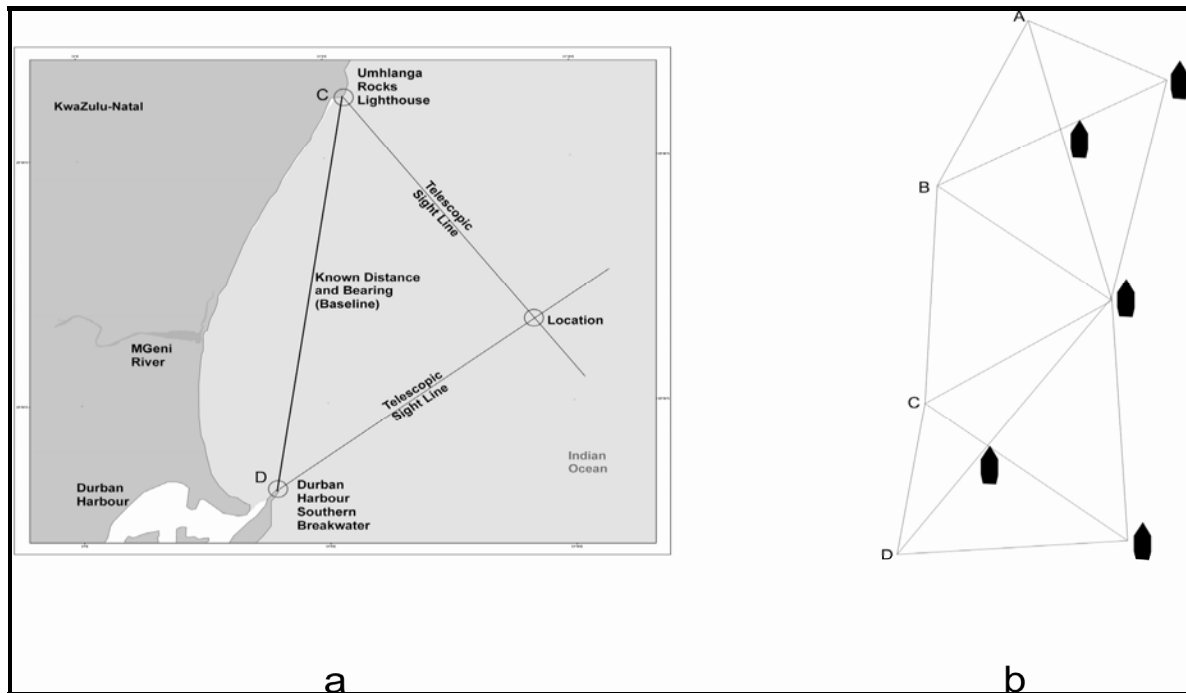
Figure 2.8. (a) The principle of triangulation used for marine navigation using the Durban Harbour Breakwater and Umhlanga Rocks Lighthouse as an example to set up a baseline of known length and azimuth (bearing) (C – D). (b) The triangle network is extended by using additional known beacons (C, D) setting up additional baselines. The intersection points form triangles and these intersection points establish where marker buoys are deployed and subsequent bathymetric measurements are made.

2.3.2 Radio navigation

Radio simplified navigation at sea and it was more accurate than celestial navigation or triangulation. Two methods were used to position a vessel: the measurement of the travel times of a pulsed radio wave transmission using a directional antenna and the measurement of phase differences in continuously transmitted radio waves. Both pulsed-wave and continuous-wave systems are divided into high, medium and low frequency systems.

Measurement of a pulsed radio signal travel time between one or more fixed land based antenna at a known location and a vessel at sea with an active directional antenna using a system of Radio Direction and Ranging (RADAR) where the 299 792 km.s^{-1} speed of radio waves allowed distance and bearing to be calculated. Figure 2.9 indicates how antennae in known positions simultaneously transmit pulsed radio waves to allow vessels to measure the different pulse travel times simultaneously and calculate their positions by radio triangulation where two or more signals are coincident. Omega or Differential Omega made use of pulsed

radio wave measurements (Jones, 1999). Transmitted continuous radio waves from synchronised stations that follow hyperbolic paths (Figure 2.10), allow for phase comparisons of two or more coincident signals by a vessel (Jones, 1999). The DECCA Navigator – used in South Africa from 1960 to 1990 (Guy, 2000) made use of this method of phase comparison of coincident signals.
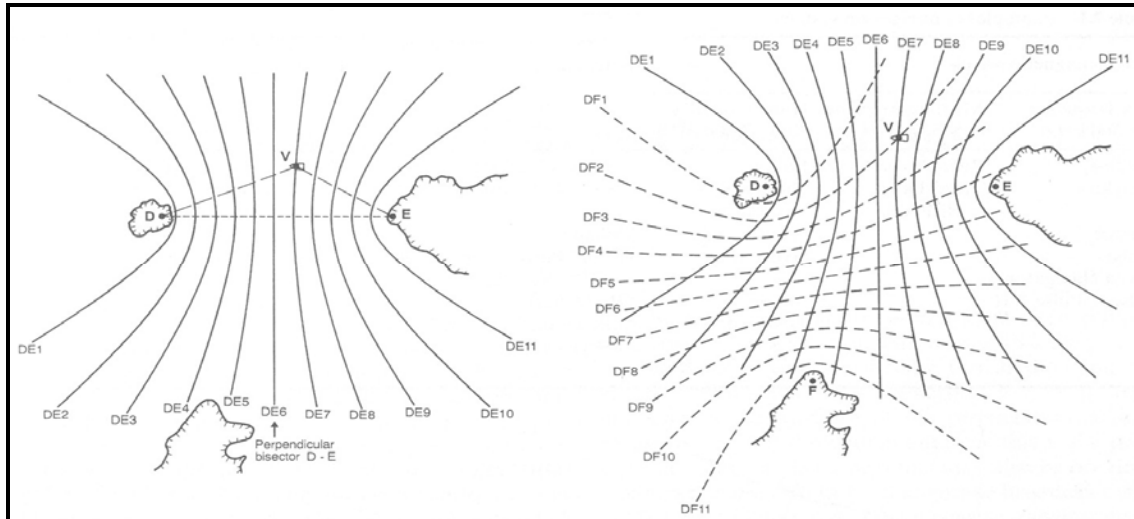
Figure 2.9. Position fixing by a vessel (V) using simultaneous measurement of pulsed radio wave travel times from different land based stations (D, E and F) emitting continuously. The hyperbolic overlaps of the three antennae together indicate vessel position (Jones, 1999).
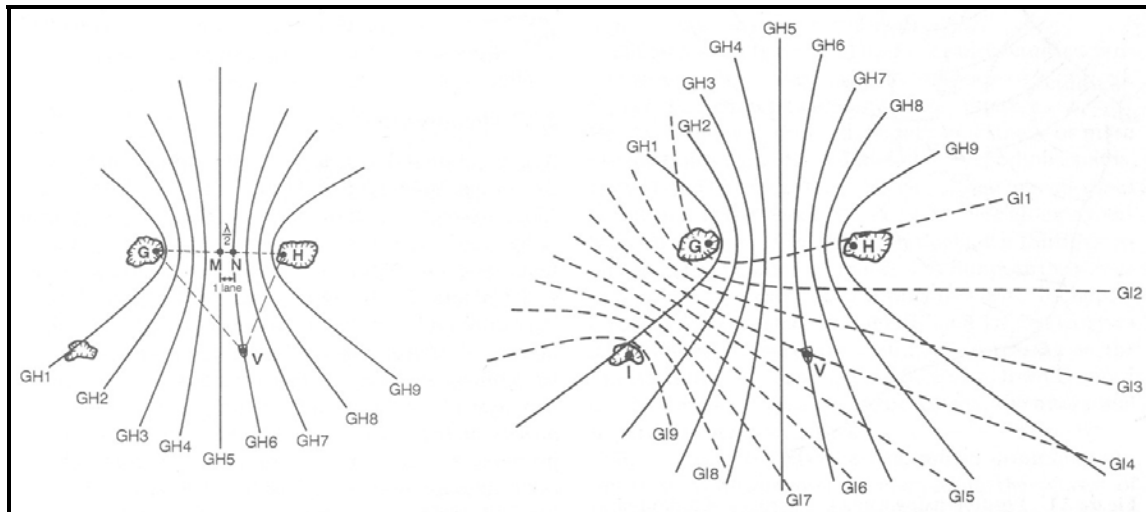
Figure 2.10. Position fixing by a vessel (V) using simultaneous measurement of phase differences between synchronously transmitted continuous radio waves from different land based stations (G, H and I). (Jones, 1999).

High frequency systems

These comprise the S-Band (1.65 GHz to 5.2 GHz) or X-Band (5.2 GHz to 11.9 GHz) used for a ships RADAR operated in line of sight of land where targets of known position are ranged with a rotating directional antenna to an accuracy of 50 m. Offshore work further from land made use of moored surface buoys with radar reflectors or transponders sending an amplified signal back to ship when ships RADAR transmission was detected. Long slack buoy lines causing positional errors in winds and variable seas and RADAR signal backscatter from sea roughness were both error sources. High frequency systems work better in the tropics where they are not influenced by ionospheric interference. Shoran was a high frequency system operating at 220 MHz to 400 MHz with an 80 km range with extended Shoran extending this to 100 km. The Sercel Syledis system operating in the 420 MHz to 450 MHz range produced 5 m accuracies. Some portable devices such as the 5.48 GHz Racal Micro-Fix provided accuracies of 1 m (Jones, 1999) similar to that of differential GPS (Jones, 1999).

Medium frequency systems

These systems cover the 1.5 MHz to 5 MHz band and operated out to approximately 800 km in either hyperbolic (continuous wave) or ranging (pulsed) mode or both in hybrid systems. Racal Hyperfix and BRAS-3 RS-10 are examples and ranges of 700 km in the day and 300 km at night with 1 m to 2 m accuracies were achievable (Jones, 1999).

Low frequency systems

These systems operate in the 10 kHz to 300 kHz band over ranges of more than 1 000 km with accuracies of 500 m to 4 km. Loran-C (operating at 100 kHz) was a pulse based system measuring return time of pulses with 2 000 km separations between a master and up to four secondary transmitters. Since pulses are used, ionospheric interference is limited compared to continuous wave systems. Sky wave returns can increase ranges to 4 500 km in the day and 5 500 km at night with accuracies of 3 km to 4 km. In differential mode, accuracies of better than 50 m can be obtained (Jones, 1999).

DECCA Navigator is a continuous-wave low frequency system operating at 70 kHz to 130 kHz with daytime ranges of 800 km and 400 km at night. A master transmits at a given frequency and several, normally 3 slave transmitters, transmit harmonic frequencies of the master frequency phase locked and controlled by the master.

The ship receiver has multiplier circuits producing different frequencies for phase comparison with the different master-slave pair having different colour hyperbolic lattices such as red, green and purple (Jones, 1999; Guy, 2000). Accuracy is 15 m along a baseline but away from the base line between 50 m and 400 m up to 400 km away from transmitters (Jones, 1999). DECCA was set up in Namibia and South Africa in the late 1960's with a total of 5 out of 7 proposed shore stations. It was operated for 30 years, used extensively by hydrographical survey organisations such as the South African Navy until its disbandment in March 1998 (Guy, 2000). All 6 South African Navy Fair Charts used in this work made use of the DECCA system for positioning (Appendix 3C).

Omega and Alpha are low frequency worldwide coverage systems transmitting 200 kHz, 11.33 kHz and 13.6 kHz continuous-wave signals every 10 seconds for 1 second duration each with all stations synchronized by an atomic clock. Daytime accuracy is 1.8 km, while accuracy at night is 3.7 km but down to 500 m in differential mode (Jones, 1999). The continuous-wave DECCA had a higher power output than pulsed-wave Omega and thus a longer range of 1 000 km. Omega however could operate up to 2 000 km using ground waves and 5 000 km using sky-waves, but these methods produced significant errors (Guy, 2000).

2.3.3   Satellite navigation

Satellite navigation systems can be divided up into systems where the Doppler shifts in received radio signals are measured for positioning and systems where time measurement is used:

- Transit Satellites (or NAVSAT) – using Doppler shift measurements

- United States Navigation Satellite Timing and Ranging Global Positioning System (Navstar GPS) and the Russian Global Orbiting Navigation Satellite System (GLONASS) –using time measurements

Transit satellites (NAVSAT)

These were the first satellites used for navigation. Doppler shifts in received radio signals from satellites allowed positions to be calculated if a satellite tracking station could track the satellites orbit. The latitude of the overhead north-south orbiting satellite and the receiving station were almost identical and the frequency-time curve gave the longitude separation. The only requirement was for the receivers position to be known to within 200 km (Jones, 1999). The first transit satellites were deployed in the 1960's and transmitted at 150 MHz to 400 MHz (Blondel and Murton, 1997; Jones, 1999) with accuracies of between 30 m and 100 m with only up to 20 observations possible per day (Blondel and Murton, 1997; Jones, 1999) and continuous positional fixes not possible. In higher latitudes, above 55°, position fixes were separated by 1 hour but by up to 2 hours at the equator and the vessel speed had to be known (Jones, 1999). This system was used in South Africa up to 1988 (Guy, 2000) and remained in use worldwide until the 1990's when the Global Positioning System (GPS) was deployed by the US Department of Defence (Jones, 1999). NAVSAT may have been used for navigational positioning in certain South African Navy Fair Charts used here (Appendix 3C).

GPS and GLONASS satellites

The US Department of Defence developed the Navigation Satellite Timing and Ranging Global Positioning System (Navstar GPS) (Figure 2.11) which was deployed in the 1990's during which time the Russians deployed the Global Orbiting Navigation Satellite System (GLONASS). The positioning dependence on time ranging rather than Doppler shift did not require low altitude, high velocity satellite orbits. Greater coverage was possible and higher satellite orbits reduced effects of the lower atmosphere on signal improving navigation accuracy. There are 24 GPS satellites orbiting the Earth at a height of approximately 20 200 km. These comprise 21 Block 1 satellites at 63° to the Equator and 3 Block 2 satellites at 55° to the Equator in 6 equally spaced orbits with 4 satellites per orbit each completing an orbit in 11 hours 58 minutes – ensuring satellite visibility for 5 hours and at least 4 satellites visible at any time to an observer. In comparison, the 24 GLONASS satellites orbit at 19 100 km with orbital periods of 11 hours 16 minutes at 65° to the Equator. GPS transmits on two L-Band frequencies, L1 at 1 575.42 MHz and L2 at 1 227.60 MHz synchronised with 10.23 MHz atomic clocks from ground tracking stations (Figure 2.11), while GLONASS transmits at 1 607.0 MHz and 1 250.0 MHz (Jones, 1999).
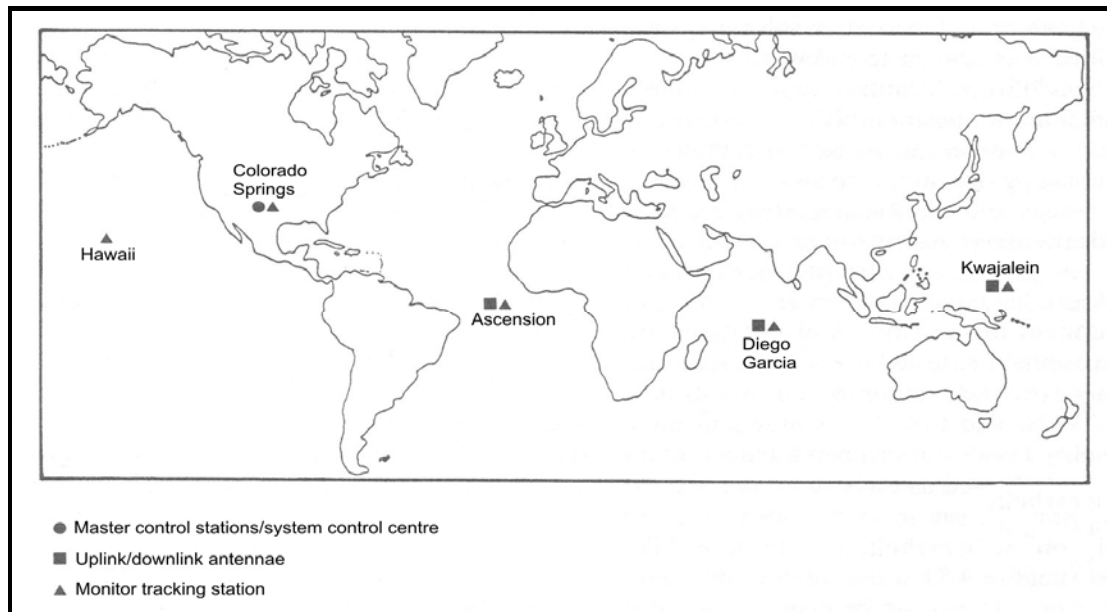
Figure 2.11. The GPS ground control stations – close to the Equator and uniformly spaced. The master station in Colorado Springs provides satellite orbit and performance information. All stations track and issue commands to the satellites (Jones, 1999).

Known ranges to three satellites allow receiver latitude, longitude and height to be calculated and a fourth satellite allows the clock offset between the satellites and receiver to be calculated for a more accurate reading. Unlike transit satellites the atmospheric effects on the signal are corrected making GPS and GLONASS based positioning more accurate and independent of vessel speed (Jones, 1999). In GPS both a P or precision transmission and a CA or coarse acquisition transmission are broadcast. Horizontal accuracy using the CA and P codes is between 5 m and 15 m and using the CA code alone reduces this to 100 m. This Selective Availability (SA) was a form of control by the US Department of Defence who corrupted the P code transmission (Blondel and Murton, 1997; Jones, 1999) which has subsequently been abandoned but can be reinstated at any time.

Differential GPS can be implemented when an observational GPS has the capability and is within 2 000 km of a fixed GPS receiver of known position in which case error causing influences are assumed to affect both the fixed and observational GPS station equally. The fixed station uses its known position to calculate positional error between its position and that computed by the satellites. This is transmitted to the observational GPS for calculation of its position more accurately. Horizontal accuracy can be less than 1 m but depends on the number of fixed stations and error signal transmission rate (Jones, 1999).

All 5 of the ACEP multi-beam echo-sounder datasets and 14 of the MGU single-beam echo-sounder datasets used in this work were acquired using differential GPS navigation technology. One MGU dataset used standard GPS navigational technology (Appendix 3C).

2.4   Dataset co-ordinate systems and datums

Bathymetric datasets acquired for this work had co-ordinates either in degree-based, angular units or in metre-based distance measuring units, both of which require the choice of a suitable horizontal datum. The differences are described along with the reasons for the choice of the UTM metre-based co-ordinate system for this work. The choice of an appropriate vertical (tidal) datum is also required for each bathymetric dataset.

2.4.1   Geographic co-ordinate systems

Geographic co-ordinate systems consist of a grid of standard parallels of latitude and standard meridians of longitude depicting angular measurement units such as degrees. They are used on ellipsoids or spheres, where constant lengths, angles and areas cannot be honoured as shown in figure 2.12. For example, the convergence of lines of longitude at the poles results in one degree longitude being zero km at the poles, whereas, one degree longitude is about 112 km at the Equator (Zakrzewska, 2004).

2.4.2   Projected co-ordinate systems

Projected co-ordinate systems are based on an underlying geographic co-ordinate system, but are capable of displaying two-dimensional constant lengths, angles and areas in distance measuring units (metres in the case of these datasets) rather than angular units such as degrees. To accomplish this, an X and Y grid with an arbitrary origin at the grid centre is defined to develop a 2-dimensional map of an area of interest, after which a map projection transforms the equivalent area from the 3-dimensional Earth to this flat, 2-dimensional map. Four projection types exist with one of these, the conformal projection, used for the Universal Transverse Mercator (UTM) co-ordinate system which is used by the MGU. Local shape is preserved in a conformal projection by maintaining all angles, good for large scale, more detailed mapping of small areas (Zakrzewska, 2004).
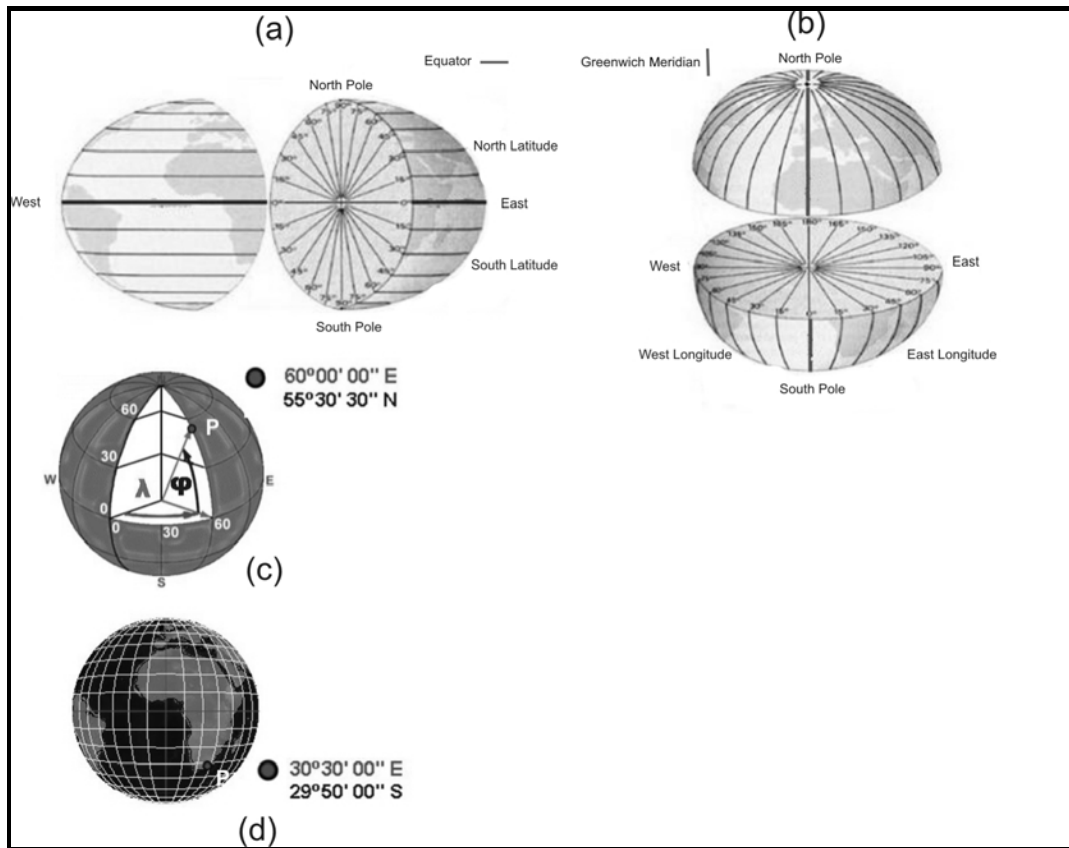
Figure 2.12. (a) Standard parallels of a geographic co-ordinate system with the Equator as the origin showing north and south latitudes, (b) standard meridians with the Greenwich Meridian as the origin showing east and west longitudes of a geographic co-ordinate system. (c) Longitude (λ) is the angle measured in the equatorial plane between a point and the Greenwich Meridian with east positive and west negative and latitude (φ) is the angle measured in the meridional plane between a point and the Equator with north positive and south negative. (d) The location of a point by defining its longitude and latitude position on the Earth after Zakrzewska (2004).

Universal Transversal Mercator (UTM) co-ordinate system

Ridd (1991) notes that scale of observation is relevant to spatial data analysis in GIS, with a larger denominator indicative of a smaller map scale and correspondingly larger real world physical environmental distance traversed by one map unit. Correspondingly, a map scale of 1:3 000 000 indicates smaller scale with more real world distance covered by one map unit than a map at a scale of 1:300 000. Scale of observation also determines the appropriate co-ordinate system to use which can cause confusion. In general, smaller map scales, where spherical or ellipsoidal GIS themes are used, for instance the use of the Earth to display GIS

datasets, make the geographical co-ordinate system preferable. Another instance where this co-ordinate system is useful includes the display of GIS datasets extending across multiple UTM Zones (Figure 2.13).

However the accuracy requirement for MGU survey work in KwaZulu-Natal involves large scale, more detailed mapping of small areas, often only within the UTM Zone 36 S (Figure 2.13) requiring the use of the applicable, projected, metre-based UTM Zone 36 S co-ordinate system rather than a degree-based geographical co-ordinate system. Although the 1:3 000 000 map scale of the final bathymetric dataset (Figure 5.1) is small, it covers UTM Zone 36S, and this along with its larger scale mapping requirements along with most acquired MGU data using the UTM Zone 36 S co-ordinate system, led to the adoption of the UTM Zone 36 S co-ordinate system for all datasets including the final bathymetric dataset for this work (Figure 2.13).
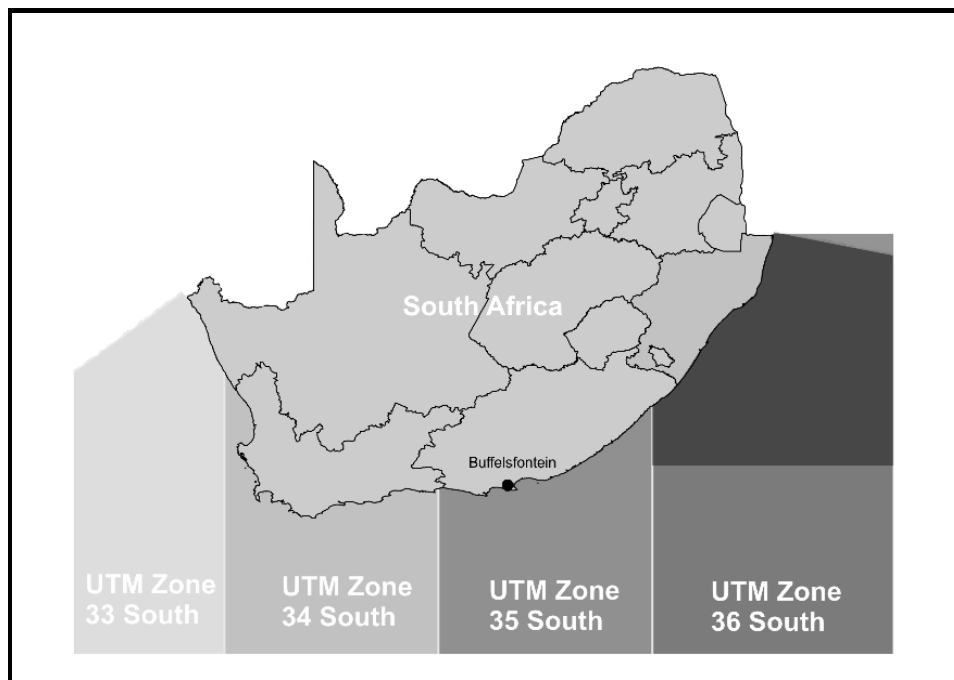
Figure 2.13. The South African marine UTM co-ordinate system zones. The KwaZulu-Natal marine environment (dark grey) falls within UTM Zone 36 S.

2.4.3 Horizontal datums

Bathymetric datasets reviewed here had either geographic-based angular measurement co-ordinates or metre-based, distance measuring co-ordinates. These, together with one of two standard ellipsoids determined one of two possible map datums, essential for their correct spatial projection. These two datums were the older Cape Datum, defined by the Modified

Clarke 1880 Ellipsoid, and the newer World Geodetic System of 1984 (WGS84) Datum, defined by the Ellipsoid of the same name. The Cape Datum is a local datum with its origin at Buffelsfontein (Figure 2.13) whereas the WGS84 Datum is a geocentric datum with its origin at the centre of the Earth, the reason it is preferred for GPS positioning systems. The two ellipsoids each have a larger semi-major equatorial axis (a), and a smaller semi-minor polar axis (b) and a ratio of each known as a flattening ratio as in table 2.1.

Table 2.1. Comparison of the dimensions of the semi-major axis (a) and semi-minor axis (b) and flattening ratios (a-b)/a for the Modified Clarke 1880 Ellipsoid and the WGS84 Ellipsoid.

Variable Name	Modified Clarke 1880 Ellipsoid	WGS84 Ellipsoid
Semi-major axis (a)	6 378 249.145 m	6 378 137.298 m
Semi-minor axis (b)	6 356 514.967 m	6 356 752.314 m
Flattening ratio (a-b)/a	0.003408	0.003353

These different values (Table 4.2) result in changes when transforming datasets from the Cape to the WGS84 datum of these amounts:

(0.5" or 15.43 m and 2.8" or 86.43 m northwards)

(0.7" or 21.62 m and 2.6" or 80.25 m eastwards)

GIS software, such as ESRI ® ArcGIS ® proved essential to the accomplishment of the projection and transformation of these spatial bathymetric datasets. Brief overviews of GIS data types are thus presented.

2.4.4 Vertical datums

Foxgrover et al. (2004) used GIS to integrate diverse bathymetric datasets for their work to determine erosion and bathymetric change in San Francisco Bay from 1858 to 1983. Many tidal datums were used in their study area over their observation period, leading to data uncertainty, especially in shallow areas. In addition, Ng' ang' a et al. (2004) in their technical review of the 3D marine cadastre requirements, mentioned the existence of many vertical or chart datums as a source of confusion. Tidal datums such as mean low water, low water, lowest astronomical tide, mean low water spring tide are some of the tidal datums in use today (Monahan and Nichols, 1999; Fowler and Treml, 2001). In South Africa, Mean Sea Level (MSL), known as the *National Land Levelling Datum* and Lowest Astronomical Tide (LAT), known as *CHART DATUM* are most frequently used, where MSL is currently considered to be 0.913 m above *CHART DATUM* for Durban and 1.015 m above *CHART DATUM* for Richards Bay (Kampfer, 2007). These are the two ports applicable to this work.

2.5 Geographical Information Systems (GIS)

2.5.1 Overview

Van Zwieten (2008) notes that a geographical information system (GIS) merges data management and spatially related map based locations into a user-friendly graphical interface. From this it is possible to produce multiple diverse data themes (for example a political map and a topographic map) with great accuracy and quality. Digital GIS data has advantages over analogue data. It can be displayed more legibly and is scalable, allowing visual or computer aided analysis and searches which can be advantageous, especially with large spatial datasets where time and costs can be saved. Modification of digital spatial data is also easier and quicker than modification of analogue spatial data. Relating diverse digital spatial data and non-spatial data can benefit many endeavours, such as banking, health care, policing and leisure. Scott (2006) has also indicated the proven usefulness of Geographical Information Systems (GIS) as a tool in marine sciences to store, manipulate, interrogate and edit spatially diverse geographical scientific data It has even been suggested by Antenucci et al. (1991) that data sharing will be a key influence to the continued growth of GIS technology. Essential to the creation of these accurate, useful GIS datasets is the establishment of a map datum, based on the correct ellipsoid and an appropriate co-ordinate system.

2.5.2 GIS integration background

Bonham-Carter (1994) and Foxgrover et al. (2004) note that GIS systems are used to integrate diverse spatial datasets to allow for its analysis to enable predictions to support decisions. Flowerdew (1991) has identified three technical issues related to dataset integration: data modelling, data vintage and data quality problems. Thus, resolution or precision of this integrated GIS bathymetric dataset to map real world features depends upon its underlying data modelling capability in conjunction with its vintage and its quality. The last two issues can be addressed by a term known as metadata. Larsen (1996) defined this as data about data or a means of describing a dataset. The quality of GIS results has been recognised by Van Deursen et al. (1991) Wadge (1992) and Guptil (1996) to be dependant on the descriptive quality of this metadata for dataset acquisition and processing. Modelling ability of the final GIS bathymetric dataset is influenced by the individual GIS bathymetric datasets and thus their metadata. Such metadata include: vintage or year of acquisition, seasonal weather at the time of acquisition, acquisition and navigational positioning instruments, processing software and

operator bias. Whereas the MGU and ACEP bathymetric metadata were good (Appendices 3A to 3C), the only meaningful metadata for the South African Navy bathymetric datasets were the year of acquisition (Appendix 3A) and the type of bathymetric acquisition instrument used (Appendix 3B). From these metadata the use of an analogue echo-sounder for the Fair Chart bathymetric dataset acquisition was deduced, while the positioning instrument was deduced from metadata about the year of acquisition (Appendix 3A). Comparison with MGU and ACEP bathymetric datasets where possible, proved useful in determining these bathymetric datasets' quality. Bathymetric dataset integration led to the recognition of two GIS data types, the raster or field data model and the vector or object data model, which as noted by Bonham-Carter (1994) could be used either separately or simultaneously in a GIS theme. Goodenough (1988) Zhou (1989) and Lunetta et al. (1991) have addressed the advantages and disadvantages of both types in works on the integration of raster-based satellite imagery data and vector-based topographic data, with table 2.2 conceptualised by Dangermond (1991) indicating these differences as applied to this work.

Table 2.2. Raster and vector data types and their application to marine data representation shown in bold (Dangermond, 1991).

Vector preferred	Raster preferred
Lines real: coastline / **study area** / **track lines** / **bathymetric contours**	Lines artificial / apparent – represented by adjacent cells of similar colour
Data certain: **point datasets** (**sounding data**)	Data probabilistic: **data interpolation** (**DEM or relief image**)
Descriptive query: (**dataset statistics in Appendices 3A to 3D**)	Prescriptive analysis
Computer mapping (**creating contour maps, DTM's and TIN's**)	Spatial statistics
Spatial DBMS': (**datasets in personal geodatabase manageable in MS Access ® or ESRI ® ArcGIS ®**)	Spatial modelling: **able to represent differing elevations using different shades or colours**

Raster data

Raster model space is continuous and is divided up into equally spaced units known as cells on a map. These map units or cells have attribute values which vary continuously (for instance, different colour values) while a related user-defined environmental variable such as elevation varies in the real world while the map and real world are related spatially via the GIS system software. User-defined environmental variable values can be explicit or implicit, derived via software interpolation. Map surfaces created by software interpolation of explicit elevation values yield a Digital Elevation Model (DEM). Its object resolution is proportional to its point

density, user-defined environmental variable interval and the software interpolation precision of cells in an appropriate raster grid. This implies that raster data stored is directly proportional to raster resolution required. Spatially geo-referenced raster file types used in this project and supported by ESRI ® ArcGIS ® have included the MrSID ® and GeoTIFF. Raster datasets were mainly used as map backgrounds to enable the digitising of point and polyline vector data to be included in the final bathymetric dataset.

Vector data

Whereas raster model space is continuous, vector model space is discreet and object orientated. Vector model space thus consists of objects such as points, polylines or polygons defined by object properties such elevation, rock type, geological fault type or name. Datasets used in this work were point vector datasets, which can have regular grid-like spacing similar to that of a grid-based raster dataset. These types are known as isotropic point vector datasets. The ACEP multi-beam datasets, ETOPO5-, Smith and Sandwell- and GEBCO freely available vector bathymetric grids are examples of this type of point vector dataset (Figures 3.16 to 3.20 and 3.24, 3.25 and 3.27). However a point vector dataset can also be anisotropic or irregular, unlike a raster dataset. The MGU, South African Navy bathymetric datasets (Figure 3.5 to 3.15) and the final bathymetric dataset are examples of this type of point vector dataset. These differences in raster and vector properties influence spatial GIS model space, related data properties and data storage requirements.

From the above it can be seen that vector model space favours this work more than raster model space. Vector spatial data formats used in this project and supported in ArcGIS included:

- The ESRI ® Shapefile ®

- The AutoDesk ® AutoCAD ® DXF ® file

- The ESRI ® Geodatabase ® feature class

ESRI ® Shapefiles ®

The ESRI ® Shapefile ® is a non topological composite spatial data file type with multiple individual files with different extensions (ESRI, 2007) and was initially used when point data were imported into and displayed in GIS format. Exported AutoCAD ® DXF ® contour data from surfer was also imported into GIS format initially using the ESRI ® Shapefile ® format.

Paul Young

AutoDesk Drawing Exchange Files ® (DXF ®)

The Autodesk ® AutoCAD ® Drawing Exchange Format file with the *.DXF extension was the intermediary file type used to export contours maps produced in Golden Software ® Surfer 8 ® for import into ESRI ® ArcGIS ®. The reason for this was that contour maps exported by Golden Software ® Surfer 8 ® as Shapefiles did not retain contour elevation value attribution whereas DXF ® files did.

ESRI ® Geodatabases ®

The ESRI ® Geodatabase ® is a database system with spatial capabilities and properties built around a database management system (DBMS) tool. A DBMS allows the management of large data amounts beyond the capability of traditional stand alone file management software tools such as the Windows Explorer and, more commonly in the GIS arena, ESRI ® ArcGIS ®. The powerful DBMS is based on Structured Query Language (SQL), a data management language designed to process and analyse data structured in the records (rows) and fields (columns) structure commonly found in GIS systems. The DBMS can be leveraged by GIS software to allow for GIS system scaling or growing complexity with data needs and uses over time. The main spatial vector data format stored in geodatabases is the feature class. Feature classes along with raster datasets and tables represent the three initial basic elements constituting the first step in the design of a geodatabase. Attributes and rules describing these three elements are stored using tables of records (rows) and fields (columns). The addition of topologies, networks and subtypes add to the complexity or upward scaling of the geodatabase design (ESRI, 2007). All point vector datasets were finally stored as geodatabase feature classes.

University of KwaZulu-Natal   -57-   Integrated marine GIS bathymetric
dataset for KwaZulu-Natal

3 DATASET REVIEW

3.1 Introduction

The datasets used in this study comprised 29 near-shore and 3 deep-water datasets. The 29 near-shore datasets used for this work were more dense, averaging approximately 2 000 points per km^2 but up to approximately 57 000 points per km^2. The 3 deep-water datasets used were of lower data densities, with 1 point every 1 852 m (GEBCO dataset) or 3 704 m (Smith and Sandwell dataset). The third, the digitised contour dataset of the northern Natal Valley after Dingle et al. (1978) with diverse data densities varying from 0.02 to 1 point per km^2.

The 15 MGU near-shore datasets used in this work were acquired between 1990 and 2005. All except one made use of digital single-beam echo-sounders and differential GPS. The exception made use of GPS navigational technology and was acquired with an analogue single-beam echo-sounder (Appendices 3A to 3C). All datasets were anisotropic and in a digital format. Processing to correct errors, mostly zero or positive depth values, was required.

The 9 South African Navy Admiralty- and Fair Chart sounding datasets were acquired between 1911 and 1993. Six made use of analogue single-beam echo-sounders and DECCA or possibly NAVSAT based navigation while 3 made use of lead lines and triangulation- or marine chronometer and sextant based navigation (Appendices 3A to 3C). These were digitised earlier by MGU workers either from sounding data or from contour data. All except one dataset, subsequently digitised by the author, were in anisotropic, digital format. Processing included the removal of zero or positive depth values and the conversion from fathoms to metres (AFC 34).

The 5 African Coelacanth Ecosystem Programme (ACEP) acquired in 2002 made use of a digital multi-beam echo-sounder and differential GPS navigation (Appendices 3A to 3C). All datasets were in isotropic, digital format for this work.

Deep-water datasets used in this work included the freely available, grid-like Smith and Sandwell bathymetric dataset predicted from satellite acquired gravitational data available in version 8.2 since 2000, the freely available GEBCO bathymetric grid dataset derived from digitised contours available in version 1.02 since 2003 and the Marine Geoscience Unit's contour dataset of the northern Natal Valley after Dingle et al. (1978). The isotropic, digitally

available Smith and Sandwell and GEBCO datasets were extracted for the study area and processed for zero or positive depth values. The contour dataset of the northern Natal Valley after Dingle et al. (1978) was digitised by the author for this work.

3.2 Organisations acquiring near-shore data

The near-shore datasets used were sourced from three organisations; the Council for Geoscience, the South African Navy and Marine Geosolutions (MGS) on behalf of the African Coelacanth Ecosystem Programme (ACEP).

3.2.1 Marine Geoscience Unit (MGU) data

The MGU acquired near-shore data in KwaZulu-Natal have either been collected using Tethys, the Durban MGU's survey vessel or other vessels of opportunity. Differential GPS (DGPS) positioning is used, with the metre-based UTM Zone 36 S co-ordinate system based on a central meridian of 33° E most often while the degree-based geographic co-ordinate system is seldom used. The WGS84 Datum based on the WGS84 Ellipsoid is the standard used for MGU marine survey work, while older work has used the Cape Datum based on the Modified Clarke 1880 Ellipsoid. The 15 MGU acquired near-shore datasets used extend southwards from Kosi Bay to Port Edward in KwaZulu-Natal (Figure 3.1). Appendices 3A to 3D list information about these datasets.

MGU single-beam echo-sounders were initially calibrated with a standard speed of sound in sea water of 1 500 ms^{-1} after considering their operating frequency and pulse widths. This value was then adjusted by measuring a known depth after which the new derived value was programmed into the echo-sounder. As explained in section 2.2.1, the speed of sound in sea water is temperature, salinity and depth dependant. To take these factors into account, a sound velocity probe is lowered to the seabed to allow the average sound velocity to be calculated and programmed into the echo-sounder.

The Cape Town MGU research unit acquired continental shelf data in the 1970's and 1980's which resulted in the establishment of a suitcase database – a catalogued collection of suitcases containing paper cruise records, many of which were not digital (Rogers, 2008, *pers. comm.*). The Marine Geoscience Unit's contour map of the northern Natal Valley, digitised for this project is based on some of these annotated analogue sounding data from unpublished University of Cape Town (UCT) and British Admiralty plotting sheets (Dingle et al., 1978).

3.2.2   South African Navy

South African Navy bathymetric data (Figure 3.2) are of strategic national importance for marine safety and navigation around South Africa (Guy, 2000). The South African Navy is the national custodian of these data (Rheeder, 2001, *pers. comm.*) and the MGU acquired these data via exchange agreements. Data were collected by the South African Navy survey platform, the SAS Protea up to 1993 (South African Navy Hydrographic Office, 1995a). Data are used for the production and supply of paper Admiralty Fair Charts (AFC's), Fair Charts (FC's) and SAN Charts. The South African Navy Hydrographic Office (SANHO) also produces standardised national tide tables for each port, which since July 2007, have been available online (South African Navy Hydrographic Office, 2007). The digitising of AFC and FC sounding data or contour data have been undertaken to add to the MGU's digital bathymetric database. Figure 3.2 shows the 9 South African Navy Admiralty and Fair Chart datasets used and appendices 3A to 3D list information about them.

3.2.3   Marine Geosolutions (MGS)

KwaZulu-Natal based Marine Geosolutions (Pty) Ltd (MGS) surveyed five blocks mapping a total of 23 canyons on the Zululand continental margin (Figure 3.3) aboard the MV Ocean Mariner (Ramsay and Miller, 2006). This was undertaken in March and April 2002 for the National Research Foundation (NRF) funded African Coelacanth Ecosystem Programme (ACEP) with a RESON ® SeaBat ® 8111 multi-beam echo-sounder using differential GPS for positioning (Appendices 3A to 3D) (Ramsay and Miller, 2006).

Figure 3.1. Coloured areas indicating extents of coverage of each of the 15 MGU acquired high-resolution single-beam echo-sounder datasets. The South African Maritime Zones give an indication of seaward extent of each dataset. Little MGU dataset coverage exists beyond 12 nautical miles or 22.2 km and little contiguous data exist beyond 3 nautical miles or 5.5 km.

Figure 3.2. Coloured areas indicating extents of coverage of each of the 9 South African Navy acquired high-resolution single-beam echo-sounder datasets. The South African Maritime Zones give an indication of seaward extent of each dataset. South African Navy dataset coverage exists beyond 24 nautical miles or 44.4 km but little contiguous data exist beyond 12 nautical miles or 22.2 km.

Figure 3.3. Coloured areas indicating the 5 East Coast survey block extents for the ACEP acquired high-resolution multi-beam echo-sounder datasets. The South African Maritime Zones give an indication of seaward extent of each dataset. These datasets offer limited very high resolution coverage extending in these areas beyond 3 nautical miles or 5.5 km and possibly just beyond 6 nautical miles or 11.1 km in the case of Sodwana survey block.

3.3 Areas mapped by the Marine Geoscience Unit (MGU)

Extensive coverage of the near-shore areas of KwaZulu-Natal has been achieved by the MGU since the early 1990's represented by the 14 MGU acquired high-resolution datasets (Figure 3.1), and 11 digitised South African Navy paper chart datasets (Figure 3.2). These digital bathymetric datasets have been used to map the following areas from north to south (Figure 3.4):

- The Maputaland continental shelf including the iSimangaliso Wetland Park, formerly the Greater St. Lucia Wetland Park (GSLWP) covers the shelf from Leven Point to Kosi Bay. It extends from the shoreline out to between 1.9 nautical miles or 3.5 km (Ramsay et al., 2006) and 6 nautical miles or 11.1 km offshore. Continental shelf depths of down to 60 m were initially mapped. The later inclusion of multi-beam data in five additional survey blocks, donated by the African Coelacanth Ecosystem Programme (ACEP), led to some areas being mapped down to maximum depths of approximately 838 m (Green and Uken, 2008) in this dataset (Block 1, Figure 3.4).

- The Richards Bay and Thukela continental shelf covering the area from north of the port of Richards Bay to the Thukela River mouth. It extends from the shoreline out to between 12 nautical miles or 22.2 km and 24 nautical miles or 44.4 km down to depths of approximately 300 m (Block 2, Figure 3.4).

- The Durban continental shelf covering the area from Umhlanga Rocks north of the port of Durban to Brighton Beach south of the port of Durban. It extends from the shoreline out to between 3 nautical miles or 5.5 km and 6 nautical miles or 11.1 km. Continental shelf depths of 200 m are mapped (Block 3, Figure 3.4) using the MGU acquired Durban Bight and Blood Reef datasets.

- The Aliwal Shelf covering the Aliwal Shoal Reef and adjacent continental shelf (Block 4, Figure 3.4) within the Aliwal Shoal Marine Protected Area (MPA) off Scottburgh. It extends from 2.7 nautical miles or 5 km offshore to approximately 6 nautical miles or 11.1 km offshore and has depths ranging from approximately 10 m down to approximately 110 m.

MGU data acquired from digitised South African Navy paper contour maps have been used to produce bathymetric maps of these areas from north to south (Block 5 and 6, Figure 3.4):

- The northern section of the southern KwaZulu-Natal continental shelf covering the area from the Mlazi River mouth to Port Shepstone from the shoreline out to an average of approximately 6.6 nautical miles or 12 km down to a depth of 150 m (Block 5, Figure 3.4). Data were based on Admiralty Fair Chart 18.

- The southern section of the southern KwaZulu-Natal continental shelf covering the area from Port Shepstone to Port Edward from the shoreline out to an average of approximately 7 nautical miles or 13 km down to a depth of 500 m (Block 6, Figure 3.4). Data were based on Admiralty Fair Chart 19.

The near-shore bathymetric dataset metadata are presented in appendices 3A to 3D.

Figure 3.4. MGU near-shore high-resolution contour datasets. These have been produced by the integration of 14 MGU acquired single-beam echo-sounder datasets with 9 digitised South African Navy single-beam echo-sounder Fair Chart and lead line Admiralty Fair Chart datasets along and 2 digitised Admiralty Fair Chart contour datasets and 5 ACEP acquired multi-beam echo-sounder datasets. Contour dataset coverage is approximately 75% contiguous out to approximately 6 nautical miles or 11.1 km with the Richards Bay/Thukela continental shelf dataset extending beyond 12 nautical miles or 22.2 km seawards off the Richards Bay area and beyond 24 nautical miles or 44.4 km seawards off the Thukela River mouth area.

3.4 MGU digitally acquired near-shore datasets

3.4.1 Maputaland continental shelf

NRF Block A, B and C datasets

The Marine Geoscience Unit (MGU) was also data custodian of the National Research Foundation (NRF) funded Innovation Fund Project 24401 between 2002 and 2005. An expert GIS based tool was developed to manage marine resources within the iSimangaliso Wetland Park on the Maputaland coast (Ramsay et al., 2006). Other stakeholders included Marine Geosolutions (Pty) Ltd (MGS), the Oceanographic Research Institute (ORI), Ezemvelo KwaZulu-Natal Wildlife (EKZNW) and Graham Muller Associates (GMA). Bathymetric data was collected by the MGU and MGS between 2003 and 2005 covering Blocks A, B and C, Island Rock and Kosi Bay as well as 2 mile-, 5 mile- and 9 mile reef off Sodwana Bay (Figures 3.5 to 3.7).

The NRF Block A and B bathymetric dataset (Figure 3.5) and Block C bathymetric dataset (Figure 3.6) are spatially separate having been acquired using a RESON ® Navisound 210 ® digital single-beam echo-sounder with a beam-width of 9° aboard the MV Ocean Mariner in 2003 . Positioning was achieved using a Fugro ® OmniStar ® 12 channel differential GPS system using a virtual base station capable of sub-metre accuracy. The maximum measurable depth of the Navisound 210 ® is 600 m (RESON Inc., 2002). The echo-sounder was interfaced to a TSS ® HS50 ® heave compensator to correct vessel movement owing to swell. Data were collected at one second intervals using Navlog Systems ® acquisition with a depth precision of 0.01 m (Ramsay et al., 2006).

This survey covered a distance of 121 km of the northeastern KwaZulu-Natal coast from Leven Point in the south to Kosi Bay in the north and extended for a distance offshore to 3.5 km, covering approximately 420 km^2 of seafloor. Survey speed was 4 to 5 knots with a line spacing of 170 m (Ramsay et al., 2006). Data densities for Block A and B (Figure 3.5) were 1 926.10 records per km^2 (Appendix 3D) with 216 629 anisotropic records covering 112.47 km^2. Data densities for Block C (Figure 3.6) were 1 956.59 records per km^2 (Appendix 3D) with 23 753 anisotropic records covering 12.14 km^2. Data densities were similar to the 2 000 records per

square kilometre of the South African Navy Fair Chart 202 (FC 202) dataset. The use of differential GPS navigation with modern digital single-beam echo-sounder and descriptive metadata confirmed the good quality of these datasets, in addition, they offer the only dataset coverage for the area.

NRF Kosi Bay 2005 dataset

The NRF Kosi Bay bathymetric survey of April 2005 was undertaken in the near shore area of Kosi Bay (Figure 3.5). The processed bathymetry supplemented the adjacently mapped NRF Block A bathymetry to improve the northwestern shallow near shore reef area that was not accessible by the initial survey platform, the MV Ocean Mariner. To accomplish this, the Durban MGU's survey vessel Tethys was used and instrumentation, co-ordinate system and tidal correction were the same as for the NRF Block A, B and C datasets. Data densities of 1 989.15 records per km^2 (Appendix 3D) were achieved by 14 481 anisotropic records covering approximately 7.28 km^2, similar to that of the NRF Block A and B and NRF Block C datasets with similar dataset quality while also offering the only dataset coverage for the area.

NRF Island Rock 2005 dataset

The NRF Island Rock bathymetric survey of April 2005 (Figure 3.6) was undertaken in the near shore area of the Island Rock reef complex in northeastern KwaZulu-Natal located between the NRF Block A and B dataset and the NRF Block C dataset (Ramsay et al., 2006). Survey vessel, instrumentation, co-ordinate system and tidal correction were the same as that used for the Kosi Bay 2005 dataset. Data densities of 104.89 records per km^2 (Appendix 3D) are reflected by 7 597 anisotropic records covering approximately 72.43 km^2, far sparser than that of the NRF Block A and B, the NRF Block C and the Kosi Bay 2005 datasets. Sparser dataset densities make this dataset quality less than that of the other NRF datasets; however it offers the only dataset coverage for the area.

Figure 3.5. Ship tracks for the MGU acquired single-beam echo-sounder datasets covering the NRF Block A and B and Kosi Bay areas (Ramsay et al., 2006).

Figure 3.6. Ship tracks for the MGU acquired single-beam echo-sounder datasets covering the NRF Block C and Island Rock areas (Ramsay et al., 2006).

Sodwana Bay datasets

The Sodwana Bay dataset (Figure 3.7) was integrated from a combination of data sources. The first was collected between Leven Point and Gobey's Point on two separate cruises between 1990 and 1991. The first of these cruises made use of the RV Benguela research vessel from the former Sea Fisheries Research Institute, now Marine and Coastal Management (MCM) using a hull mounted SIMRAD ® EK 120 ® analogue single-beam echo-sounder whose paper chart was annotated every 10 minutes. In addition, the former South African Geological Survey now the Council for Geoscience research ski boat, Geocat with a 12 kHz ELAC ® digital single-beam echo-sounder was used (Ramsay, 1991). The details are shown in table 3.1.

Table 3.1. Vessel and bathymetric transducer deployment details for the Sodwana Bay surveys from 1991 to 1992 (Ramsay, 1991).

Vessel	RV Benguela	GEOCAT
Vessel Owner	Former Sea Fisheries Research Institute	Former South African Geological Survey
Length	44 m	6.4 m
Draught	3 m	0.5 m
Tonnage	560 T	2 T
Transducer Depth	3 m	0.5 m (1991)

Overall, 226 line km were surveyed with a line spacing of 250 m at between 3.5 and 5.5 knots, from depths of 5 m to 100 m. Two coast perpendicular lines to investigate a submarine canyon and dune field (Ramsay, 1991). Navigation was achieved by the JRL 4200 ® GPS with geographic co-ordinates based on the WGS84 Datum (Ramsay, 1991). Software downloaded navigation data at 30 second intervals over an RS 232 link while simultaneously allowing the helmsman to maintain course. Navigation data were converted to then standard metre based South African Latitude of Origin "Lo" 33 co-ordinate system using a central meridian of 33° E based on the Cape Datum using the standard Modified Clarke 1880 Ellipsoid (Ramsay, 1991) by applying these corrections:

WGS84 Datum based latitude – 1.7" or approximately 52.47 m   (Ramsay, 1991)

WGS84 Datum based longitude + 0.8" or approximately 24.69 m   (Ramsay, 1991)

Figure 3.7. Ship tracks for the MGU acquired Sodwana Bay datasets (Ramsay, 1991; Ramsay et al., 2006). The high density closely spaced ship tracks for the digital single-beam echo-sounder coverage of the 2004 NRF Sodwana Bay survey area are seen surrounded by the less dense lower resolution Leven Point to Gobey's Point 1990 to 1991 dataset.

The survey of 25 points by triangulation with two theodolites was used to indicate a mean difference between the GPS and surveyed values of 48 m with the smallest difference of 8 m being established as the most accurate (Ramsay, 1991). Depths with a precision of 0.01 m were reduced to Mean Sea Level (MSL).

The second bathymetric dataset (Figure 3.7) was collected in 2004 and 2005 for the NRF using the MGU's survey boat Tethys at a survey speed of 4 to 5 knots with a line spacing of 75 m over the Sodwana Bay reefs with the same instrumentation as the other NRF datasets (Ramsay et al., 2006). These northern, central and southern Sodwana Bay areas considered together are 9.22 km^2 with 424 648 anisotropic data points producing data densities of 46 057.27 records per km^2 (Appendix 3D) the highest considered in this study.

Earlier data acquired aboard the RV Benguela and the Council for Geosciences Geocat were combined with the newer NRF data to produce one Sodwana Bay dataset.

Red Sands Reef and Ntabende Hill datasets

These datasets cover the continental shelf between Leven Point and Ntabende Hill (Figure 3.8) with 336 line km at 250 m line spacing and were surveyed aboard the RV Benguela and the MGU's Tethys at 4 to 6 knots between 1990 and 1995 (Ramsay, 2000). A 200 kHz Odom ® EchoTrac 3100 ® digital single-beam echo-sounder with a 10° beam angle acquired the bathymetric data with 2 m positioning accuracy from a Trimble ® Navstar ® 12 channel differential GPS system (Ramsay, 2000). Red Sands Reef the southern-most dataset, covers the seafloor in the St. Lucia Marine Reserve Sanctuary between Leven Point and Red Sands. Ntabende Hill, covers the seafloor between Red Sands and Ntabende Hill (Ramsay, 2000). The Red Sands Reef dataset covers an area of 138.27 km^2 with 12 690 anisotropic data points giving data densities of 91.78 records per km^2. The Ntabende Hill dataset covers an area of 75.92 km^2 with 1 051 anisotropic data points resulting in data densities of 13.84 records per km^2 (Appendix 3D). Both were the only datasets for some of the area and thus portions of both were included in the final bathymetric dataset.

Figure 3.8. Ship tracks for the MGU acquired single-beam echo-sounder Red Sands and Ntabende Hill datasets (Ramsay, 2000).

3.4.2   Richards Bay continental shelf

Richards Bay dataset

A total of 1 500 line km was collected at a coarse line spacing of 600 m aboard the MV Ocean Mariner in 1996 in an unusual north-south orientation (Figure 3.9). The echo-sounder was the same as that used for the Red Sands Reef and Ntabende Hill datasets with the same tidal corrections to MSL while positioning made use of real-time differential GPS accurate to within 5 m with the base station positioned on the top of the Richards Bay Port Control Tower with navigation in geographic co-ordinates using the WGS84 Datum (Lord et al., 1996). The original data were converted in ESRI ® ArcGIS ® to the UTM Zone 36 S co-ordinate system. In 2004, Richards Bay National Ports Authority (NPA) hired the Institute of Natural Resources (INR) who approached the MGU to produce a GIS environmental management tool presenting an opportunity for a data quality audit, eventually undertaken by the author (Leuci et al., 2004). Data errors were corrected including positive or zero-value bathymetric data, reducing the dataset size from approximately 130 539 points to its current 128 720 points with a survey area of 482 km^2 giving data densities of 267.05 records per km^2 (Appendix 3D). This dataset intersected a common area with Fair Charts 166 to 168 and 202 along with Admiralty Fair Chart 34.

3.4.1 Durban continental shelf

Durban Bight dataset

This dataset comprised 870 line km of bathymetry with a line spacing of 100 m to 150 m and was collected between Durban Harbour and Umhlanga Rocks in KwaZulu-Natal in 1999 (Figure 3.10) using the same echo-sounder as the Richards Bay dataset with a boat mounted motion reference unit correcting for heave and swell effects (Miller, 2000; Richardson, 2005). Tidal correction to Mean Sea Level (MSL) was done and positioning was achieved with the same differential GPS system and co-ordinate system used for the NRF datasets (Miller, 2000; Richardson, 2005). The final processed dataset of 282 596 data points included the originally acquired Durban Bight data with additional Durban Harbour, Vetch's Pier and Limestone Reef (Richardson, 2005). This dataset was found to cover 139.74 km^2 giving data densities of 2 022.30 records per km^2 (Appendix 3D), similar to that of the NRF acquired datasets. It

intersected the MGU Blood Reef and Fair Chart 165 datasets and offers the best coverage.

Figure 3.9. Ship tracks for the MGU acquired single-beam echo-sounder Richards Bay continental shelf dataset (Lord et al., 1996).

Figure 3.10. Ship tracks for the MGU acquired single-beam echo-sounder Durban Bight, Durban Outer Shelf and Blood Reef datasets (Miller, 2000; Richardson, 2005; Cawthra, 2006).

Durban Outer Shelf dataset

This alternating coast parallel and perpendicular survey lines were surveyed at 5 knots in 2006 between the Durban harbour approaches and the southern extent of the Blood Reef survey area. Depths of 45 m on the eastern boundary (Figure 3.10) extended down to maximum depths of almost 200 m, 10 km offshore. Line spacing was 2 km and a RESON ® Navisound 210 ® dual frequency single-beam echo-sounder with a beam-width of 9° was used (RESON Inc., 2002) with depths corrected to Mean Sea Level. Positioning was achieved using a 12 channel, CSI Wireless ® DGPS Max ®, differential GPS capable of a 1.2 m horizontal measurement accuracy and positional update rate of 5 Hz. An embedded SBX dual channel minimum shift key (MSK) demodulator gives the CSI Wireless ® DGPS Max ® the capability of receiving differential GPS corrections from medium frequency radio beacons allowing it to apply real time differential correction to the GPS signal it simultaneously receives (CSI Wireless Inc., 2005). This dataset traverses 25 km with 15 651 anisotropic data points giving 626 records per line km (Appendix 3D).

Blood Reef dataset

The Blood Reef dataset (Figure 3.10) was surveyed to extend the Durban Bight dataset coverage in 2006 and was part of the Blood Reef geophysical survey programme (Cawthra, 2006). It extends from the Durban Harbour southern breakwater to Brighton Beach in the south. Bathymetry was collected with the same echo-sounder as the Durban Outer Shelf bathymetric dataset and reduced to Mean Sea Level (MSL) with the same positioning system and co-ordinate system as that of the Durban Bight bathymetric dataset (Cawthra, 2006). At 19.33 km^2 this dataset covers a smaller area than the Durban Bight dataset with 343 149 anisotropic data points giving a data densities of 17 752.15 records per km^2 (Appendix 3D) and is much higher than the northern, adjacent Durban Bight dataset and the second highest considered in this study. The data intersects the MGU Durban Bight and the South African Navy Fair Chart 165 datasets and offers the best coverage available.

3.4.2   Aliwal Shoal and adjacent shelf dataset

The Aliwal Shoal bathymetric dataset was acquired in March 2001 to provide the first accurate coverage of this previously unmapped reef complex off Scottburgh to be used by the broader scientific community (Bosman et al., 2005). Bathymetric data were surveyed at a speed of 2.5 knots with a 120 m line spacing for a total of 266 line km using the same echo-sounder as the Durban Bight bathymetric dataset with data corrected to Mean Sea Level (Bosman et al., 2005). Positioning made use of the same differential GPS system as that of the Durban Bight dataset and used the same co-ordinate system (Bosman et al., 2005). An additional 108 line km of boomer seismic data were acquired coast-perpendicular at a survey speed of 5 knots with a 1 km line spacing resulting in 1 data point every 1.3 m on the seafloor (Bosman, 2004). *Kriging*, using an octant search, a grid interval of 110 metres and a search radius of 3000 metres was used to interpolate 68 646 usable data points derived from the integration of bath datasets to produce a bathymetry map (Bosman, 2009, *pers. comm.*). The Aliwal Shoal and adjacent shelf dataset (Figure 3.11) was obtained by the author as an integrated grid produced from the single-beam echo-sounder and seismically-derived bathymetric datasets and covers an area of 60.12 km^2 with its 43 675 data points giving data densities of 726.46 records per km^2 (Appendix 3D). Its echo-sounder bathymetric component offers the best coverage of the area; however bathymetric resolution by the seismic dataset is poor, warranting caution upon integration into the final dataset. Nevertheless the regional 1:3 000 000 mapping scale of the final dataset was anticipated to filter possible artefacts.

Figure 3.11. The Aliwal Shoal and adjacent shelf bathymetric dataset. Ship track, single-beam echo-sounder data, acquired in 2001 (Bosman et al., 2005) were integrated with seismically derived bathymetric data to produce one bathymetric grid dataset.

3.5 MGU digitised near-shore contour maps

Bathymetric contour maps were produced between Port St. Johns and Durban from these four paper South African Navy Admiralty Fair Charts (AFC's) 17 to 21, 23 and 29 (Birch, 1981). Since the four AFC's were not in the MGU digital database, these contour datasets were digitised and geo-referenced by the author with geographic co-ordinates based on the Cape Datum with the Modified Clarke 1880 Ellipsoid.

The four bathymetric AFC datasets where acquired using a lead line between 1924 and 1927 with original depths in fathoms or English feet and tidal correction was the same as for all South African Navy datasets (South African Navy Hydrographic Office, 1995a). Available metadata suggested the same positioning, bathymetric acquisition instrument and map datum as Admiralty Fair Chart 34 (Guy, 2000).

3.5.1 Mlazi River to Port Shepstone continental shelf dataset

This dataset was digitised from Admiralty Fair Chart 18 (AFC 18) (Figure 3.12). It covers an area of 238.2 km^2 with 5 324 anisotropic data points giving data densities of 22.35 records per km^2 (Appendix 3D). This dataset offered the best coverage of the area except for a small intersection with the Aliwal Shoal and adjacent shelf dataset.

3.5.2 Port Shepstone to Port Edward continental shelf dataset

This dataset was digitised from Admiralty Fair Chart 19 (AFC 19) (Figure 3.12). It covers an area of 1 158.95 km^2 with 28 982 anisotropic data points giving data densities of 25 records per km^2 (Appendix 3D). Again, this dataset offered the best coverage of the area.

Figure 3.12. MGU digitised Mlazi River to Port Shepstone and Port Shepstone to Port Edward contour datasets (Birch, 1981). The Mlazi River to Port Shepstone contour dataset was based on the Admiralty Fair Chart 18 dataset while the Port Shepstone to Port Edward dataset was based on the Admiralty Fair Chart 19 dataset. The bathymetric data from these Admiralty Fair Charts were not included in the MGU digital database.

3.6 MGU digitised near-shore datasets

3.6.1 Maputaland continental shelf

Fair Charts 200, 204 and 205 (FC 200, FC 204 and FC 205) datasets

Fair Chart 200 (FC 200) is the Jesser Point to Ponto Du Ouro Southern Sheet which only extends north to Lala Nek (Figure 3.13). Fair Chart 204 (FC 204) is the Cape St. Lucia to Jesser Point Northern Sheet while Fair Chart 205 (FC 205) is the Cape St. Lucia to Jesser Point Southern Sheet (Figure 3.13). Acquisition vintages indicated depths were measured in metres with a single-beam echo-sounder, assumed to be an analogue device in the absence of better metadata. Fair Chart was 200 acquired in 1992 and the other two in 1993. The collected data for all these Fair Charts were used to produce paper charts to a scale of 1:75 000 (South African Navy Hydrographic Office, 1995a). The positioning method was unknown, however, according to available metadata, hydrographic surveys undertaken after 1960 for the production of South African Navy Fair Charts made use of electronic positioning systems such as DECCA navigator or possibly NAVSAT (Guy, 2000). The original scanned raster map used the Cape Datum with the Modified Clarke 1880 Ellipsoid and the UTM Zone 36 S co-ordinate system (South African Navy Hydrographic Office, 1995a). All three datasets were included in one final dataset to extend the NRF Innovation Fund Maputaland Dataset. Fair Charts 200, 204 and 205 together cover approximately 5 691.35 km^2 with 35 859 anisotropic records producing data densities of 6.3 records per km^2 (Appendix 3D). Dataset densities are much lower than MGU datasets' densities, but higher than the available deep-water dataset densities, thus resulting in their prioritisation for use. These datasets intersect with the MGU and ACEP datasets.

Figure 3.13. MGU digitised South African Navy Fair Chart 200, 204 and 205 Maputaland datasets (South African Navy Hydrographic Office, 1992; South African Navy Hydrographic Office, 1993b; South African Navy Hydrographic Office, 1993c).

3.6.2   Richards Bay continental shelf

Fair Charts 166, 167 and 168 (FC 166, FC 167 and FC 168) datasets

The Fair Charts 166, 167 and 168 (FC 166, FC 167 and FC 168) cover the Richards Bay area (Figure 3.14). Acquisition vintages of 1981 for all three datasets derived from available metadata suggested the DECCA or NAVSAT positioning system was used, while an analogue single-beam echo-sounder bathymetric acquisition instrument was assumed in the absence of better metadata. Depths were originally acquired in metres (South African Navy Hydrographic Office, 1995a; Kampfer, 2007). The data collected for FC 166 and FC 167 were used to produce paper charts at a scale of 1:20 000 while those for FC 168 were used to produce a paper chart at a scale of 1:40 000 (South African Navy Hydrographic Office, 1995a). The original map projection for the raster map of FC 167 used the Cape Datum with the Modified Clarke 1880 Ellipsoid and the UTM Zone 36 S co-ordinate system (South African Navy Hydrographic Office, 1995a). A point vector dataset was digitised from the FC 167 raster dataset. The datum of FC 166 and FC 168 were unknown as they were obtained digitally in a geographic co-ordinate system. However comparison with The MGU's Richards Bay Shelf and the FC 167 datasets established them to be in the WGS84 Datum. Fair Chart 166 covers approximately 147.81 km^2 with 14 135 anisotropic records producing a data density of 95.63 records per km^2 (Appendix 3D). Fair Chart 167 covers an area of approximately 85.37 km^2 and consists of 9 409 anisotropic records producing a data density of 110.21 records per km^2 (Appendix 3D). Fair Chart 168 covers approximately 86.95 km^2 with 3 448 anisotropic records producing a data density of 39.65 records per km^2 (Appendix 3D). These datasets overlap with the MGU Richards Bay dataset.

Figure 3.14. MGU digitised South African Navy Fair Chart 166, 167 and 168 Richards Bay datasets and Admiralty Fair Chart 34 and Fair Chart 202 Thukela Shelf datasets (South African Navy Hydrographic Office, 1911; South African Navy Hydrographic Office, 1981b; South African Navy Hydrographic Office, 1981c; South African Navy Hydrographic Office, 1981d; South African Navy Hydrographic Office, 1993a).

3.6.3   Port Durnford to the Thukela River continental shelf

Fair Chart 202 (FC 202) dataset

Fair Chart 202 was a wreck investigation for the M.V. Petingo in the Richards Bay area (Figure 3.14). Acquisition vintage of 1993 suggested that the DECCA or even the NAVSAT positioning system was used (Guy, 2000). The absence of better metadata once again led to the assumption of an analogue single-beam echo-sounder bathymetric acquisition instrument with depths in metres (South African Navy Hydrographic Office, 1995a; Kampfer, 2007). A large scale paper chart at a scale of 1:3 000 was produced to aid wreck investigation. The original vector dataset was obtained digitally in a geographic co-ordinate system but the datum and ellipsoid were unknown. However comparison with the MGU's Richards Bay and AFC 34 datasets established it as being in the WGS84 Datum. Fair Chart 202 covers an area of approximately 0.668 km^2, a small area compared to the other Fair Charts, consisting of 1 336 anisotropic records producing data densities of 2 000 records per km^2 (Appendix 3D), denser than the other Fair Charts reviewed. This Fair Chart's dataset densities and its newer vintage resulted in its inclusion. This dataset overlaps the MGU Richards Bay and Admiralty Fair Chart 34 datasets.

Admiralty Fair Chart 34 (AFC 34) dataset

Admiralty Fair Chart 34 covers the area from Port Durnford to the Thukela River mouth in the study area (Figure 3.14). As with all Admiralty Fair Charts, depths were measured with a lead line (Guy, 2000) originally in fathoms with a paper chart scale of 1:63 342 (South African Navy Hydrographic Office, 1995a). The positioning method is unknown, although from available metadata, it was deduced that triangulation, daytime astronomical fixes using horizontal sextant angles or dead reckoning were used (Guy, 2000). The dataset was initially obtained digitally in a geographic co-ordinate system. The original map projection used is thus unknown but the vintage from metadata suggested that the Cape Datum based on the Modified Clarke 1880 Ellipsoid was most likely. Depth conversion from fathoms to metres were required (Kampfer, 2007). AFC 34 covers an area of approximately 2 375 km^2 and consists of 25 128 anisotropic records producing data densities of 10.58 records per km^2 (Appendix 3D). This was

the only near shore dataset mapping this part of the continental shelf, which resulted in its inclusion in this study; however it does overlap slightly with the MGU's Richards Bay and Fair Chart 202 datasets.

3.6.4 Durban continental shelf

Fair Chart 165 (FC 165) dataset

Fair Chart 165 was a survey of the Durban Port approaches (Figure 3.15). Its acquisition vintage of 1981 suggested the same positioning system and bathymetric acquisition instrument type as the preceding Fair Charts (Guy, 2000) with depths measured in metres to produce a paper chart at a scale of 1:20 000 (South African Navy Hydrographic Office, 1995a). The original scanned raster map used the Cape Datum with the Modified Clarke 1880 Ellipsoid and the UTM Zone 36 S co-ordinate system (South African Navy Hydrographic Office, 1995a). The Fair Chart 165 dataset covers an area of approximately 63.82 km^2 and consists of 4 016 anisotropic records producing data densities of 62.93 records per km^2 (Appendix 3D). It overlaps with the MGU's Durban Bight and Blood Reef datasets.

Figure 3.15. MGU digitised South African Navy Fair Chart 165 Durban dataset (South African Navy Hydrographic Office, 1981a).

3.7 ACEP digitally acquired multi-beam datasets

3.7.1 Maputaland continental shelf

Five datasets in five survey blocks (Figure 3.3) were acquired for the African Coelacanth Ecosystem Programme (ACEP) to map all known submarine canyons between Leven Point and Island Rock on the northern KwaZulu-Natal continental shelf and slope (Ramsay and Miller, 2006). Marine Geosolutions (MGS) managed the bathymetric data acquisition aboard the survey vessel, the MV Ocean Mariner (Miller and Ramsay, 2002) in March and April 2002 using a RESON ® SeaBat 8111 ® multi-beam echo-sounder with a RESON 6042 ® multi-beam acquisition, processing and presentation system (Ramsay and Miller, 2006). The echo-sounder is a 100 kHz system with 101 different 1.5^o by 1.5^o beams producing a 150° bathymetric swath of up to 7.4 times the water depth between 5 m and 150 m and has a 1 000 m depth measuring capability (RESON Inc., 2006b). It was interfaced to a TSS ® DMS05 ® motion sensor to correct for vessel heave, pitch and roll while a Meridian ® Surveyor ® gyrocompass interfaced to the echo-sounder provided accurate electronic vessel heading information (Ramsay and Miller, 2006). Positioning used a Fugro ® Starfix ® 12 channel Trimble differential GPS with an update rate of 10 Hz and a virtual base station solution of less than 5 seconds with sub-metre horizontal measurement accuracy which was based on the RTCM SC-1.04 version 2.0 format (Miller and Ramsay, 2002). Thirty-six gigabytes (GB) of raw multi-beam bathymetric data were collected from which an ASCII grid was derived (Miller and Ramsay, 2002). Depth values were reduced to Mean Sea Level (MSL) in the CARIS ® HIPS ® multi-beam software package using Richards Bay tidal data from the South African Navy (Miller and Ramsay, 2002). Precision was 0.001 m. These data allowed new canyons to be mapped and an accurate GIS was produced for future exploration planning (Ramsay and Miller, 2006). These datasets offer the highest resolution, largest area multi-beam seafloor coverage on the South African East Coast.

Ten metre isotropic point spacing is common to all these survey block multi-beam datasets from the binning process. The northernmost Mabibi survey block (Figure 3.16) covers an area of 34.42 km^2 with 321 832 data points producing the lowest data densities of 9 350.15 records per km^2 (Appendix 3D), while south of this, the largest, Sodwana survey block (Figure 3.17)

covers an area of 118.71 km^2 with 1 142 901 data points producing higher data densities of 9 627.67 records per km^2 (Appendix 3D). Just south of Jesser Point, the Diepgat survey block (Figure 3.18) covers an area of 27.15 km^2 with 261 089 data points producing similar data densities to the Sodwana survey block of 9 616.54 records per km^2 (Appendix 3D), while south of the Diepgat survey block, the Leadsman survey block (Figure 3.19) covers an area of 28.64 km^2 with 274 115 data points producing data densities between those preceding of 9 571.05 records per km^2 (Appendix 3D). The southernmost Leven survey block (Figure 3.20) covers an area of 40.16 km^2 with 391 222 data points producing the highest data densities of all survey blocks of 9 741.58 records per km^2 (Appendix 3D). These datasets intersect with MGU acquired NRF datasets and Fair Charts 200, 204 and 205.

Figure 3.16. ACEP acquired multi-beam echo-sounder Mabibi survey block dataset (Ramsay and Miller, 2006). The dataset is a grid derived from multi-beam data whose acquisition and processing was managed by MGS for the ACEP Programme.

Figure 3.17. ACEP acquired multi-beam echo-sounder Sodwana survey block dataset (Ramsay and Miller, 2006). The dataset is a grid derived from multi-beam data whose acquisition and processing was managed by MGS for the ACEP Programme.

Figure 3.18. ACEP acquired multi-beam echo-sounder Diepgat survey block dataset (Ramsay and Miller, 2006). The dataset is a grid derived from multi-beam data whose acquisition and processing was managed by MGS for the ACEP Programme.

Figure 3.19. ACEP acquired multi-beam echo-sounder Leadsman survey block dataset (Ramsay and Miller, 2006). The dataset is a grid derived from multi-beam data whose acquisition and processing was managed by MGS for the ACEP Programme.

Figure 3.20. ACEP acquired multi-beam echo-sounder Leven survey block dataset (Ramsay and Miller, 2006). The dataset is a grid derived from multi-beam data whose acquisition and processing was managed by MGS for the ACEP Programme.

3.8 KwaZulu-Natal deep-water datasets and the acquiring organisations

The regional component of this study required the investigation of lower resolution deep-water datasets from six sources with the eventual selection of three. The Cape Town MGU research collaboration produced the contour map and the accompanying physiographic provinces of the northern Natal Valley after Dingle et al. (1978) from which digitised contour data were derived (Figure 3.21). The South African Navy provided the digitised point SAN Chart data (Figure 3.22). The National Oceanographic and Atmospheric Administration's (NOAA) and National Geophysical Data Centre (NGDC) supplied the freely available GEODAS ship track dataset (Figure 3.23) and the ETOPO5 5-minute grid based dataset (Figure 3.24). The Smith and Sandwell version 8.2 (Figure 3.25) was a 2-minute Mercator projected dataset available freely from the SCRIPPS Institution of Oceanography at the University of California, San Diego. The British Oceanographic Data Centre (BODC) supplied the freely available GEBCO 1-minute grid based dataset (Figure 3.26).

3.8.1 Digitised northern Natal Valley contour dataset

The northern Natal physiographic provinces after Dingle et al. (1978) and related bathymetry were considered authoritative for the deep-water bathymetry for this work. This dataset (Figure 3.21) was the first deep-water dataset examined. The bathymetric contours this dataset are based upon were produced from unpublished data sourced from the University of Cape Town and British Admiralty bathymetric plotting sheets (Dingle et al., 1978). The contour map was scanned as two raster images. Both were geo-referenced using geographic co-ordinates based on the Cape Datum using the standard Modified Clarke 1880 Ellipsoid. Contours were digitised discontinuously at scales between 1:1 000 000 and 1:250 000 in ESRI ® ArcGIS ®. A depth-value coded polyline shape file was created from the discontinuously digitised contours. From these, a depth-value coded point shape file was created. Depths had a precision of 1 metre. The digitised data were anisotropic with areas on the Mozambique Ridge and deep ocean basin having sparse, irregular data densities varying from 0.02 to 1 point per km^2.

Figure 3.21. MGU digitised deep-water dataset based on the northern Natal Valley contour map (Dingle et al., 1978). This dataset coverage has been excluded in areas of better near-shore dataset coverage.

3.8.2   Digitised South African Navy SAN Chart dataset

The SAN Chart data are a collection of digital data from various SA Navy datasets (Figure 3.22). The acquisition method was unknown but being of SA Navy Origin it is reasonable to assume that a mixture of lead line and single-beam echo-sounder transducers were used to collect the data. Positioning was unknown but tests with known datasets indicated the use of a WGS84 Datum. Depth precision was 0.1 m. The sparse deep-water coverage resulted in its exclusion.

3.8.3   GEODAS ship track dataset

GEODAS (GEOphysical DAta System) is the National Geophysical Data Centre (NGDC) interactive database for geophysical data searches, including, seismic, magnetic, gravitational, gridded elevation and, ship track multi- and single-beam bathymetry. The GEODAS database is available online for free download or on DVD, available for purchase (Metzger and Campagnoli, 2007). In both cases GEODAS navigation software is used to extract desired data from the database. This project initially required the extraction of single-beam and multi-beam ship track bathymetric data (Figure 3.23) using geographic co-ordinates with a WGS84 Datum. Bathymetric transducers and positioning methods used to acquire all the data in the study area were not known. However, vintage suggested possibly lead lines, single-beam and multi-beam echo-sounders being used for bathymetry while early horizontal sextant systems, analogue systems such as DECCA as well as more recent GPS and perhaps differential GPS could have been used for positioning. The NGDC's GEODAS dataset has been known to include errors which span a lack of control on data quality to minimise the unknown inclusion of raw, unprocessed bathymetric data. (Chandler and Wessel, 2008). Currently no mechanism for worldwide raw data sharing and correction for the prevention of error correction duplication exists and this, combined with the NGDC's role as a data library in limiting data revision and correction to source institutions does not easily facilitate peer review mechanisms (Chandler and Wessel, 2008). However this disadvantage is offset firstly against this existence of archived NGDC data and secondly against the cost of data acquisition in unmapped remote areas (Chandler and Wessel, 2008). The GEODAS ship track bathymetry was nevertheless known to have been used in the development of the Smith and Sandwell satellite derived

bathymetry (Smith and Sandwell, 1997; Sandwell and Smith, 2000) and the GEBCO dataset (GEBCO Task Group, 2003). Removal of inaccurate GEODAS ship track bathymetry during the development of the Smith and Sandwell satellite derived bathymetry was also achieved (Smith and Sandwell, 1997). The establishment of the contour map of the northern Natal Valley after Dingle et al. (1978) as authoritative over most of the deep-water region in this study, in conjunction with the use of the GEODAS data in both the Smith and Sandwell satellite derived bathymetry and possibly the GEBCO datasets, resulted in the GEODAS data being discarded.

Figure 3.22. MGU digitised South African Navy SAN Chart KwaZulu-Natal deep-water dataset (South African Navy Hydrographic Office, 1995b). This dataset coverage has been excluded in areas of better near-shore dataset coverage.

Figure 3.23. GEODAS ship track deep-water KwaZulu-Natal dataset (Metzger and Campagnoli, 2007).

3.8.4   ETOPO5 5-minute global gridded dataset

The Earth Topography 5-minute global gridded dataset (ETOPO5) seen in figure 3.24 was the first freely available dataset to be considered for this project. The National Geophysical Data Centre (NGDC) is the custodian of these data. Numerous data sources listed in Appendix 3E were assembled in 1988 into a global 5-minute or 9 260 m grid (Moore and Eakins, 2009). The digital bathymetry was based on Digital Data Base 5-minute (DBDB5) a digital US Navy computer interpolated database from existing ocean contour maps in the 1980's (Olsen, 2008a). This was in turn based on the Digital Data Base Variable Resolution (DBDBV) which at the time consisted of data of only 5-minute resolution and is now of 0.5-, 1-, 2- and 5-minute resolution (Olsen, 2008b). True 5-minute (approximately 9 260 m) latitude and longitude resolutions are encountered over ocean floors, and the well covered areas of the USA, Europe, Japan and Australia, but up to 1° (approximately 111 120 m) is the norm in other data deficient areas (Moore and Eakins, 2009). The vertical depth resolution at each grid point is approximately 1 m in the well covered areas, whereas vertical resolutions of a few metres, even to as much as 150 m may be encountered in poorly covered areas with bathymetric detail found to be sparse in areas shallower than 200 m (Moore and Eakins, 2009). In addition, the interpolation algorithm used by the US Navy to create the oceanic grid (DBDB5) was assigned an upper bathymetric cut-off value of 10 m with all shallower data designated as on-land; all oceanic bathymetric data were then coded at 1 m or deeper (Moore and Eakins, 2009).

The original transducers used to acquire the data the ETOPO5 dataset is based on are unknown, but could possibly have included lead lines and single-beam echo-sounders and perhaps some early multi-beam echo-sounders. The geographic co-ordinates were initially assumed to be based on a WGS84 Datum, however it was subsequently established that the reference datum was older than WGS88 or WGS84 possibly even a sphere, as opposed to an ellipsoid with depth values measured relative to Mean Sea Level (MSL) (Sloss, 2001, *pers. comm.*). Dataset vintage, co-ordinate system referencing to a sphere and, not more accurately to an ellipsoid, and the existence of more recent, accurate and precise freely available data have resulted in the exclusion of this dataset from this study.

Figure 3.24. ETOPO5 5-minute gridded dataset for KwaZulu-Natal (Moore and Eakins, 2009). Note the areas adjacent to the coastline where better near-shore dataset coverage is available, resulting in the exclusion of ETOPO5 data in these areas.

3.8.5   Smith and Sandwell 2-minute bathymetric dataset

The Smith and Sandwell 2-minute satellite derived bathymetry version 8.2 covering the study area was one of the two freely available datasets (the GEBCO gridded dataset was the other) evaluated for the deep offshore areas (Figure 3.25). The dataset is calculated from satellite altimeter data and derived from gravity anomaly (geoid height) measurements (Marks and Smith, 2006). The dataset is based on a Mercator projection spanning 72° N to 72° S using the WGS84 Ellipsoid with geographic co-ordinates and a longitude sampling of 2-minutes (3 704 m or 0.03333^{o}). The Mercator projection results in an increasing latitude sampling distance with latitude and becomes infinite at the poles. Increased areas at higher latitudes were found to spread the correspondingly increased satellite track density at higher latitudes to make data densities more uniform (Marks and Smith, 2006). Grid based bathymetric value location was not possible resulting in individual pixels being assigned bathymetric values (Marks and Smith, 2006). Bathymetric precision was 1 m. The points constrained by ship track and multi-beam bathymetry were coded to the nearest odd integer while the grid points based on bathymetry predicted from gravity were coded to the nearest even integer (Smith and Sandwell, 1997; Sandwell and Smith, 2000) providing a method of separating the two. Ongoing removal of inaccurate ship track data, some of which included the NGDC's GEODAS data, have led to dataset improvements (Smith and Sandwell, 1997; Marks and Smith, 2006). The process used to create the global bathymetry dataset is given in Appendix 2A. In areas of sparse ship track coverage outside the preferred 20 km to 200 km waveband, predicted bathymetry can be assumed to be inaccurate unless constrained by ship track data (Sandwell and Smith, 2000). In addition areas of thick sediment infilling have been established to make the predicted bathymetry unreliable (Sandwell and Smith, 2000). Also, within the established waveband, sea surface roughness is known to affect the accuracy of predicted bathymetric measurements and large seas, common in the study area would affect sea surface roughness introducing these errors. Other global bathymetric grids derived from this dataset and are listed in table 3.2.

Table 3.2. Global bathymetric grids as they apply to the study area. All except one are based on the Smith and Sandwell bathymetry predicted from satellite gravity. The only grid not based on Smith and Sandwell data, the GEBCO grid is included as it was one of the grids reviewed (Marks and Smith, 2006). The last column indicates dataset components applying to the study area only.

Dataset Name	Spacing	Node Type	Projection	Coverage	Deep-water data for the study area based on
Smith and Sandwell	2' longitude	Pixel	Mercator	72° N to 72° S	Satellite gravity
GINA	30"	Pixel	Geographic	Global	Smith and Sandwell
ETOPO2	2'	Grid	Geographic	Global	Smith and Sandwell
DBDB2	2'	Grid	Geographic	Global	Smith and Sandwell below depths of 1 000 m
GEBCO	1'	Grid	Geographic	Global	Mostly 500 m hand-drawn contours at scale of 1:10 000 000
S2004	1'	Grid	Geographic	Global	Smith and Sandwell below depths of 1 000 m

Detailed individual evaluation of each grid was undertaken by Marks and Smith (2006) which led to the conclusion that the original Smith and Sandwell data were probably the best freely available global bathymetric grid. It had been found that both the DBDB2 and ETOPO2 datasets are interpolated grids that smoothed the original data into a grid which limited sharp feature resolution (Marks and Smith, 2006). Additionally, ETOPO2 was found to be problematic since its grid node bathymetric values were incorrectly registered in longitude and latitude during assembly resulting in a north-east shift of topographic features (Marks and Smith, 2006). DBDB2 was found to contain additional high-resolution survey data with errors while the GINA grid had also been smoothed (Marks and Smith, 2006). An unpublished S2004 grid was also available, consisting of GEBCO data in regions shallower than 200 m as well as north of 72° N and south of 72° S and Smith and Sandwell data in regions deeper than 1 000 m as well as south of 70° N and north of 70° S with a blend of both between 200 m and 1 000 m deep on a 1-minute grid with geographic co-ordinates (Marks and Smith, 2006). However little information on the control by use of ship track data of the GINA, ETOPO2, DBDB2 and S2004 grids could be established whereas both the GEBCO and Smith and Sandwell data included such information (Marks and Smith, 2006).

Figure 3.25. Smith and Sandwell 2-minute gridded dataset for KwaZulu-Natal (Smith and Sandwell, 1997). Note the areas adjacent to the coastline where better near-shore dataset coverage is available, resulting in the exclusion of Smith and Sandwell data in these areas.

3.8.6 GEBCO 1-minute bathymetric grid dataset

The GEBCO bathymetric grid consists of data collected from various global organisations (Appendix 3F). A 1- by 1-minute (1 852 m at the equator) worldwide grid was assembled and the oceans divided up as represented in figure 3.26. However, the 1-minute E-W distances shorten with increasing latitude from the equator with the resultant longitudinal separation distance of the eastern and western extents found to be cos(latitude) x 1 852 m which applies from the Equator up to approximately 72° latitude (Goodwille, 2004).
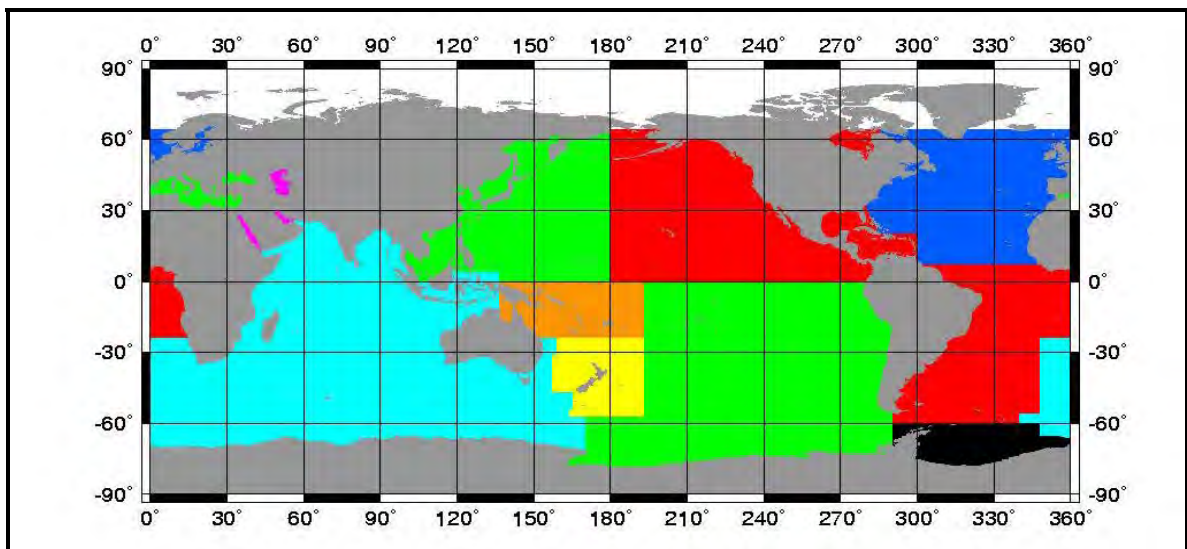
Figure 3.26. Components of the GEBCO 1-minute global bathymetric grid (GEBCO Task Group, 1997). **Cyan**: Indian Ocean (KwaZulu-Natal marine environment location). **White**: Arctic Ocean (64° N to North Pole). **Red**: South Atlantic, NE Pacific, Gulf of Mexico, Sections of North Atlantic and Hudson Bay. **Green**: NW and SE Pacific, Mediterranean Sea, Black Sea. **Black**: Weddell Sea. **Dark Blue**: North Atlantic and Baltic Sea. **Magenta**: Red Sea, Caspian Sea and Persian Gulf. **Orange**: Equatorial Western Pacific. **Yellow**: New Zealand Waters.

Gridding areas were made manageable through division into sub-grids of 10° by 10° with additional 5° overlaps to smooth out edge matching irregularities with adjacent grids. This gives a set of sub-grids of 20° by 20° (Goodwille, 2004). The following data were then input into the grid:

- Digitised GEBCO Digital Atlas (GDA) bathymetric contours (considered authoritative) based on available digital contour data and digitised paper contour maps at a scale of 1:10 000 000 at a contour interval of 500 m;

- Land elevations from the GLOBE database;

- Coastlines (0 metres) from the WVS database at 1:1 000 000 scale (not used as the KwaZulu-Natal coastline for the integrated GIS contour dataset);

- Antarctic coastlines from the SCAR database;

- Additional shallow-water contours, echo-sounding or swath bathymetry survey data (swath bathymetry unlikely in KwaZulu-Natal);

- Additional contours in featureless areas;

- Additional individual echo-soundings

Where multiple bathymetric values existed in a 1- by 1-minute bin for a given 1- by 1-minute grid point at the bin centre, the median value was assigned to the grid point thus filtering spurious bathymetry, smoothing the grid and reducing its computation time. Any empty grid points remained empty until filled by the surface-fitting and interpolation of the gridding process (Goodwille, 2004). The gridding programme (the surface command in Wessel and Smith's GMT) performed the surface fitting using 3-D bi-cubic spline under tension to pass the surface to within 1 m of the input bathymetric values and then interpolate a bathymetric value for every grid point on the surface. The 5° overlap between each adjacent 10° by 10° sub-grid minimised adjacent sub-grid overlap errors. Adjusting the surface optimally to fit the input bathymetry is known as its tension: a low tension produces a stiffer surface tending to bypass some input data; a high tension produces a surface tending to oscillate as it attempts to pass all input data values (Goodwille, 2004). The extremes are a smooth or bumpy surface with somewhere in-between being desirable. The resulting grid was compared to the GEBCO Digital Atlas (GDA) contours, considered authoritative, consisting mostly of standard 500 m intervals and in rare cases 200 m and 100 m (Goodwille, 2004).

Artefacts occurred, mostly as overshoots at the summits of high topography (seamounts, ridges and continental shelves) where sparse shallow-water data did not adequately constrain the algorithm and at the foot of such features where the standard GEBCO intervals of 500 m were insufficient to constrain the surface-fitting algorithm. Featureless areas such as abyssal plains, sediment fans, wide continental shelves and basins also produced erroneous bathymetry. Overshoots and erroneous bathymetry in featureless areas were corrected by additional digital sounding data, digitizing analogue sounding data, using digital contours or digitizing analogue contours where these data were available (Goodwille, 2004). Minor errors from mislabelled contour values and isolated poor quality bathymetry were easily removed. The GEBCO Digital Atlas (GDA) had concentrated on deep water bathymetry work with standard 500 m contour intervals from 500 m down to abyssal depths with occasional 200 m and 100 m contours (Goodwille, 2004). The GDA tended to bias the gridding process to produce a gridded bathymetry at intervals known as terracing (Goodwille, 2004). The grid is based on the WGS84 Datum and Ellipsoid with geographic co-ordinates and a longitude and latitude precision of 1-minute (1 852 m at the Equator or 0.01667^{o}) with depth precision of 1 m.

GEBCO Sheet G.08 (Cyan, figure 3.26) is the main input for the part of the GEBCO dataset covering the study area (Figure 3.27). Depths are in corrected metres using Carter's Tables with 1 m precision using the WGS84 Datum with geographic co-ordinates (GEBCO Task Group, 2003). The technical development details along with the numerous data sources of this sheet are given in Appendix 3F. It is assumed that extra contours and sounding data used to develop the worldwide GEBCO 1- by 1-minute grid would be different from those sources listed in Appendix 3F as GEBCO Sheet G.08 sources. The Sheet G.08 scale is 1:1 000 000 consisting of the World Vector Shoreline (WVS) for the zero metre land boundary with standard GEBCO 500 m contour intervals, a 200 m contour in places and on some wide shelves locally, a 100 m contour (GEBCO Task Group, 2003).

Given the narrowness of the KwaZulu-Natal continental shelf between the southern KwaZulu-Natal border and Durban as well as between Cape St. Lucia and Kosi Bay, it can be concluded that there is unlikely to be a 100 m contour on GEBCO Sheet G.08. This then implies that the bathymetry down to the shelf edge, at approximately 100 m as assumed by researchers, is not covered by GEBCO Sheet G.08 and bathymetry up to as shallow 200 m may be covered by the GEBCO Sheet G.08. Future work needs to establish if any other input

data to the GEBCO worldwide bathymetric grid were included in addition to GEBCO Sheet G.08 and if they are possibly shallower than 500 m, 200 m or even 100 m for the KwaZulu-Natal marine environment.

The use of this dataset resulted from the fact that the ship track data information used to constrain the grid construction existed along with the possibility of better shallow water coverage (Marks and Smith, 2006). However the digitising of 500 m contours at 1:10 000 000 limited horizontal resolution to 30 km and ocean floor slope to 1° (Marks and Smith, 2006). In general the interpretation of large scale long wavelength features (greater than 160 km) were found to be similar to that of the Smith and Sandwell dataset limited only by ship track data control for each dataset (Marks and Smith, 2006).

Figure 3.27. GEBCO 1-minute gridded dataset for KwaZulu-Natal (British Oceanographic Data Centre, 2003). Note the areas adjacent to the coastline where better near-shore dataset coverage is available, resulting in the exclusion of GEBCO data in these areas.

4   INTEGRATION METHOD

4.1 Introduction

Podobnikar et al. (2000) mentions that integration of diverse data sources and subsequent interpolation requires the systematic management of data processing steps. GIS aids the integration management process by combining a visual, spatial software interface and a Relational Database Management System (RDBMS). The visual interface simplifies human interaction with spatial data; and the RDBMS simplifies management and processing of large amounts of often irregularly spaced or anisotropic, repetitive spatial data. Meaningful digital interpretation of the natural environment then requires the conversion of this processed, irregularly spaced data into a regularly spaced (isotropic) grid or a triangulated irregular network (TIN) to describe elevation with points, lines or areas in a belonging co-ordinate system (Podobnikar et al., 2000; Billen et al., 2008). The integrated final dataset was anisotropic since the majority of its constituent, integrated datasets were individually anisotropic, except the GEBCO, Smith and Sandwell and 5 ACEP survey block datasets.

Various software packages interpolate anisotropic explicit data into a grid or TIN. Merwade et al. (2008) notes that while GIS software has become more flexible and user-friendly its development along with geostatistical software has been largely independent. This is one of the suggested reasons for GIS software lacking complex geostatistical routines to create contour maps. Nevertheless, works by Foxgrover et al. (2004) have made use of a finite difference interpolation technique in the TopoGrid module in ESRI ® ArcInfo ® GIS software. However the cost of ESRI ® ArcInfo ® has prohibited its use in the MGU. Others such as Yongshe and Journel (2008) have made use of specialist geostatistical software such as BGoest, a geostatistical algorithm package with *Block Kriging* capabilities, built into the Stanford Geostatistical Modelling Software (SGeMS) (Remy et al., 2008).

The separate development of GIS and geostatistical interpolation software and the prohibitive cost, as in the case of ESRI ® ArcInfo ®, has led to the use of Golden Software ® Surfer 8 ® for interpolation by the MGU. Golden Software ® Surfer 8 ® supports 12 geostatistical interpolation methods which, along with its user-friendly interface, flexibility and low cost has

made it the preferred MGU map production software.

The integration method involved the initial non-spatial processing of bathymetric datasets after which GIS conversion and GIS-based processing was done. All processed data were then integrated into a final dataset. This final dataset was interpolated to produce a final GIS contour dataset at a scale of 1:3 000 000. Bathymetric dataset record processing was initially done in Microsoft ® Access since its built-in user-friendly RDBMS allowed for processing large amounts of data to remove erroneous point data. These were then converted to GIS format vector bathymetric datasets in ESRI ® ArcGIS ® for spatial data processing after which the GIS software was used to prepare the individual vector bathymetric datasets for integration into a final anisotropic dataset. Explicit point data were then interpolated in Golden Software ® Surfer 8 ® to produce an isotropic bathymetric grid from which a final GIS bathymetric contour dataset at a scale of 1:3 000 000 was produced.

4.2 Point vector dataset processing and integration

4.2.1 Non-spatial dataset processing

Non-spatial bathymetric dataset files had delimiting ASCII characters (tab, comma or space), separating each unique field (column) and end of line characters indicating the next new data record (row) with this sequential file structure repeated in proportion to the number of records in the bathymetric dataset. Bathymetric dataset records consisted of their UTM co-ordinate positioning fields given as "Eastings" and "Northings" and bathymetric depth field given as "MSLDepth". Figure 4.1 indicates the two possible display methods with text editors such as UltraEdit ® displaying records separated by the delimiting character (in this example, a space, Figure 4.1b), whereas a column view (Figure 4.1a) is used by Golden Software ® Surfer 8 ®, Microsoft ® Access ® or ESRI ® ArcGIS ®. UltraEdit ® was flexible and was also capable of viewing data in columns.

All data files were imported into Microsoft ® Access ® as tables with the "Eastings", "Northings" and "MSLDepth" bathymetric fields set to double precision using the Access Database Management System (DBMS). An example of an imported bathymetric data table in Microsoft ® Access ® is given in figure 4.2a along with the data field descriptions (Figure 4.2b). Appendix 5A – Microsoft ® Access ® Data Types, contains the different numeric field precision types supported by Microsoft ® Access ®.

The Microsoft ® Access ® DBMS allowed for easy, rapid structuring of queries based on Structured Query Language ® (SQL ®) for processing large amounts of data as well as setting numeric precision. One centimetre numeric precision or two decimal places was considered sufficient spatial accuracy for metre-based UTM co-ordinate fields. Where geographic co-ordinates were encountered, one centimetre numeric precision (or 0.0000001°) corresponded to seven decimal places. This decimal precision was required for accurate conversion of geographic co-ordinates to UTM co-ordinates. The depth field's highest numerical precision varied according to the dataset with the highest precision being 1 cm or two decimal places.

Figure 4.1. Two different display methods of data files encountered in this work, as used by the different software: (a) Tabular as viewed in Golden Software ® Surfer ®, Microsoft ® Excel ® and Access ® or ESRI ® ArcGIS ® or (b) Tab-delimited as viewed in the UltraEdit ® text editor.

SQL used by the RDBMS allowed for easy, rapid removal of invalid depths greater than or equal to zero as in the case of the Richards Bay, Sodwana Bay, Smith and Sandwell and GEBCO datasets. Incorrect initial precision settings in Microsoft ® Access ® of the "DD_Lon" Longitude and "DD_Lat" Latitude fields resulted in the imported GEBCO and Smith and Sandwell datasets, whose co-ordinates were in degrees having duplicate co-ordinate values.
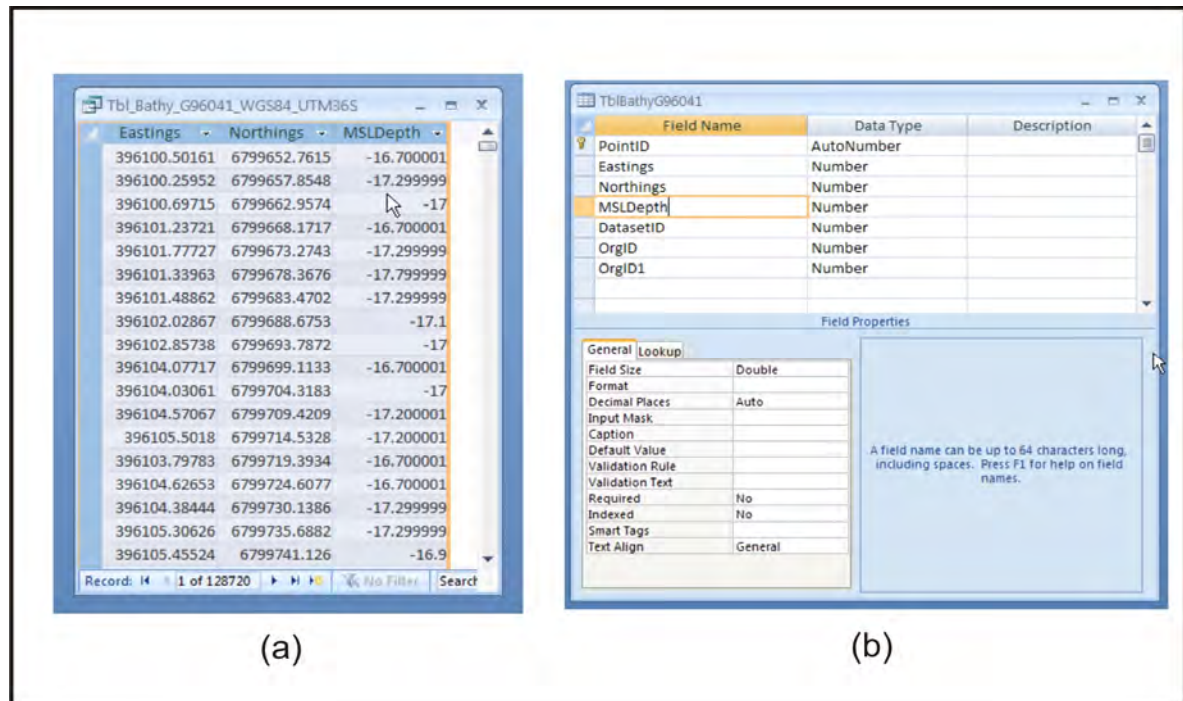
Figure 4.2. (a) A non spatial bathymetric data table displayed in Microsoft ® Access ® showing the data field names "Eastings", "Northings" and "MSLDepth" also showing how (b) individual data field properties can be interrogated in Microsoft ® Access ® to change the precision.

4.2.2   Spatial dataset conversion

ESRI ® ArcGIS ® was then used to convert non-spatial bathymetric to spatial vector GIS bathymetric datasets. The ESRI ® personal Geodatabase ® feature class GIS storage structure was used since the underlying ESRI ® data structure was a Microsoft ® Access ® database. The GIS data conversion process for each bathymetric dataset related it to the real-world environment after the addition of the spatial fields, "ObjectID" and "Shape", both part of the GIS software spatial system management. This allowed for their correct map projection by means of an appropriate co-ordinate system (for example, degree-based geographic or metre-based UTM Zone 36 S) and horizontal datum (for example, Cape or WGS84). Figure 4.2a indicates a non-spatial data table, in contrast to a GIS spatial attribute table in figure 4.3 where the unique identifier index field, "ObjectID" and a spatial field, "Shape" are seen. The display of a GIS spatial attribute table in both figure 4.3a and figure 4.3b demonstrate the compatibility between Microsoft ® Access ® and ESRI ® ArcGIS ®.

Figure 4.3. (a) GIS attribute table for personal geodatabase vector feature class as viewed in (a) Microsoft ® Access ® and (b) ESRI ® ArcGIS ®. The additional data fields "ObjectID" and "Shape" indicate this to be a spatial dataset in contrast to a data table as shown in figure 4.2. The "ObjectID" field allows for spatial indexing to improve data processing performance while the "Shape" field indicates the spatial geometric component.

4.2.3 Spatial dataset processing

As noted by Van Deursen et al. (1991) Wadge (1992) Guptil (1996) and Larsen (1996) metadata are essential when working with diverse datasets collected by third parties. The 5 ACEP and 15 MGU near-shore bathymetric datasets had good descriptive metadata, whereas the 9 South African Navy near-shore bathymetric datasets did not (Appendices 3A to 3C). For these, the year of acquisition became a crucial metadata proxy. Good descriptive metadata existed for the GEBCO and Smith and Sandwell deep-water bathymetric datasets whereas works by Dingle et al. (1978) were used as a metadata proxy for the deep-water, digitised contour dataset of the northern Natal Valley.

Vertical (tidal) datum

The correct vertical (tidal) datum is important; works by Foxgrover et al. (2004) Ng' ang' a et al. (2004) and Le Bas and Huvenne (2008) highlight some of the difficulties relating to the use of incorrect tidal datums. MGU and ACEP bathymetric datasets depths were relative to MSL, South African Navy bathymetric datasets required conversion from *CHART DATUM* or LAT to

MSL using the South African Navy tide tables for the nearest port – Richards Bay for the Maputaland and Richards Bay datasets and Durban for Durban datasets (South African Navy Hydrographic Office, 1995a; Kampfer, 2007). All deep-water bathymetric datasets were relative to MSL.

Horizontal datum, co-ordinate system and map unit

Foxgrover et al. (2004) again highlight georeferencing and map projection issues, especially with their older bathymetric datasets from 1858 up until as late as the 1950's. It is however noted that their georeferencing and map projection work became simpler with their more modern bathymetric datasets from the 1950's onwards. Their older bathymetric datasets up to the 1980's were based on the North American Datum of 1927 (NAD27). Their bathymetric datasets were converted to UTM co-ordinates based on the North American Datum of 1983 (NAD83). The American NAD27 and South African Cape Datums are equivalent local datums while similarly the American NAD83 and South African Hartebeesthoek 1994 Datums are also equivalent local datums. The WGS84 Datum has similar dimensional properties to the two local NAD83 and Hartebeesthoek 1994 Datums. ESRI (2007) provides an explanation of the differences between local and geocentric datums. Ng' ang' a et al (2004) note that GPS positioning, based on the WGS84 Datum is now widespread and workers such as Elema and de Jong (1999) have noted the International Hydrographic Organisation (IHO) also strongly supports initiatives to reference hydrographic charts to the WGS84 Datum.

All 32 bathymetric datasets for this work required the same horizontal datum, co-ordinate system and map units. The metre-based UTM Zone 36 S co-ordinate system based on the WGS84 Datum was chosen. Dataset conversion was accomplished using ESRI ® ArcGIS ®. According to available metadata, all 5 ACEP multi-beam and 13 of the 15 MGU single-beam near-shore bathymetric datasets required no conversion. All 9 of the South African Navy near-shore datasets required conversion. The 3 deep-water datasets comprising the GEBCO, the Smith and Sandwell and the digitised contour data of the northern Natal Valley after Dingle et al. (1978) required conversion. The dataset conversion details are given in table 4.1

Table 4.1. Datasets listed requiring map co-ordinate and datum conversions. The original details are shown. All were converted to the UTM36 S co-ordinate system based on the WGS84 Datum. Geographic co-ordinate units are in degrees (^{o}). UTM36 S and Lo33 co-ordinate units are in metres (m). In all, 2 of the 15 MGU near-shore, all 9 South African Navy near-shore and all 3 deep-water datasets required conversion. All 5 ACEP datasets and 13 MGU datasets required no conversion.

Dataset	Organisation	Original co-ordinates (units) /datum
Leven Point to Gobeys Point	MGU	Lo33 (m) /Cape Datum
Richards Bay Continental Shelf	MGU	Geographic (^{o}) / WGS84 Datum
Fair Chart 200, 204 and 205	South African Navy	UTM36S (m) /Cape Datum
Fair Chart 166	South African Navy	Geographic (^{o}) / WGS84 Datum
Fair Chart 168	South African Navy	Geographic (^{o}) / WGS84 Datum
Fair Chart 167	South African Navy	UTM36S (m) /Cape Datum
Fair Chart 202	South African Navy	Geographic (^{o}) / WGS84 Datum
Admiralty Fair Chart 34	South African Navy	Geographic (^{o}) / Cape Datum
Fair Chart 165	South African Navy	UTM36S (m) /Cape Datum
Umlazi River to Port Shepstone (AFC18)	South African Navy	Geographic (^{o}) / Cape Datum
Port Shepstone to Port Edward (AFC19)	South African Navy	Geographic (^{o}) / Cape Datum
GEBCO 1-minute gridded dataset	Freely available	Geographic (^{o}) / WGS84 Datum
Smith and Sandwell 2-minute gridded dataset	Freely available	Geographic (^{o}) / WGS84 Datum
Northern Natal Valley contour dataset	MGU	Geographic (^{o}) / Cape Datum

4.2.4   Spatial dataset integration

Near-shore dataset integration

Four areas of the continental shelf existed where near-shore bathymetric dataset integration was required: Maputaland, Richards Bay, Durban and the continental shelf south of Durban. Perimeter polygon vector feature classes were digitised in ESRI ® ArcGIS ® around each near-shore bathymetric dataset in these areas, to exclude data where spatially adjacent datasets intersected (Figures 3.1 3.2 and 3.3). Available metadata resulted in the ranking of datasets in the following descending order of priority for data exclusion:

- The 5 ACEP multi-beam echo-sounder survey block bathymetric datasets

- The 14 MGU digitally acquired bathymetric datasets using differential GPS and digital single-beam echo-sounders

- The MGU acquired bathymetric dataset using GPS and an analogue single-beam echo-sounder

- The 6 South African Navy Fair Chart bathymetric datasets

- The 3 South African Navy Fair Chart bathymetric datasets

Metadata for the Blood Reef bathymetric dataset indicated a more recent acquisition date, a more modern echo-sounder with a narrower beam-width and higher dataset density than the Durban Bight bathymetric dataset (Appendices 3A to 3D). This resulted in the adjacent, overlapping Durban Bight data being excluded. Similarly, metadata indicated the more recently acquired 2004 to 2005 NRF Sodwana Bay dataset to be more favourable than the Leven Point to Gobey's Point dataset collected in 1990 to 1991 (Appendices 3A to 3D). The limited available metadata for the South African Navy bathymetric datasets indicated that Fair Charts 166 to 168 used the same instruments and were acquired in the same year (Appendices 3A to 3C) resulting in all overlapping data being retained.

Deep-water dataset integration

The digitised contour data of the northern Natal Valley after Dingle et al. (1978) Smith and Sandwell and GEBCO bathymetric datasets were excluded in areas of intersection with the digitised polygons representing the near-shore bathymetric datasets. The remaining digitised contour data of the northern Natal Valley after Dingle et al. (1978) were considered authoritative. Concluding remarks by Marks and Smith (2006) stating that *"the original Smith and Sandwell dataset may well be the best choice"* led to the adoption of the remaining Smith and Sandwell bathymetric dataset for the deep-water areas not covered by the digitised contour data of the northern Natal Valley after Dingle et al. (1978). Bathymetric data shallower than 200 m in the remaining GEBCO bathymetric dataset were retained for areas where no other bathymetric data may have existed, but were subsequently not used. All bathymetric datasets were exported from ESRI ® ArcGIS ® to ASCII, comma-delimited files and all were integrated into one final bathymetric dataset for interpolation in Golden Software ® Surfer 8 ®.

4.3 Final bathymetric dataset interpolation

4.3.1 Introduction

Podobnikar et al. (2000) and Bjørke and Nilsen (2009) have defined interpolating as a means of deriving output data elements in a regular rectangular array or grid from irregularly spaced input data known as the data neighbourhood with Podobnikar et al. (2000) describing how elevation is defined by points, lines or polygons in a specified co-ordinate system. Merwade et al. (2008) also noted that many interpolation methods and software packages exist for grid development with more recent neural network algorithms and robust interpolators having been combined into newer machine-learning techniques. As established by Marsh and Brown (2008) in the neural network (NN) classification of multi-beam bathymetric data from Stanton Bank, other authors such as Alexandrou and Pantzartzis (1993) Müller et al. (1997) Zhou and Chen (2005) Müller et al. (2007) have also used artificial neural networks (ANN's) for bathymetry and seafloor interpretation. This suggests that neural networks may become an important tool to interpret bathymetric data.

The finite difference interpolation capability of ESRI ® ArcInfo ®'s TopoGrid module used by Foxgrover et al. (2004) and the *Block Kriging* interpolation capability of the specialist geostatistical module BGoest in the SGeMS software used by Yongshe and Journel (2008) highlight some of the different geostatistical software packages and available interpolation methods in use. Interpolation methods can either be exact, attempting to honour input data points coincident with an interpolated grid node, or smoothing, tending to do the opposite. Golden Software ® Surfer 8 ®, the interpolation software used in this work, requires a minimum of four non-collinear XYZ data points by one of its twelve exact or smoothing interpolation methods, some of which have both capabilities (Golden Software, 2002). It is however noted by Bjørke and Nilsen (2009) that accurate interpolation is limited by noise in input data which will subsequently be modelled by the interpolation algorithm. They however suggest using arithmetic averaging as a simple but robust means to solve this problem.

4.3.2 Interpolation method and choice

The need to honour input data as required in this work led the choice from one of seven, Golden Software ® Surfer 8 ® exact interpolators: *Kriging*, *Radial Basis Function*, *Inverse Distance to a Power, Modified Shepard's Method, Nearest Neighbour, Natural Neighbour*, and

Triangulation with Linear Interpolation. Bakkali and Amrani (2008) identified *Kriging*, *Radial Basis Function, Inverse Distance to a Power, Modified Shepard's Method* and *Triangulation with Linear Interpolation* as the preferred exact interpolation method choices for their work on removing resistivity data noise in Moroccan phosphates.

Triangulation with Linear Interpolation, based on Renka's algorithm, performs Delaunay triangulation (Okabe et al., 1992). Lawson (1972) noted that using this interpolation method with datasets having sparse areas could cause triangular facets on the interpolated grid surface, and this combined with the known areas of sparse data densities in the final bathymetric dataset resulted in its abandonment.

Inverse Distance to a Power and *Modified Shepard's Method* have been described by Bakkali and Amrani (2008) as similar interpolation methods. *Modified Shepard's Method* is able to reduce the effects of "bulls-eye" contour appearances making it the favourable choice over *Inverse Distance to a Power*.

Radial Basis Function is a well established scattered data interpolation method (Franke and Nielson, 1980) and as also noted by Fasshauer et al. (1998) is a diverse group of interpolation tools. Smoothly interpolated surfaces are considered best achieved by the *Radial Basis Function's Multiquadratic* option (Hardy, 1971; Chen et al., 1996)

Kriging, as noted by Cressie (1991; 1993) and Swan and Sandilands (1995) is a geostatistical interpolation method that has proven useful in many fields, capable of producing appealing maps from irregularly spaced data and according to Davis (1986) the defaults can be used to produce an accurate grid of the input data. Davis and McCullagh (1975) have noted its dependence on spatial and statistical relationships to calculate the developed surface. More complicated forms of *Kriging* such as *Regressive-Kriging* and *CoKriging* exist (Hengl et al., 2007) however Golden Software ® Surfer 8 ® supports only *Ordinary Kriging* (no drift) or *Universal Kriging* (with linear or quadratic drift) both of which are more widespread, simpler to configure and less demanding on computer resources; *Regressive-Kriging* may even require specialised computers other than Personal Computers (Hengl et al., 2007).

Golden Software (2002) indicates *Kriging* as the default interpolator in Surfer 8 ® and this combined with its widespread acceptance and use by the MGU for contour map interpolation led to its adoption for the final bathymetric dataset interpolation to produce the 1:3 000 000

scale GIS contour dataset. *Kriging* was classified as one of the slower interpolation methods supported by Golden Software ® Surfer 8 ®, often seen as its disadvantage; however the final integrated bathymetric dataset's large size of 4 007 970 records suggested long interpolation times regardless of the interpolation method. Based on the recommendations of Davis (1986) the *Kriging* default configuration was used with some modifications. A circular 8-sector 500 km search radii was chosen to minimise the possibility of grid node blanking causing degrading of the contour data (Golden Software, 2002). The aim of producing a contour dataset at a regional scale of 1:3 000 000 capable of near-shore higher scale mapping led to an initial grid spacing of 1 000 m, after which a 500 m spacing was found more favourable. The grid based on the 1 000 m spacing was completed in 42 hours, whereas the grid based on the 500 m spacing took 193 hours to complete. Appendix 5B shows the grid details for the 500 m grid spacing.

5 DISCUSSION

5.1 Introduction

GIS applications such as this work accomplish the mapping of the natural environment by relying on semantic digital interpretation, using diversely integrated, heterogeneous datasets rendering more objective statistical quality control methods difficult, instead requiring visual, more subjective quality control (Podobnikar et al., 2000; Billen et al., 2008; Durbha et al., 2008; Reitsma et al., 2008). Billen et al. (2008) furthermore note that research with poorly defined constraints and little descriptive metadata defining underlying data relationships can make statistical analysis and interrogation of datasets difficult requiring a more flexible, interactive visual environment, making use of the human brain to identify patterns. Mapping and GIS software offer this type of environment as noted by Bonham-Carter (1994) and Foxgrover et al. (2004). The general absence of good control points in the marine environment, typical in this work and essential for statistical quality control, combined with the heterogeneous nature of the integrated datasets in the final bathymetric dataset add to the complexity of statistical analysis making the visual quality control offered by ESRI ® ArcGIS ® useful. Visual quality control of contours was therefore used to highlight artefacts at the proposed regional scale of 1:3 000 000 and at higher near-shore local scales of up to 1:45 000. In addition, Golden Software ® Surfer 8 ®'s ability to render a grid whose density was proportional to object mapping resolution, as a 3-dimensional elevation surface (Golden Software, 2002) made it a useful visualisation aid for artefact identification. User-friendly configuration of the lighting, overlays, view and scale settings were important for this work, with the rainbow 2 colour ramp established as the most favourable colour scheme for artefact identification (Appendix 4A).

5.2 Regional 1:3 000 000 contour dataset

The final GIS contour dataset of the KwaZulu-Natal marine environment is presented both in figure 5.1 at a scale of 1:3 000 000. Contour intervals are: 5 m between depths of 5 m and 100 m, 10 m between depths of 100 m and 200 m and 100 m for depths more than 200 m.

Visual quality control of the near-shore features was possible as previous MGU near-shore contour mapping work had been done as shown by the blue contours in figures 5.2 to 5.13. The

higher-resolution mapping capability made possible by the previously mapped near-shore contour datasets can be attributed to the higher underlying bathymetric dataset densities and the smaller interpolation grid spacing that was possible. Consequently, better resolution was achieved by the final dataset where control by the original near-shore bathymetric datasets was evident. Contour mapping detail offered by the final dataset was best where the 5 dense multi-beam echo-sounder East Coast survey blocks were acquired. This is attributable to the small grid spacing of 10 m and the isotropic nature of the input point data. This allowed for grid node interpolation, closely honouring the input point data, while the dense, more accurate input data allowed for better interpretation than the irregularly space, often less dense single-beam echo-sounder acquired and digitised near-shore bathymetric data.

Despite the diversity of the individual bathymetric datasets integrated into the final bathymetric dataset, it was able to map deep-water submarine features identified by Dingle et al. (1978) along with near-shore areas, some of which have been selected in this work. This indicates the success of the diverse dataset integration and the chosen grid interpolation spacing of 500 m for the final bathymetric dataset to simultaneously interpret the deep-water and near-shore features. However, noticeable dataset errors can be seen at a regional scale (Figures 5.1 and 5.16), south of 31°S. The main deep-water regional features included the two canyons of the Thukela Cone: the Thukela and 29° 25' S Canyons (Figure 5.1). Inclusion of the 5 ACEP multi-beam survey blocks allowed the final contour dataset to detect the Canyons, identified by the survey blocks described in Ramsay and Miller (2006) (Figures 5.2 to 5.6). Inclusion of the NRF bathymetric datasets allowed the final bathymetric contour dataset to resolve near-shore features, such as the Sodwana Bay Two-, Four-, Six and Nine-Mile reefs (Figure 5.3) and the Kosi Bay reefs (Figure 5.7) described by Ramsay (1996) and the NRF project reported in Ramsay et al. (2006). Leadsman Shoal (Figure 5.5) and Red Sands Reef (Figure 5.8) were also resolved by the final contour dataset as a result of the inclusion of MGU datasets from the previous works of Ramsay (2000). The final contour dataset between Durban and Richards Bay displayed more detail off Richards Bay (Figure 5.9) after the inclusion of the MGU Richards Bay continental shelf bathymetric dataset after Lord et al. (1996). Higher resolution off the Thukela River mouth (Figure 5.10) was possible due to the inclusion of the South African Navy's AFC 34 and MGU Richards Bay continental shelf dataset after works done for the Institute of Natural Resources (INR) by Leuci et al. (2004). Resolution between Virginia Beach and the Thukela River mouth was limited because of the lack of recent, high-resolution data.

The MGU high-resolution Durban Bight and Blood Reef datasets, however, improved the final bathymetric contour dataset resolution between Virginia Beach and Brighton Beach (Figure 5.11) after bathymetric works by Richardson (2005) and Cawthra (2006). Figure 5.12 shows how the inclusion of the MGU's Aliwal Shoal bathymetric dataset after Bosman et al. (2005) allowed the final bathymetric contour dataset to resolve Aliwal Shoal and how the Protea Banks Reef (Figure 5.13) between Margate and Shelly Beach was resolved due to the inclusion of digitised bathymetric contour data after Birch (1981).

Figure 5.1. The Integrated marine GIS bathymetric contour dataset for KwaZulu-Natal. The northern Natal physiographic provinces after Dingle et al. (1978) are also shown. The South African 200 nautical mile Exclusive Economic Zone (EEZ) is in light blue. Regional scale artefacts from conjoined arc-like contours can be seen and artefacts from the presence of noisy satellite altimetry data south of 31° S and east of 34° E are also visible.

Figure 5.2. Mabibi survey block mapped using the KwaZulu-Natal contour dataset (black). The ACEP Mabibi survey block contour dataset is used as a comparison (blue).

Figure 5.3. Sodwana survey block and reefs mapped using the KwaZulu-Natal contour dataset (black). The NRF contour dataset and the ACEP Sodwana survey block contour dataset are used as a comparison (blue).

Figure 5.4. Diepgat survey block mapped using the KwaZulu-Natal contour dataset (black). The ACEP Diepgat survey block contour dataset is used as a comparison (blue).

Figure 5.5. Leadsman survey block mapped using the KwaZulu-Natal contour dataset (black). The ACEP Leadsman survey block contour dataset is used as a comparison (blue).

Figure 5.6. Leven survey block mapped using the KwaZulu-Natal contour dataset (black). The ACEP Leven survey block contour dataset is used as a comparison (blue).

Figure 5.7. Kosi Bay Reefs mapped using the KwaZulu-Natal contour dataset (black). The NRF contour dataset is used as a comparison (blue).

Figure 5.8. Red Sands Reef, Leadsman Shoal, Leadsman (northernmost) and Leven (southernmost) survey blocks mapped using the KwaZulu-Natal contour dataset (black). The NRF contour dataset including the ACEP Leadsman and Leven survey block contour datasets are used as a comparison (blue).

Figure 5.9. Richards Bay continental shelf mapped using the KwaZulu-Natal contour dataset (black). The MGU Richards Bay contour dataset is used as a comparison (blue).

Figure 5.10. Thukela continental shelf mapped using the KwaZulu-Natal contour dataset (black). The MGU Thukela contour dataset is used as a comparison (blue).

Figure 5.11. Durban continental shelf mapped using the KwaZulu-Natal contour dataset (black). The MGU Durban Bight and Blood Reef contour datasets are used as a comparison (blue).

Figure 5.12. The Durban to Aliwal Shoal region mapped using the KwaZulu-Natal contour dataset (black). The MGU Mlazi River to Port Shepstone contour dataset is used as a comparison (blue).

Figure 5.13. The Protea Banks reef mapped using the KwaZulu-Natal contour dataset. The MGU Port Shepstone to Port Edward contour dataset is used as a comparison.

5.3 Data artefacts

5.3.1 Conjoined contours

In the areas deeper than 200 m, not constrained by high density ship track data, visual inspection showed that the general contour trend is maintained as a result of the Golden Software ® Surfer 8 ® *Kriging* algorithm function as an exact interpolator (attempting to honour original input data) with its 500 m grid spacing. However, the contours approximated a series of conjoined arcs instead of smooth curves more noticeable in the deep-water areas of underlying low data densities (Figures 5.1, 5.9, 5.10, 5.12 and 5.13). Figures 5.14, 5.15 and 5.16 visually enhance some of the noticeable artefacts. These are shown by purple, yellow, and red and to a lesser extent by blue polygons where the topography is less variable. Conjoined, arc-like contour induced, artefacts are shown by purple and polygons in figure 5.16 at the margin of steeper and more gradual topography where little or no data exists as indicated by figure 3.21.

As noted by Merwade et al. (2008) and Billen et al. (2008) good bathymetric data interpolation is dependant on: the availability of well constrained, known control points, point measurement density, distance between point measurements and orientation of point measurements, also noted by Sinclair (1998) in the case of MGU bathymetric field work undertaken. Additionally, interpolation methods for producing grids, based on local, partial data neighbourhoods (search radii in Surfer 8 ®) instead of all data can be based on user defined (subjective) assumptions (Franke and Nielson, 1980). Interpolation, as noted by Bjørke and Nilsen (2009) can also be negatively affected by noise, thus introducing artefacts. Irregular data overages of the final bathymetric dataset caused by the combination of individual, constituent higher density near-shore and lower density regional deep-water datasets, when considered with the 500 m grid spacing and the search radii of 500 km for the *Kriging* algorithm in Golden Software ® Surfer 8 ®, have caused interpolation problems in areas of sparse dataset coverage (Figure 5.1). This is the likely cause for the conjoined arc-like appearance of the contours. The effects are enhanced along margins of variable topography like the Mozambique Ridge (purple polygons, Figure 5.16). However, south of the northern Natal physiographic provinces (31° S, Figures 5.1 and 5.16) these conjoined contour artefacts are absent because the Smith and Sandwell (1997) satellite altimetry based data densities are more regular.
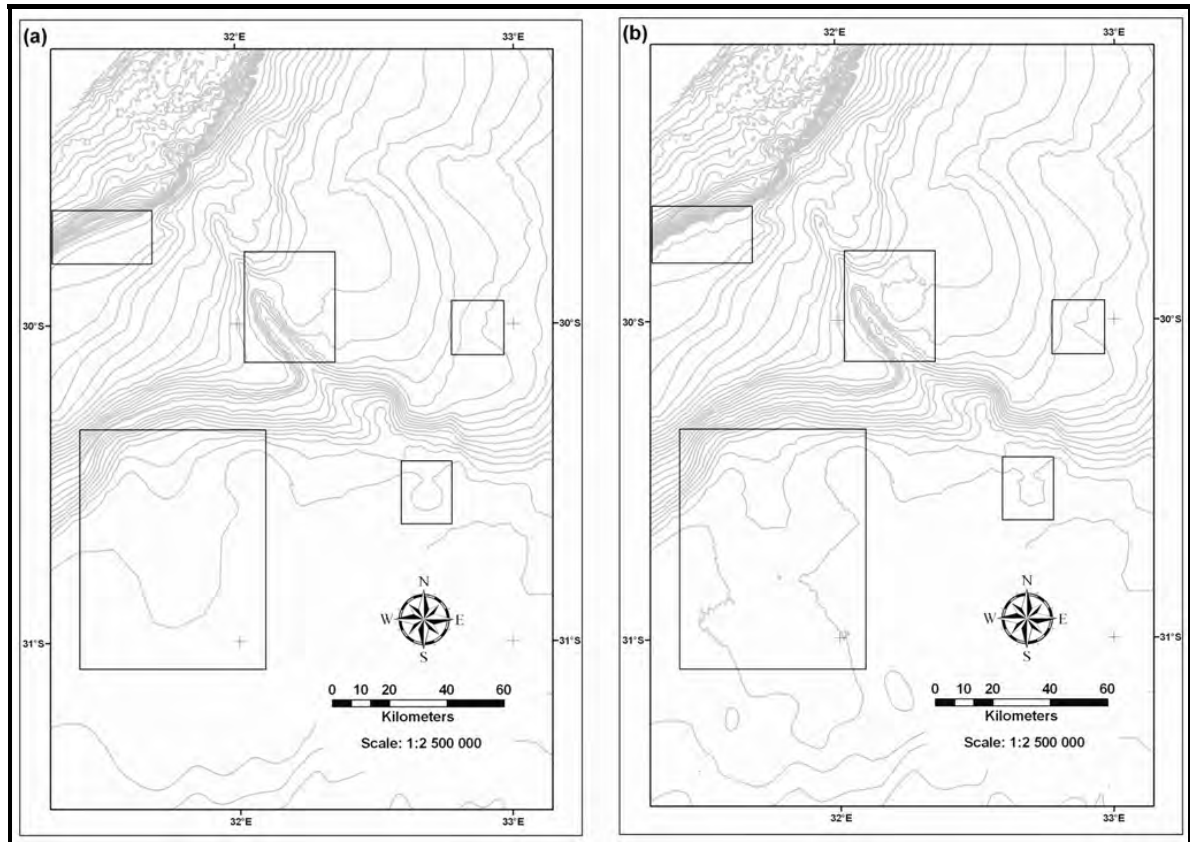
Figure 5.14. **(a)** The improved contour dataset after using ESRI ® ArcGIS ® contour editing capability on **(b)** the original contour dataset in the areas highlighted by the rectangles. These artefacts occurred where the Smith and Sandwell (1997) satellite altimetry based dataset and the digitised contour dataset of the northern Natal Valley after Dingle et al. (1978) were merged between 30° 30' S and 31° 15' S and in areas of variable data densities where steep topography became more gradual.

Gridding three individual datasets (the Smith and Sandwell (1997) satellite altimetry based deep-water dataset, the digitised contour dataset of the northern Natal Valley after Dingle et al. (1978) and all the near-shore datasets) with different configurations for the Golden Software ® Surfer 8 ® *Kriging* algorithm to produce three individual contour maps, which could be integrated, may improve the appearance of conjoined contours. However the aim of this work was to produce one useful diverse final dataset from which to derive a single grid for the construction of the best possible contour dataset. In addition, the use of GIS contour editing techniques would introduce user bias. Nevertheless, the contour editing ability of ESRI ® ArcGIS ® was used selectively to correct some of the more noticeable conjoined arc-like contour artefacts where the digitised contour dataset of the northern Natal Valley after Dingle et al. (1978) and the Smith and Sandwell (1997) satellite altimetry based dataset were merged between 30° 30' S and 31° 15' S (Figure 5.14).

GIS contour editing techniques were also used to improve the dataset in the vicinity of the Thukela Canyon (Figure 5.14) and along the adjoining Central Terrace, deep ocean basin and Mozambique Ridge physiographic provinces (Figure 5.15) where variable data densities occurred particularly where steep topography became more gradual.
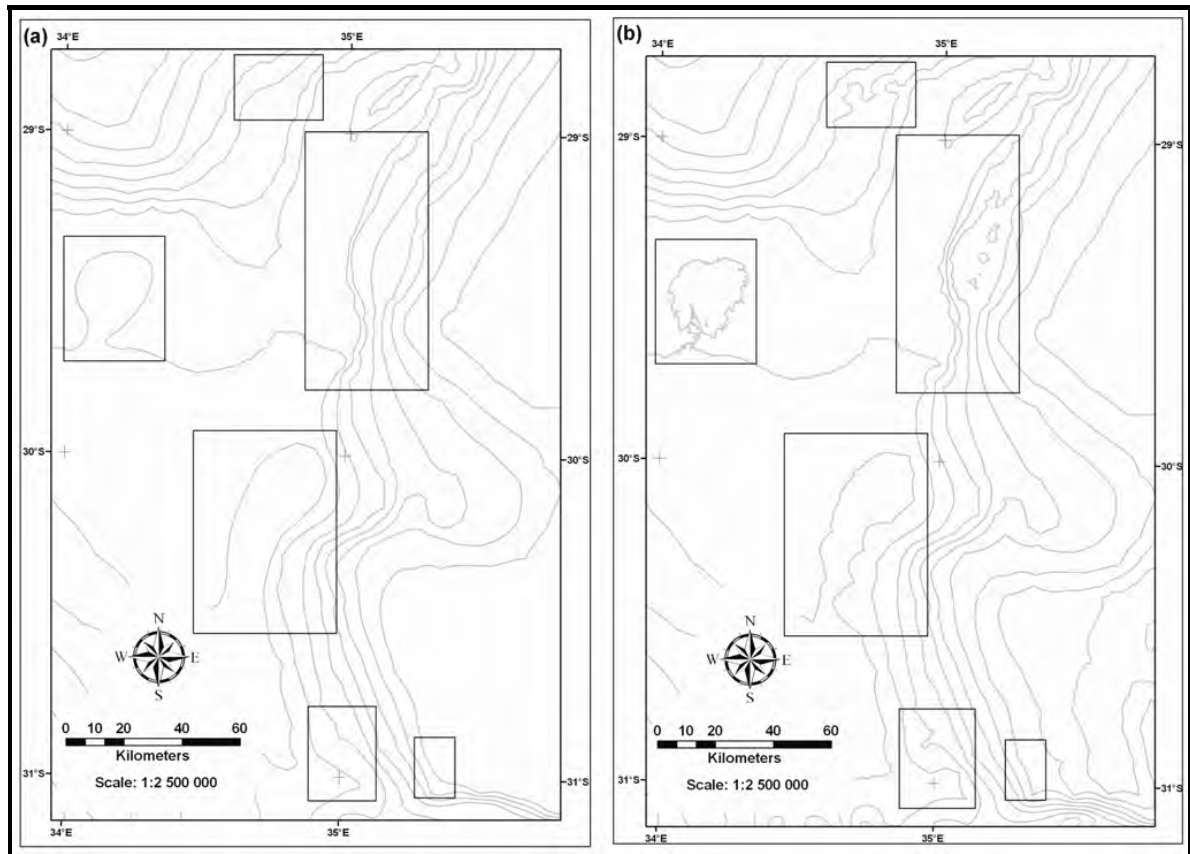
Figure 5.15. **(a)** The improved contour dataset after using ESRI ® ArcGIS ® contour editing capability on **(b)** the original contour dataset in the areas highlighted by the rectangles. These artefacts occurred in areas of variable data densities where steep topography became more gradual.

5.3.2 Noisy satellite altimeter data

Marks and Smith (2006) evaluated the Smith and Sandwell (1997) satellite altimetry based dataset version 8.2 and GEBCO datasets used here. These datasets differ fundamentally in that the former is predicted from satellite measured gravity while the latter is based on digitised paper contour data at 500 m contour interval at a scale of 1:10 000 000. Both contain metadata on the distribution of the underlying ship track data used. The concluding remark by Marks and Smith (2006) that the "*the original Smith and Sandwell dataset may well be the best choice*", and its choice for inclusion in the S2004 bathymetric grid at depths below 1000 m led to its

inclusion in the final dataset south of 31° S in spite of its noise signal component.

Replacing the Smith and Sandwell (1997) satellite altimetry based dataset with a smoother dataset could be done to remove the characteristic bumpy texture of satellite altimetry data (Marks and Smith, 2006) and for this task the GEBCO dataset would be the best alternative recommendation as the other publicly available bathymetric grids are derived from the Smith and Sandwell dataset (Table 3.2). However the GEBCO dataset has known limitations in the featureless deep ocean basins (Goodwille, 2004) with Marks and Smith (2006) even mentioning that both the Smith and Sandwell (1997) and GEBCO datasets have similar large scale feature resolution, with both dependant on the underlying ship track data control in the area being mapped.

South of 31° S, contours do not posses the arc-like appearances as described earlier. They are nevertheless jagged and irregular, presenting a bumpy seafloor because of the presence of high frequency noise data along with some of the signal data, particularly where it was used to map the steeper topography (Marks and Smith, 2006). These artificial contour artefacts are shown particularly between 34° E and 36° E (red polygon, Figure 5.16) in areas of steeper topography and to a lesser degree east of 34° E where the topography is less steep (yellow polygon, Figure 5.16).

Figure 5.16 highlights obvious regional scale differences in the final bathymetric dataset between the authoritative, digitised contour dataset of the northern Natal Valley after Dingle et al. (1978) component north of 31° S and the less reliable Smith and Sandwell (1997) satellite altimetry based dataset component south of 31° S. Figure 5.17 firstly presents an area off the Thukela Cone southern margin bounding the cross section A-B in figure 5.16 where bathymetric data were extracted from both datasets.
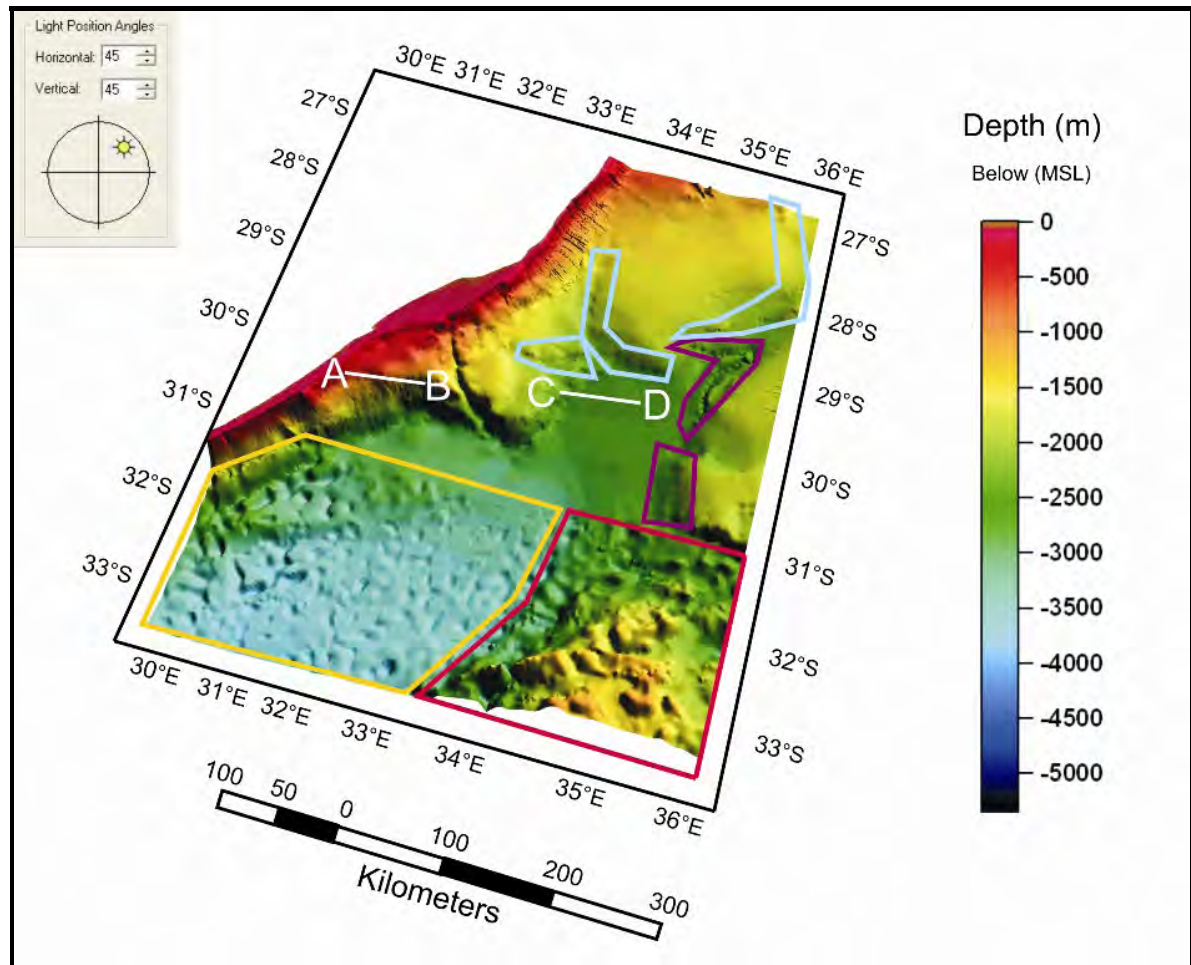
Figure 5.16. A 24-bit colour rendering of the final grid is shown. A depth dependant 3-dimensional surface was generated in Golden Software ® Surfer 8 ® for the visualisation of regional scale dataset errors. Conjoined arc-like contour artefacts (purple and blue polygons) were produced where sparse data constrains the ability of the contour producing software. These are more pronounced where variable topographic areas on the west and east side of the Mozambique Ridge (Physiographic Province 13) are adjacent to its summit (purple polygons) and less pronounced where data are sparse and topography is less variable (blue polygon) such as the deep ocean basin (physiographic provinces 14 and 15). Artefacts from noisy satellite altimetry data are also seen (red and yellow polygons), again more pronounced in areas of steeper variable topography (red polygon) and not as pronounced in areas of less steep, less variable topography (yellow polygon) such as the deep ocean basin (physiographic provinces 15 and 16). A-B and C-D are cross sections through the final dataset referred to in figures 5.17 and 5.18.

Data counts, bathymetric minima, maxima and mean values (Figure 5.17b) as well as contour maps (Figure 5.17c) and bathymetric profiles are similar (Figure 5.17d). The anisotropic nature (Figure 5.17a) of the authoritative, digitised contour dataset of the northern Natal Valley after Dingle et al. (1978) has produced the familiar arc-like contour artefacts (red contours, Figure 5.17c), whereas the isotropic nature (Figure 5.17a) of the Smith and Sandwell (1997) satellite altimetry based dataset has produced the more regular contours (blue contours, Figure 5.17c).

A depth discrepancy of 200 m also exists between the 2 datasets. This could be attributable to the lack of good control by ship track data in the Smith and Sandwell (1997) satellite altimetry based dataset, or as noted by (Chandler and Wessel, 2008) the presence of unreliable, erroneous ship track data used in the initial development of the Smith and Sandwell (1997) satellite altimetry based dataset.

Figure 5.18 presents an area in the deep ocean basin between the Thukela Cone and Mozambique Ridge bounding cross section C-D in figure 5.16. This area was chosen to extract cross sectional bathymetric data from both datasets constrained between a single 100 m contour interval as was applied to the deep-water areas in this work. The anisotropic digitised contour dataset of the northern Natal Valley after Dingle et al. (1978) has lower data densities than the isotropic Smith and Sandwell (1997) satellite altimetry based dataset – 230 compared to 2 325 data points for the same area in figure 5.18. The digitised contour dataset of the northern Natal Valley after Dingle et al. (1978) has values for a minimum depth of 2 800 m, a maximum depth of 2 000 m, and a mean depth of 2 480 m vs. corresponding values of 2 870 m, 1 876 m and 2 536 m for the Smith and Sandwell (1997) satellite altimetry based dataset. Figure 5.18b shows the conjoined arc-like contours caused by the anisotropic digitised contour dataset of the northern Natal Valley after Dingle et al. (1978) and the smooth contours of the isotropic Smith and Sandwell (1997) satellite altimetry based datasets. However, the cross section C-D in figure 5.18b for each dataset differs, with the Smith and Sandwell (1997) satellite altimetry based dataset cross section (blue, Figure 5.18c) exhibiting obvious noise. This noise is responsible for the bumpy seafloor texture in figure 5.16 described by Marks and Smith (2006). It is evident south of 31° S where the final dataset is based entirely on the Smith and Sandwell (1997) satellite altimetry based dataset. The depth discrepancy is not as noticeable, possibly for the opposite reasons to those stated for figure 5.17.

Bjørke and Nilsen (2009) have commented on the negative effects of noise in anisotropic datasets from which isotropic grids are interpolated. In spite of this, Merwade et al. (2008) have mentioned the existence and use of many interpolation methods with Podobnikar et al. (2000) Billen et al. (2008) Durbha et al. (2008) and Reitsma et al. (2008) having recognised their importance for the interpolation of diverse, irregular data for meaningful environmental interpretation.
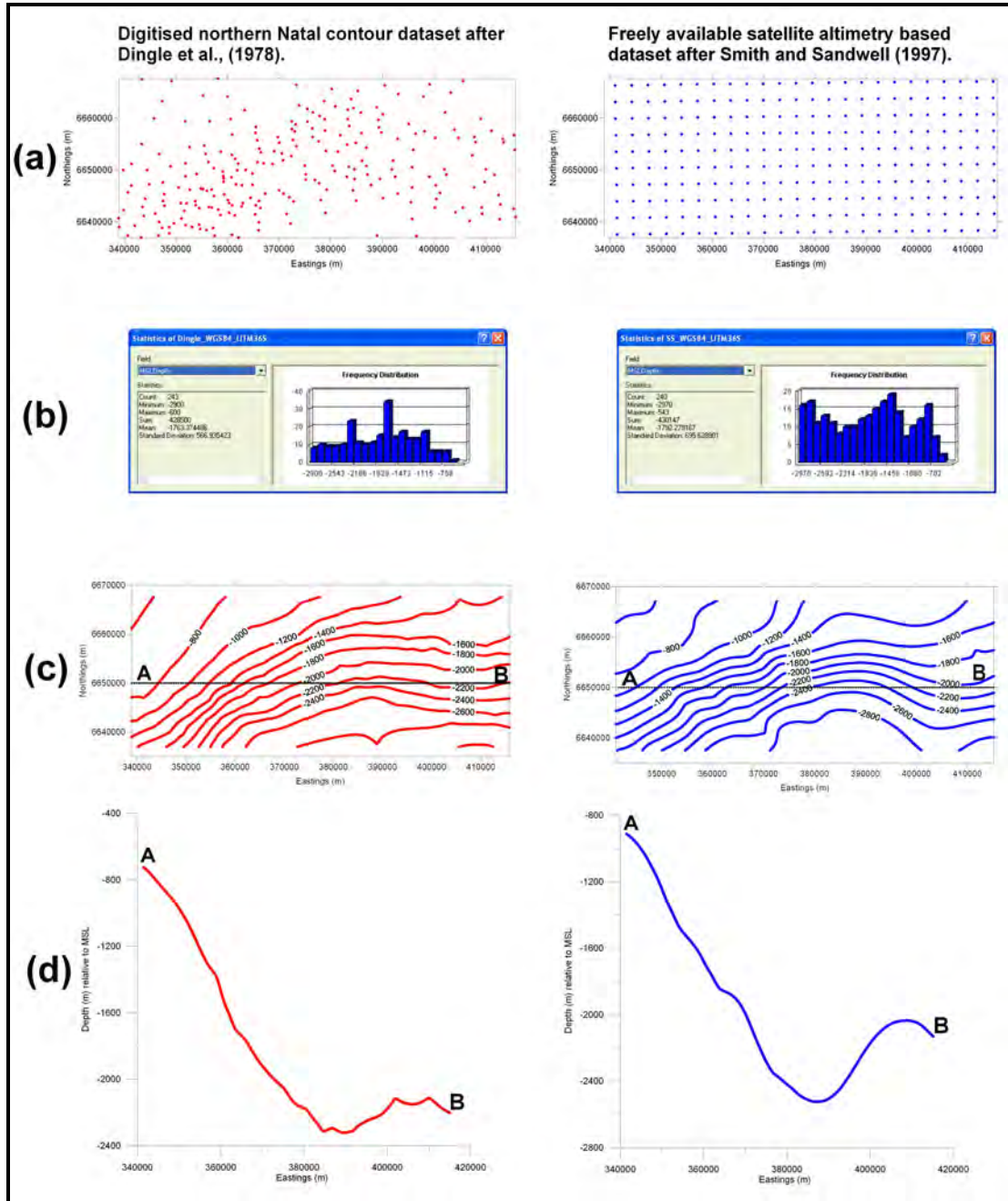
Figure 5.17. An area on the Thukela Cone southern margin is selected to compare the less reliable satellite altimetry based bathymetry dataset after Smith and Sandwell (1997) to the authoritative digitised contour dataset after Dingle et al. (1978). **(a)** The dataset after Dingle et al. (1978) is anisotropic whereas the dataset after Smith and Sandwell (1997) is isotropic. **(b)** Dataset statistics are similar and **(c)** as expected, the resultant contour datasets are also similar. **(d)** The West-East orientated cross section (A-B) indicates similar bathymetric profiles. Golden Software ® Surfer 8 ® was configured identically in both cases to generate the above contour datasets.
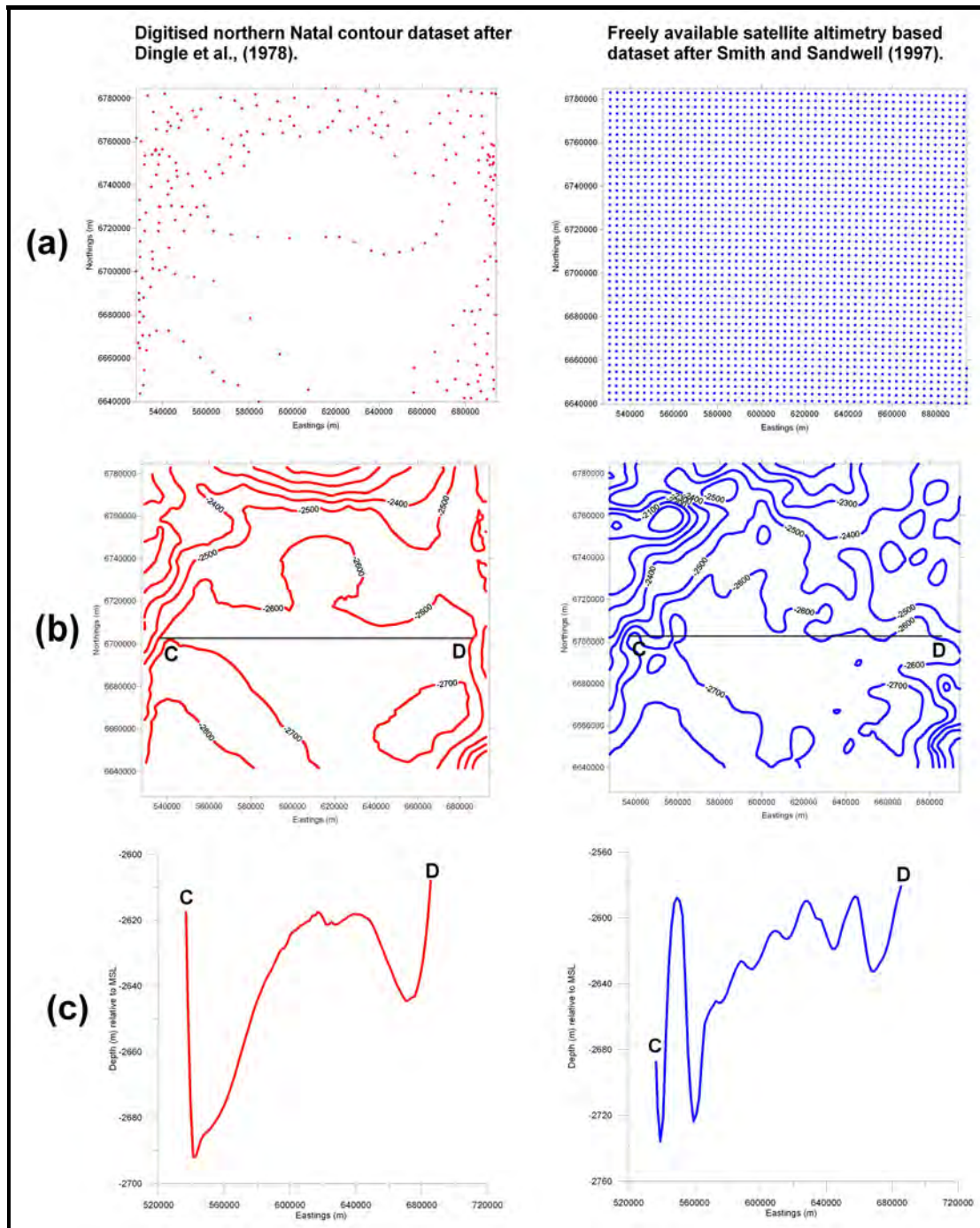
Figure 5.18. An area in the deep ocean basin between the Thukela Cone eastern margin and Mozambique Ridge is selected to compare less reliable satellite altimetry based bathymetric dataset after Smith and Sandwell (1997) to authoritative digitised bathymetric contour dataset after Dingle et al. (1978). **(a)** The dataset after Dingle et al. (1978) is anisotropic whereas the dataset after Smith and Sandwell (1997) is isotropic. Unlike in figure 5.17, dataset densities differ and **(b)** the resultant contour datasets differ. **(c)** The West-East orientated cross section (C-D) indicates different bathymetric profiles. The Smith and Sandwell (1997) bathymetric contour dataset profile (C-D) obvious noise at regular intervals.

They also suggest the use of visual instead of statistical quality control, which according to Billen et al. (2008) is more flexible and interactive to interrogate dataset quality where poorly defined constraints and little descriptive metadata exist. Bonham-Carter (1994) and Foxgrover et al. (2004) have also suggested the use of certain mapping and GIS software to accomplish this. For the visual interrogation of the final bathymetric dataset quality, ESRI ® ArcGIS ® and Golden Software ® Surfer 8 ® were thus used.

Bjørke and Nilsen (2009) have indicated that grid nodes are interpolated according to rules, prioritising certain data and excluding other data in the relevant grid node data neighbourhood. Thus, noise dominated grid node data neighbourhoods can result in noise-dominated grid nodes, in turn causing artefacts. These are evident in the final bathymetric dataset south of 31° S (Figures 5.16 and 5.19a) resembling relatively evenly spaced circular contours and in some cases dense groupings of concentric contours.

Using ESRI ® ArcGIS ®, areas of circular contours along with the outermost of the dense concentric contour groupings in figure 5.19a were used to produce the red areas in figure 5.19b. These constrained the underlying noisy satellite altimetry based bathymetric data (Figure 5.19c) extracted from the final bathymetric dataset south of 31° S. The red areas in figure 5.19b were incrementally increased, producing the grey areas in figure 5.19b. The 3 area increments were initially 2 minutes or 3 704 m, then 4 minutes or 7 408 m and finally 6 minutes or 11 112 m. This filtered noise from an incrementally larger area of interpolation data neighbourhood and was found to improve the dataset south of 31° S after four iterations. A final visual inspection resulted in additional red areas (Figure 5.19d). This further filtered the noise; resulting in a final dataset south of 31° S (Figure 5.19e) which was interpolated to produce a final, improved contour dataset south of 31° S (Figure 5.19f compared to Figure 5.19a). The final interpolated grid south of 31° S based on the dataset in figure 5.19e, was mosaicked with the originally interpolated final grid north of 31° S to produce an improved final grid from which a new 24-bit colour rendering of the final grid in figure 5.20 was produced. The new improved contour dataset south of 31° S (Figure 5.19f) was merged with the final contour dataset north of 31° S to produce an improved contour map in figure 5.1.
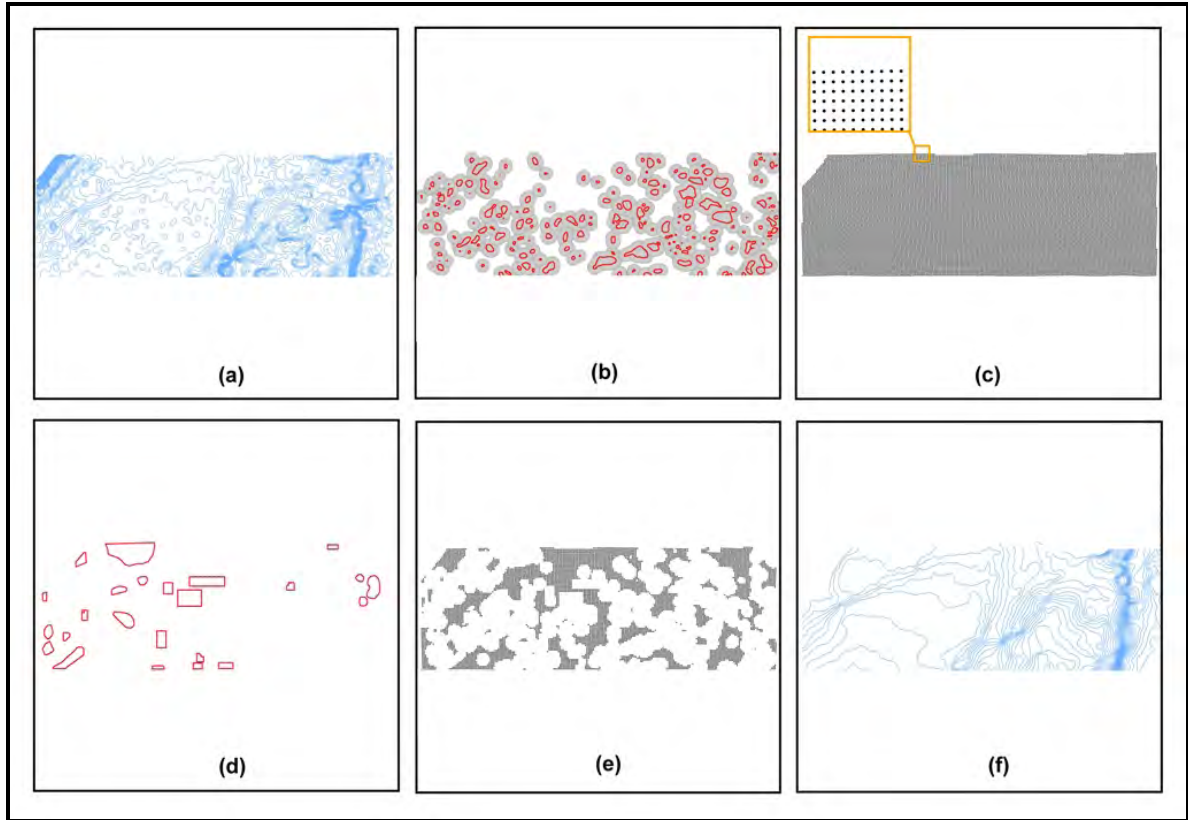
Figure 5.19. (a) Areas of circular contours along with the outermost of the dense concentric contour groupings were extracted from the noisy contour dataset south of 31° S and used to produce the red areas in **(b)**. These constrained the underlying noisy satellite altimetry based bathymetric data **(c)** extracted from the final bathymetric dataset south of 31° S. The red areas in **(b)** were incrementally increased, producing the grey areas in **(b)**. The 3 area increments were initially 2 minutes or 3 704 m, then 4 minutes or 7 408 m and finally 6 minutes or 11 112 m. This filtered noise from an incrementally larger area of interpolation data neighbourhood and was found to improve the dataset south of 31° S after four iterations. A final visual inspection resulted in additional red areas **(d)** to further filter the noise; resulting in an improved final dataset component south of 31° S **(e)** which was interpolated to produce a final, improved contour dataset component south of 31° S **(f)** when compared to **(a)**. The final interpolated grid component south of 31° S based on the dataset in **(e)**, was mosaicked with the originally interpolated final grid component north of 31° S to produce an improved final grid from which a new 24-bit colour rendering of the final grid in figure 5.20 was produced. The new improved contour dataset south of 31° S **(f)** was merged with the final contour dataset north of 31° S to produce an improved contour map in figure 5.1.
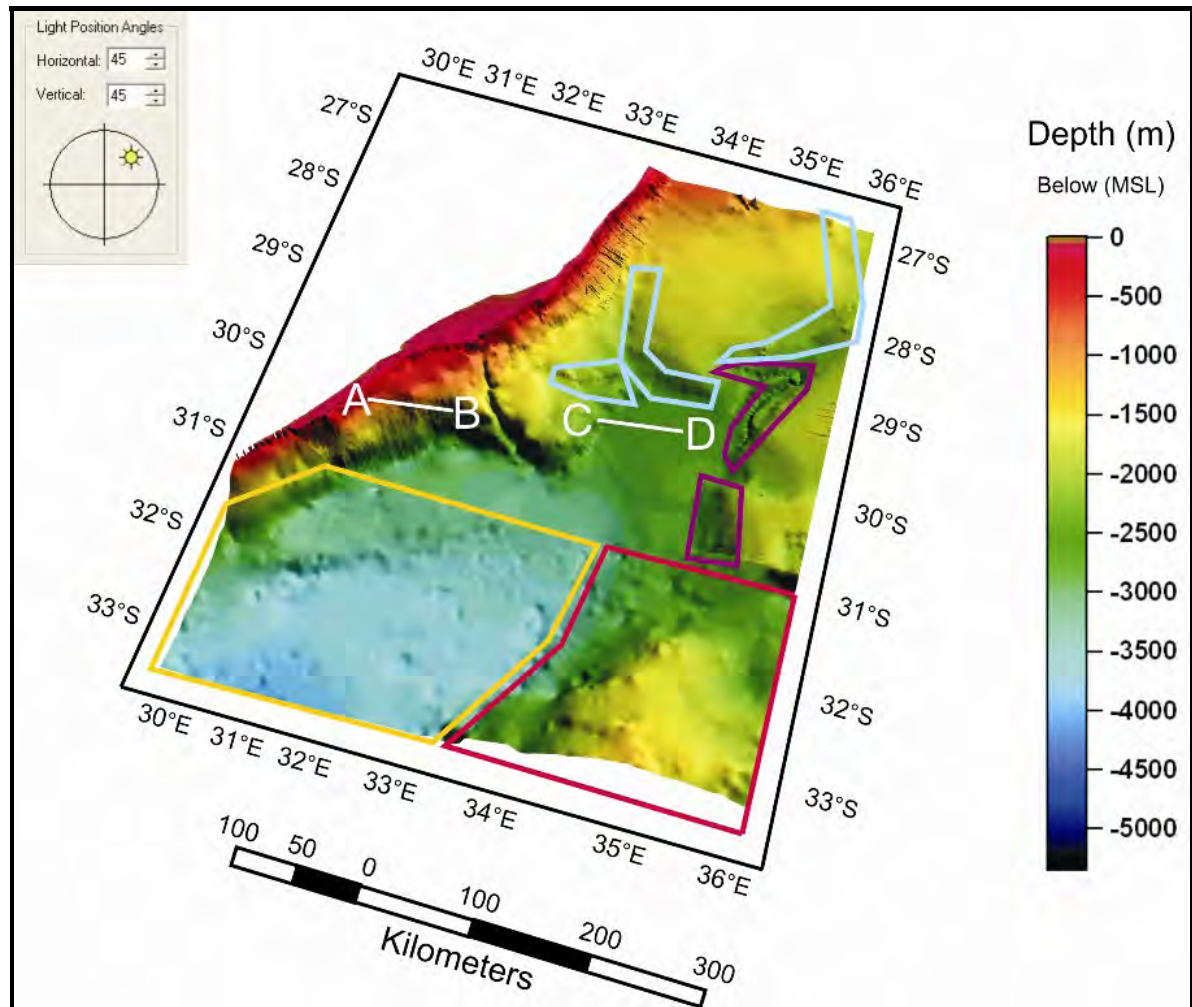
Figure 5.20. The new 24-bit colour rendering of the final grid is shown after removal of noisy data from the satellite altimetry based bathymetric dataset after Smith and Sandwell (1997). See figure 5.16 for comparison.

5.3.3 Dense concentric circular contours

At depths of between 100 m and 200 m between 29° 14' S and 29° 30' S and 31° 47' E and 32° 01' E on the Thukela continental shelf, these artefacts were encountered (Figure 5.21b). This area is based on dataset coverage by the South African Navy's Admiralty Fair Chart (AFC) 34 which made use of lead line bathymetric acquisition technology. Continuous lead line bathymetric acquisition was limited (Guy, 2000) suggesting possible sparse bathymetric coverage as a cause, confirmed by examination of Admiralty Fair Chart 34 in figure 3.14. Uncertainties relating to deeper water lead line data acquisition for Admiralty Fair Chart 34, its lower data densities in this area, the low data densities of the digitised contour data of the

northern Natal Valley after Dingle et al. (1978) and the fact that both datasets are merged here combined with a 500 m grid spacing in the Golden Software ® Surfer 8 ® *Kriging* algorithm may be the cause of these dense concentric contour mapping artefacts. The contour editing ability of ESRI ® ArcGIS ® was again used to correct these artefacts and figure 5.21a shows the improvement after this process.
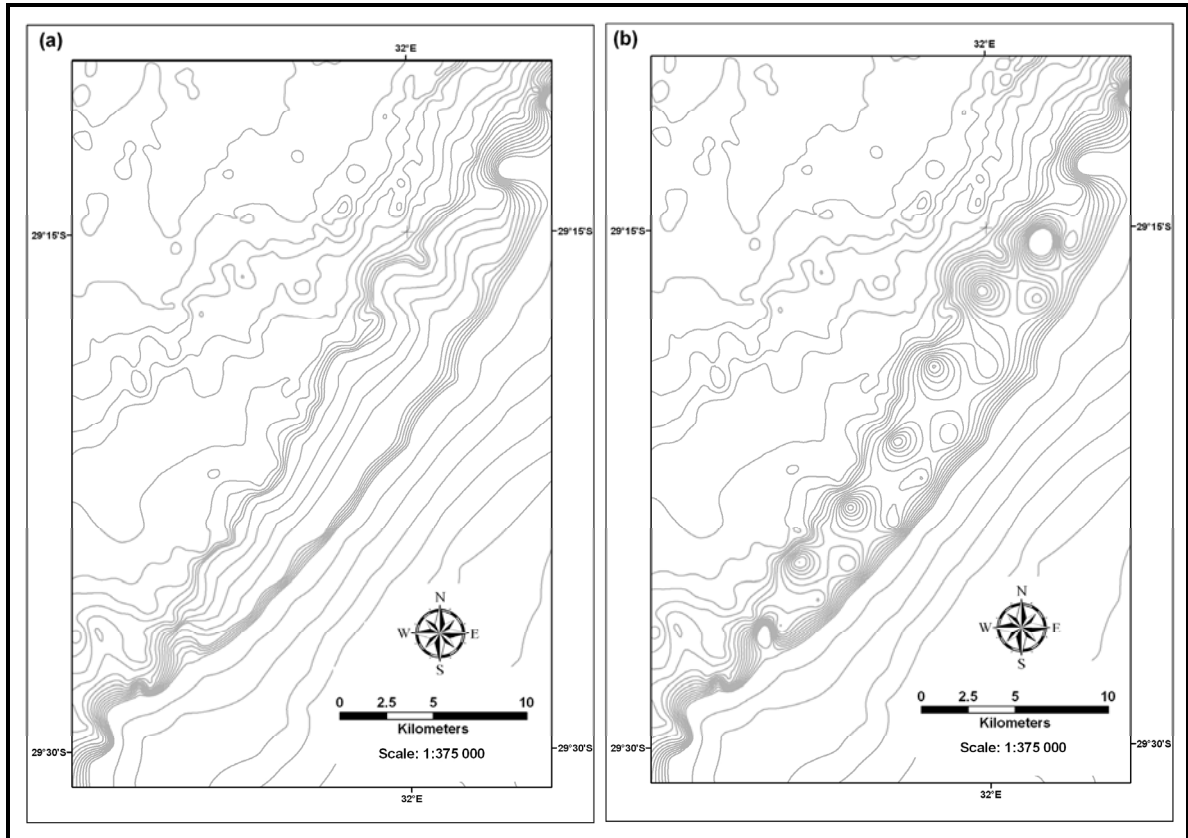
Figure 5.21. **(a)** The improved contour dataset after using ESRI ® ArcGIS ®.contour editing capability on **(b)** the original contour dataset in the areas highlighted by the rectangles. These artefacts occurred where the Admiralty Fair Chart 34 dataset and digitised contour dataset of the northern Natal Valley after Dingle et al. (1978) were merged which along with their sparse data densities in the vicinity limited the contouring ability of the Golden Software ® Surfer 8 ® *Kriging* algorithm.

5.3.4 Multi-beam dataset artefacts

The high data densities and better mapping resolution capabilities of modern multi-beam systems can introduce misleading bathymetric features (Hughes Clarke, 2003a). Multi-beam acquisition systems comprise complex inter-related instruments, such as; the transducer, acquisition and topside processing computer system, differential GPS navigation system and instrumentation computing survey vessel position, such as direction, pitch, heave, roll and yaw.

As noted by Hughes Clarke (2003b): "*Whereas inter-sensor alignment is well understood and can be easily tested for dynamically (the patch test), alignment of any one sensor with the ships coordinate system, especially for cases where installations take place underway, is not currently adequately addressed in standard dynamic survey calibration procedures. Failure to address this can result in static position biases due to incorrectly reporting the lever arm offsets. Particularly now that RTK positioning is available the importance of these small biases will be of concern.*"

The current centimetric accuracy capabilities for both multi-beam sonar and RTK type differential GPS positioning systems make instrument alignment and setup critical, more so as the instrument sensor technology improves (Hughes Clarke, 2003a). The subsequent malfunction or failure of equipment along with unfavourable sea and weather conditions can make inaccurate or aborted data acquisition more likely.

Post processing of raw multi-beam data is also time consuming and complicated, more so than that of single-beam or lead line data. Vasquez (2007) has noted that multi-beam systems can fail to track rough, variable seafloor topography and thus knowledge of multi-beam data acquisitioning and processing, knowledge of the particular acquisition system used along with knowledge of the geology and geomorphology of the area being mapped are required. Also, the default configuration of processing tools such as the widely used CUBE utility when areas of rough seafloor and steep topography have been mapped is not recommended and good area knowledge is required to configure CUBE to improve its performance (Vasquez, 2007).

Figure 5.22 highlights mapping artefacts in the Sodwana Canyon dataset. A systematic swath to swath mismatch caused by a possible roll bias was identified, not tidal variations as the water depths would exclude these. Meanwhile, the long lines and apparent terraces along the data acquisition axis were established as gridding artefacts resulting when a weighted filter with an interpolation radius too fine for the sounding density is used, particularly when data are acquired on topographically steep slopes. The filter interpolation radius for the across track sounding density may be adequate, whereas the comparatively sparse along track sounding density (possibly because of the vessel acquisition speed being too high) renders the same interpolation radius inadequate, in turn biasing the filter weighting to data in a single swathe, while excluding data from the next along track swathe until the filter radius covers it. This has led to the build up of the apparent cross track terraces and along track lines over large portions of the acquisition tracks. The solution at the time would have been to survey at slower speed to

increase the along track density or to reduce the angular sector (swathe width) however the fixed swathe width of +/- 75° for the old RESON ® 8111 ®, limiting its deep water accuracy, would have required the outer beams to be cut out to achieve the same effect. The current solution would require reprocessing the raw data with a larger weighted filter interpolation radius (Hughes Clarke, 2008, *pers. comm.*). Similar striping artefacts have also been mentioned by Blondel and Gómez Sichi (2008) as having been observed by Cullen et al. (2005) during the processing of the Mapping European Seabed Habitats (MESH) multi-beam dataset off the Stanton Banks which was found to be too complicated to correct.

In areas of rough, variable topography in one of the canyons (Area A, Figure 5.22a) other artefacts seem to be present. A shaded relief image and contour map highlight these artefacts (Areas 1, 2, 3 and 4 in Figures 5.22b and c) orientated across the track of bathymetric data acquisition. Ramsay and Miller (2006) identified area 1 in figures 5.22b and c as a margin failure, whereas it is more likely corrupt data. Vasquez (2007) has noted the possibility that multi-beam echo-sounder transducers can mistrack the seafloor, especially where it is steep (Area 1 in Figures 5.22b and c) or rough (Areas 2, 3 and 4 in Figures 5.22b and c). However, these may also be gridding artefacts (as above) where the weighted filter interpolation radius may be too small for along track interpolation, biasing the filter weighting to again show inaccurate topography, especially at the canyon edge where transitioning topography occurs. The canyon edge has a block appearance (Area B, Figure 5.22a) again possibly because of the along track terraces caused by the narrow filter interpolation radius, possible roll bias or bottom mistracking as mentioned by Vasquez (2007).

Figure 5.22. **(a)** A shaded relief map of the Sodwana survey block multi-beam ACEP data (Ramsay and Miller, 2006). Close up views of block **(A)** show **(a)** the shaded relief map and **(b)** the contour map. Both **(b)** and **(c)** indicate possible artefacts of high and low topography at locations **(1)**, **(2) (3)** and **(4)**. Block **(B)** shows the block like artefacts on the edge of a canyon.

5.4   Future work – dataset improvement

5.4.1   GIS editing of the final contour dataset

The use of ESRI ® ArcGIS ® as a contour editing tool could be used for the removal of artefacts introduced by inaccurate contouring as already undertaken and discussed in the previous chapter. This would be the quickest method for this error correction but could introduce user bias when the contours are reshaped. The final dataset and grid would not be altered and thus long grid creation times would be avoided. This method could be used to further reduce the effects of the conjoined arc-like contours and the noisy satellite altimetry data.

5.4.2   GIS editing of individual datasets in the final point dataset

ESRI ® ArcGIS ® can be used as a visual tool for the removal of inaccurate point data from the Admiralty Fair Chart 34 dataset or the digitised contour dataset after Dingle et al. (1978) using the dense concentric circular contours in the final contour dataset as a control dataset. A reconstruction of the final dataset by updating these two inaccurate datasets would be needed for the regeneration of a new grid and contour dataset. The correction of the datasets in ESRI ® ArcGIS ® would be quick but the gridding process would require approximately 193 hours for completion. The removal of inaccurate point data from the final dataset and the regeneration of a new final grid would limit user bias to the final grid and contour dataset and would be more favourable than the first option. However, this method would also not reduce the effect of the noisy satellite altimetry data or the regional conjoined arc-like contours since the *Kriging* algorithm would have the same original configuration and a long grid regeneration time would be needed as for the original dataset.

5.4.3   Multiple dataset grid generation and integration

Separate gridding of the three different datasets (Smith and Sandwell deep-water dataset, the digitised contour dataset of the northern Natal Valley after Dingle et al. (1978) and the near-shore datasets) with different settings to the Golden Software ® Surfer 8 ® *Kriging* algorithm suitable to each dataset could be done. This could allow for the production of three individual contour maps for GIS based integration into a single contour dataset. More widespread regional contour editing would be necessary as contours from the three datasets would need integration and reshaping. However, spatial displacement of contours from

adjacently merged contour datasets may be less than in the case of the first option where rerouting and replacement of contours would be done. The effects of the regional conjoined arc-like contours would be reduced but would introduce user bias when contour integration is done. The effects of the noisy satellite altimetry data may be reduced if wider grid spacing is used on the dataset but may reduce feature definition. Grid regeneration time may be quicker but grid spacing for the near-shore dataset would influence the overall time more than either of the deep-water datasets because of the higher data densities of the near-shore dataset.

5.4.4   Manual data interpolation in the final point dataset

Manual user interpolation of more data to include in the existing final dataset could reduce the effect that the gridding software limitations imposed on gridding a single large final dataset. The final dataset would be used as a control dataset in ESRI ® ArcGIS ® and additional contours would be added by the user and assigned a user interpolated depth value. The contours would be converted to points and integrated into the final dataset. This quick solution would however introduce user bias especially in areas of contrasting topography and artefacts could be added. Areas of subdued topography, such as the deep ocean basin where little ship track data are available and future collection priority is not high because of cost, could benefit from this. However this method is not recommended. Conjoined arc-like contours may be reduced in previous areas of low data densities, but the effects of the noisy satellite altimetry data would not be reduced and since the regeneration of one single large final grid from a single dataset would be required a long grid regeneration time would result.

5.4.5   Sourcing additional third-party analogue or digital data

Sourcing more paper charts and digitising either point or contour data or acquiring digital data would be the simplest most affordable method for the overall improvement of the dataset. The newer, freely available Smith and Sandwell version 11.1 predicted bathymetry dataset from satellite altimetry is now based on a 1-minute spacing instead of the 2-minute spacing of version 8.2. In addition, significant removal of inaccurate ship track data and improvement of bathymetry coverage in the 0 m to 300 m range are reported (Smith and Sandwell, 2008). This dataset could be useful for mapping the deep-water areas outside the physiographic provinces which currently use version 8.2. It could also be used to improve the final dataset coverage of certain data deficient areas like the Mozambique Ridge, since it contains metadata about its digital ship track data used for its constraint and calibration (Marks and Smith, 2006).

Sandwell et al. (2006) also propose a new satellite altimetry mission to measure the sea surface slope to an accuracy of 1 μrad (or 1 mm km^{-1}) over a mission duration of 6 years to improve range precision, reducing ocean wave-derived noise signals. They also suggest a finer cross-track spacing of 6 km and lower satellite inclination of 60° to 120° to improve resolution of the East-West components of the ocean surface slope. Using this dataset when available could also improve the final KwaZulu-Natal bathymetric dataset. The available metadata for the Smith and Sandwell dataset may also allow MGU ship track data to be constrained and calibrated, however this may be an intricate process.

5.4.6 New digital data acquisition: KwaZulu-Natal systematic mapping

From this study the obvious data gaps are the Durban Bight and adjacent area (Area 1, Figure 5.23), Durban Bluff to Aliwal Shoal area (Area 2, Figure 5.23), the Thukela Canyon (Area 3, Figure 5.23), the 29° 25' S Canyon (Area 4, Figure 5.23), both of which are located on the Thukela Cone and the Maputaland Valley (Area 5, Figure 5.23). The MGU would need to acquire new digital data but the cost of data acquisition would require a systematic prioritised area mapping approach based on areas of hydrographic, geomorphologic or geologic interest. Thus, 5 proposed areas are indicated in figure 5.23 as part of a future MGU systematic, KwaZulu-Natal marine environment mapping programme.

Durban Bight and adjacent area

The entire continental shelf out to approximately 200 m from the port of Durban in the south to the port of Richards Bay in the north (Area 1, Figure 5.23) should be resurveyed, since only the MGU's Durban Bight and Richards Bay datasets and the South African Navy Fair Charts 165, to 168 and Admiralty Fair Chart 34 offer good coverage. The main reasons for the minimal surveying of this area are:

- Unknown integrity of features mapped by Admiralty Fair Chart 34 south of the Thukela continental shelf and Richards Bay reef complex (Figures 5.9 and 5.10).

- Vintage (1911) of Admiralty Fair Chart as the only dense dataset for the area it maps (Figure 5.10).

- Data acquisition will extend the MGU's Richards Bay and Durban Bight continental shelf datasets providing good modern dataset coverage for the entire Durban Bight area from Richards Bay to Durban.

Durban Bluff to Aliwal Shoal area

Area 2 in figure 5.23 comprises the MGU's Blood Reef and Aliwal Shoal datasets, the South African Navy's Fair Chart 165 and Admiralty Fair Chart 18. Admiralty Fair Chart 18's vintage and large coverage extents, when compared to the MGU datasets present a need to map area 2 with better, more modern data.

Thukela and 29° 25' S Canyons

The two physiographic provinces (9 and 10) on the Thukela Cone (Areas 3 and 4, Figure 5.23) are larger than any of the canyons found on the KwaZulu-Natal Continental Margin south of Durban and north of Cape St. Lucia. Their size, location adjacent to the Thukela River mouth and the fact that little recently acquired digital data are available for these areas makes digital data acquisition worth considering.

Thus, a resurvey of the areas 1 to 4 in figure 5.23 using good, modern multi-beam technology and differential GPS navigational positioning would improve the bathymetric understanding of the area and contribute to the improvement of the final bathymetric dataset developed in this work. Adjacent to the Thukela Cone, this integrated dataset highlights the drainage pattern from the continental shelf between Cape St. Lucia and Kosi Bay into the abyssal plain of the northern Natal Valley. A dominant north north-west to south south-east valley extends from the deep ocean basin parallel to the coast between the Thukela Cone northeastern and eastern margin and the Central terrace. Numerous canyons have been recognised by Ramsay and Miller (2006). Green et al. (2007); Green and Uken (2008); Green et al. (2008) and Green et al. (2009) noted that the canyons did not fully incise, but merely impinged on the shelf break. The canyons are seen here to extend eastwards down the continental slope and possibly merge with a dominant un-named valley, recognised by Dingle et al. (1978), Martin (1984) and Goodlad (1986) here referred to as the Maputaland Valley (Figure 5.1). Its relief compared to the Thukela Canyon is more subdued, but similar to that of the 29° 25' Canyon. Although unclear on this dataset, this valley may extend to the Limpopo River in Mozambique, adjoining the Limpopo Cone. Works by Martin (1984) and Dingle et al. (1987) do not suggest this, but the acquisition and inclusion of new data in the additional, area 5 of figure 5.23 may verify this

finding.

Figure 5.23. Important KwaZulu-Natal marine environmental zones requiring systematic mapping.

5.5 Bathymetry and continental shelf extension

The works on 3D marine cadastre in support of good ocean governance by Ng' ang' a et al. (2004) have highlighted the essential knowledge dissemination required for effective decision-making. Brown and Blondel (2008) and Ng' ang' a et al. (2004) have also recognised that accurate information about individual resources and their relationships to one another along with human impacts on these resources are also essential for marine environmental resource management. Nichols et al. (2000) have outlined some of these important attributes as: spatial extents, bathymetry, seabed characteristics, living and non-living resources, shoreline changes, property rights and contaminants. Ng' ang' a et al. (2004) further state that ocean governance depends on multi-national statutes and due to its multi-disciplinary nature, has many research- and commercially-driven stakeholders. This has led to the adoption of the United Nations Convention on Law of the Sea (UNCLOS) to harmonise ocean governance by providing a legal framework and encouraging maritime nations to focus on their offshore resources to promote worldwide co-operative ocean governance (United Nations, 1983). Part of this governance focuses on the Exclusive Economic Zone (EEZ) comprising marine areas, seabed and subsoil up to 200 nautical mile (M) seawards from straight baselines derived to approximate the coastline (United Nations Editorial Committee, 1999). An initial desktop study using custom software such as CARIS ® LOTS ® is required to analyse UNCLOS guidelines to prepare for an Article 76 Extended Continental Shelf Claim based on the CLCS11 of 13 May 1999 document also known as the Scientific and Technical Guidelines of the Commission on the Limits of the Continental Shelf (United Nations Editorial Committee, 1999). From these guidelines, proof must be established for continental shelf extension beyond the 200 nautical mile (M) EEZ to combinations of the more distant of:

- Interconnected lines derived from points where the measurement of the sediment thickness is 1% of the shortest distance measured from this point to the foot of the continental slope or

- Interconnected lines derived from points of up to 60 nautical miles (M) seawards from the foot of the continental slope.

In addition, as suggested by United Nations Editorial Committee (1999), "*For the purposes of this Convention, the coastal State shall establish the outer edge of the continental margin*

wherever the margin extends beyond 200 nautical miles from the baselines from which the breadth of the territorial sea is measured....." it is implied that the above two rules apply only where extension beyond the 200 M EEZ is proven to be possible. These two maximal extension rules must be considered in conjunction with combinations of two constraining parameters:

- Interconnected lines derived from points up to a distance of 350 nautical miles (M) seawards from straight baselines derived to approximate the coastline or

- Interconnected lines derived from points up to a distance of 100 nautical miles (M) seawards from the 2 500 m isobath, which is a line connecting the depth of 2 500 m.

According to authors, such as Monahan and Mayer (1999) and Van de Poll et al. (1999) bathymetric data are important in Extended Continental Shelf Claims with the Scientific and Technical Guidelines of the Commission on the Limits of the Continental Shelf also highlighting this. In desktop study work undertaken by the author during the initial South African Extended Continental Shelf Claim (SAECSC), bathymetry was also assessed initially, since many, freely available, world-wide bathymetric sources (ETOPO5, ETOPO2, Smith and Sandwell and GEBCO) were found to be available in the CARIS ® LOTS ® Article 76 software. Also, it is seen above, that bathymetry plays a major role in delineating the 60 nautical miles (M) seawards from the foot of the continental slope and the 100 nautical miles (M) seawards from the 2 500 m isobath rules. In addition, according to Van de Poll, (2004), *pers. comm.*, improving the CARIS ® LOTS ® default freely available bathymetric data in support of an Article 76 Extended Continental Shelf was the most economical initial solution for the South African Extended Continental Shelf Claim (SAECSC). An extended continental shelf claim's economic importance may make the use of freely available bathymetry more favourable, however a good, periodically updated, digital bathymetric dataset, offers a maritime nation more economic opportunities, in addition to an initial extended continental shelf claim (ECSC). Extended continental shelf claims (ECSC's) highlight the dependence of humankind on the maritime and coastal zone, often in a disproportionate manner for limited resources, resulting in challenging resource management difficulties. Natural ecosystems are generally diverse, complex, uncertain and dynamic with management having to be supplemented with constantly improved scientific information, dissemination and translation to stakeholders. In addition, the treatment of ecosystems as multiple isolated components instead of integrated, inter-related components and the adoption of broad-scale decisions need to be adopted supported increasingly by

spatial (GIS based) and temporal (time varying) definitions of ecosystem components (Weinstein et al., 2007).

6 CONCLUSIONS

6.1 Overview

This project was initiated by the MGU because of the need for a single integrated GIS bathymetric contour dataset for its marine scientific work and to fulfil its statutory obligations. Past multi-disciplinary marine environment surveys undertaken have defined the KwaZulu-Natal area from a bathymetric, geological, geomorphological, oceanographic and marine biological perspective. None of those surveys had been integrated into a single, usable dataset.

Accordingly, 29 near-shore bathymetric datasets acquired between 1911 and 2006, using a wide range of methods, were examined. They had dataset densities ranging from 6 points per km^2 to 57 406 points per km^2. Of these, 15 were from the Council for Geoscience (CGS), 9 from the South African Navy and 5 from the African Coelacanth Ecosystem Programme (ACEP). Three deep-water datasets were also considered. One was digitised and had data densities varying from 0.02 to 1 point per km^2 from a contour dataset developed in 1978. The other 2 were grids, 1 developed in 2003 with 1 point every 1 852 m and the other developed in the mid 1990's with 1 point every 3 704 m. These 3 datasets were used to supplement near-shore dataset coverage gaps. Of the 29 near-shore datasets used, 19 were acquired digitally, while 10 were acquired using analogue technology. One deep water dataset, the GEBCO grid was discarded based upon its metadata as well as the concluding remark by Marks and Smith (2006) that the "*the original Smith and Sandwell dataset may well be the best choice*".

The 31 remaining bathymetric datasets were integrated to produce one useful GIS bathymetric contour dataset capable of mapping regional features at a scale of 1:3 000 000, as well as near-shore features at higher scales. In some areas integration was successful, while poor data coverage, noisy data, uneven data densities, little descriptive metadata and software biases resulted in artefacts in other areas. Some of these included conjoined arc-like contours caused by sparse, uneven data densities in conjunction with the mapping software limitations, while bumpy seafloor from noisy satellite altimetry data was also identified. In addition, data

artefacts, visible in one of the multi-beam datasets, a dataset type normally associated with good, high-resolution mapping capabilities, were filtered out in the final contour dataset at a regional 1:3 000 000 scale.

The intuitive graphic user interface (GUI) of GIS software simplified visual interrogation and editing of the regional conjoined arc-like contour artefacts north of 31° S. It also aided the editing of concentric contour artefacts where the AFC 34 dataset and the digitised contour dataset of the northern Natal Valley after Dingle et al. (1978) were integrated. However, the GIS software's flexibility and user-friendly GUI combined with its data management capability were demonstrated most notably in its use as a visual inspection tool. In this scenario, the problematic, obvious regional bumpy seafloor texture south of 31° S in figure 5.16, caused by noise in the satellite altimetry dataset after Smith and Sandwell (1997), was filtered. This edited dataset component south of 31° S was re-interpolated and the resultant grid re-mosaicked with the original final grid north of 31° S. This yielded an improved final contour dataset (Figure 5.19f vs. Figure 5.19a) and an improved colour rendered grid (Figure 5.20 vs. Figure 5.16).

As has been recorded in the body of this thesis, a range of external, multi-disciplinary organisations are showing increasing interest in the availability of such a uniform set of data in a format which can be easily and accurately interpreted. Producing the most useful end result by the integration of datasets, diverse in terms of acquisition date, method and inherent accuracy (metadata) required considerable discretion. It was the compatibility and diversity of user-friendly, powerful computer software used in this work that simplified this discretionary process to integrate the datasets for the best result.

Given the interest already shown in the dataset arising from this work, it is possible that it will be consulted by members of the public not versed in the technicalities of bathymetry. A deliberate attempt has therefore been made to include more explanatory text than might otherwise be considered absolutely necessary.

6.2 Processing technology

Currently, interpolation software, while flexible and capable of producing grids from large datasets, does have its limitations. More sophisticated forms of interpolation such as *Regressive-Kriging* or even machine-learning techniques combining neural network algorithms and robust interpolators do exist (Hengl et al., 2007) and these improve interpolation software capabilities. Moreover, technology advances in the form of affordable, powerful hardware

combined with compatible, user-friendly software, will simplify the integration of large, diverse datasets and improve the newer interpolation techniques. Accordingly, improved contour interpretation of the natural environment will result, thus reducing the generation of artefacts.

The lack of intuitive, user-friendly geostatistical software modules in GIS software because of their separate development as noted by Merwade et al. (2008) is a hindrance to the exclusive use of GIS as a spatial dataset integration tool. This will eventually be solved by technological advances and the GIS software development.

6.3 Multi-beam data

Ongoing technological developments will also improve future data acquisition quality, processing and management, simplifying the production of future datasets, particularly multi-beam bathymetric datasets. The technology driven, high-resolution, accurate mapping capability of modern multi-beam echo-sounder systems make them ideal for mapping temporal (time dependant) changes in bathymetry. Multi-beam data acquisition is rapid, often covering large seafloor areas in a single pass, especially in deeper water. However, processing multi-beam data is time consuming. Additionally, a good understanding of multi-beam echo-sounder systems with an emphasis on the particular acquisition system being used along with the area being mapped are essential for the production of good quality multi-beam datasets. The higher data acquisition densities and resolution capabilities of modern multi-beam systems make artefact generation more likely. Also, large data volumes and complexity introduce system and data management difficulties with additional costs. A consequence of the constantly improving, high-resolution, accurate mapping capabilities of multi-beam systems is that the bathymetric dataset life cycle is reduced, requiring more frequent surveying for accurate bathymetric representation of the environment. Inclusion of multi-beam data improves the overall dataset quality and resolution, by choosing the appropriate map scale and interpolation even with artefacts present. The choice of map scale and interpolation for a contour map for a specific purpose thus remains a subjective process. Brown and Blondel (2008) have also indicated the usefulness of such multi-beam bathymetric datasets to facilitate ocean governance and mitigate human impacts on the marine environment.

6.4 Bathymetry for ocean governance and research

Monahan and Mayer (1999) and Van de Poll et al. (1999) have highlighted the importance of a good bathymetric dataset for an extended continental shelf claim. Additionally, Ng' ang' a et al. (2004) have indicated the importance of a 3D marine cadastre to address the complex issues of ocean governance marine resource management of which an EEZ and extended continental shelf claim (ECSC) are part. As a result, this final digital GIS bathymetric contour dataset could be part of a 3D marine cadastre base map for KwaZulu-Natal, to which additional GIS data could be added. Interest in this GIS dataset has been demonstrated and continues to grow, most notably amongst organisations in KwaZulu-Natal, such as the School of Geological Sciences and School of Life and Environmental Sciences at University of KwaZulu-Natal (UKZN), the Oceanographic Research Institute (ORI), Ezemvelo KwaZulu-Natal Wildlife (EKZNW) and Umgeni Water as well as with Marine and Coastal Management (MCM) in Cape Town and the Council for Scientific and Industrial Research (CSIR). Integrating marine GIS data from these organisations would be beneficial in developing a 3D marine cadastre to encourage marine research and collaboration and improve marine governance in KwaZulu-Natal.

PERSONAL COMMUNICATIONS

Bosman, C., 2009. Verbal discussion via telephone of the Aliwal Shoal single-beam and seismically derived bathymetric datasets. Former MGU colleague, Norway.

Hughes Clarke, J.E., 2008. Discussion via email of Sodwana multi-beam survey block dataset artefacts. Professor, Chair in Ocean Mapping at the Ocean Mapping Group, University of New Brunswick (UNB), Fredericton, New Brunswick, Canada.

Rheeder, L.C., 2001. Verbal discussion of South African Navy datasets. South African Naval Hydrographer at the South African Navy Hydrographic Office, Silvermine, Cape Town.

Rogers, J., 2008. Verbal discussion via telephone of the MGU suitcase database. Senior Lecturer in the Department of Geological Sciences, University of Cape Town (UCT), Cape Town.

Sloss, P.W., 2001. Discussion via email of ETOPO5 and TerrainBase Reference Ellipsoid. Geophysicist at the National Geophysical Data Centre (NGDC), Boulder, Colorado, USA.

Van de Poll, R., 2004.. Verbal discussion of data sources available in CARIS LOTS version 4 for the most economical Article 76 Claim during CARIS LOTS software training in preparation for the South African Extended Continental Shelf Claim. CARIS ® Employee and UNCLOS Expert lecturing at the Institute for Maritime Technology (IMT), Simons Town, Cape Town.

INTERNET RESOURCES

Metzger, D.R. and Campagnoli, J.G., 2007.
http://www.ngdc.noaa.gov/mgg/geodas/geodas.html, Web page for Geophysical Data System (GEODAS), Boulder, Colorado, USA, 80305-3328, 1 pg.

Moore, C.J. and Eakins, B., 2009. http://www.ngdc.noaa.gov/mgg/global/etopo5.html, ETOPO5 5-minute gridded elevation data announcement 88-MGG-02, Digital relief of the Surface of the Earth, Boulder, Colorado, USA, 80305-3328, 1 pg.

Olsen, L., 2008a. http://gcmd.nasa.gov/records/GCMD_DBDB5.html, Web page for Digital Bathymetric Data Base 5-minute (DBDB5) from the U.S. Naval Oceanographic Office (NAVOCEANO). Goddard Space Flight Centre, National Aeronautical and Space Administration (NASA), 2 pp.

Olsen, L., 2008b. http://gcmd.nasa.gov/records/GCMD_DBDBV.html, Web page for Digital Bathymetric Data Base Variable Resolution (DBDB-V) from the U.S. Naval Oceanographic Office (NAVOCEANO). Goddard Space Flight Centre, National Aeronautical and Space Administration (NASA), 3 pp.

Smith, W.H.F. and Sandwell, D.T., 2008.
ftp://topex.ucsd.edu/pub/global_topo_1min/README_V11.1.txt, Web page for global seafloor topography from satellite altimetry and ship depth soundings version 11.1, 1 pg.

South African Navy Hydrographic Office, 2007. http://www.sanho.co.za/tides/tide_index.htm, South African Navy Hydrographic Office New Look Tide Data. South African Navy Hydrographic Office, Cape Town, 1 pg.

Van Zwieten, C., 2008. http://www.eepublishers.co.za/view.php?sid=13123 , Electronic article about GIS and location, PositionIT e-News. EE Publishers, 1 pg.

REFERENCES

Alexandrou, D. and Pantzartzis, D., 1993. A methodology for acoustic seafloor classification. Institute of Electrical and Electronics Engineers (IEEE) Journal of Oceanographic Engineering, 18(2): 81-86.

Antenucci, J., Brown, K., Croswell, P., Kevany, M. and Archer, H., 1991. Geographic Information Systems: A Guide to the Technology. Van Nostrand Reinhold, New York, 301 pp.

Bakkali, S. and Amrani, M., 2008. About the use of spatial interpolation methods for denoising Moroccan resistivity data phosphate "disturbances" map. Acta Montanistica Slovaca, 13 (2008)(2): 216-222.

Bang, N.D., 1968. Submarine canyons off the Natal coast. South African Geographical Journal, 50: 45-54.

Bennet, G., 2007. The Complete On-Board Celestial Navigator, 2007-2011 Edition: Everything but the Sextant. McGraw Hill, Blacklick, Ohio, USA, 174 pp.

Billen, M. I., Kreylos, O., Hamann, B., Jadamec, M. A., Kellog, L. H., Staadt, O., Sumner, D. Y., 2008. A geoscience perspective on immersive 3D gridded data visualisation. Computers And GeoSciences, 2008(34): 1056-1072.

Birch, G.F., 1981. The bathymetry and geomorphology of the continental shelf and upper slope between Durban and Port St. Johns. Anals of the Geological Survey of South Africa.(15, Chapter 1): 55-62.

Bjørke, J.T. and Nilsen, S., 2009. Fast trend extraction and identification of spikes in bathymetric data. Computers And GeoSciences, 2009(35): 1061-1071.

Blondel, P. and Murton, B.J., 1997. Handbook of Seafloor Sonar Imagery. Wiley-Praxis Series in Remote Sensing. Praxis Publishing, Chichester, West Sussex, PO19 1UD, UK, 313 pp.

Blondel, P.H. and Gómez Sichi, O., 2008. Textural analyses of multi-beam sonar imagery from Stanton Banks, Northern Ireland continental shelf. Applied Acoustics: 10 pp. (In Press).

Bonham-Carter, G.F., 1994. Geographic information systems for geoscientists: modelling with GIS. Permagon, New York, 398 pp.

Bosman, C., 2004. Cruise report for the Aliwal Shoal geophysical survey, Umkomaas, South

Africa: Phase 2 - seismic surveys, Council for Geoscience, Durban, 32 pp.

Bosman, C., Uken, R. and Smith, A.M., 2005. The bathymetry of the Aliwal Shoal, Scottburgh, South Africa. South African Journal of Science, 101(5 and 6): 255-257.

British Oceanographic Data Centre, 2003. GEBCO Digital Atlas. International Hydrographic Organisation (IHO) and British Oceanographic Data Centre (BODC).

Brown, C.J. and Blondel, P.H., 2008. Developments in the application of multi-beam sonar backscatter for seafloor habitat mapping. Applied Acoustics: 6 pp. (In Press).

Calder, B. and Smith, S., 2003. A time/effort comparison of automatic and manual bathymetric processing in real-time mode, Proceedings of the US Hydro 2003 Conference, The Hydrographic Society of America, Biloxi, MS, 17 pp.

Cawthra, H.C., 2006. A marine geophysical study of Blood Reef, Bluff, Durban, South Africa. BSc (Honours) Thesis, University of KwaZulu-Natal, Durban, South Africa, 95 pp.

Chandler, M.T. and Wessel, P., 2008. Improving the quality of marine geophysical track line data: Along-track analysis. Journal of Geophysical Research, 113(B02102): 15 pp.

Chen, W., Wang, X. and Zhong, T., 1996. The structure of weighting coefficient matrices of harmonic differential quadrature and its applications. Communication in Numerical Methods in Engineering, 12(8): 455-459.

Cressie, N.A.C., 1991. Statistics for spatial data. John Wiley and Sons, New York, 900 pp.

Cressie, N.A.C., 1993. Geostatistics: A tool for environmental modellers. In: M.F. Goodchild, B.O. Parks and L.T. Steyaert (Editors), Environmental Modelling with GIS. Oxford University Press, New York, 488 pp.

CSI Wireless Inc., 2005. CSI Wireless DGPS Max Reference Manual, DGPS Max Reference Manual, Calgary, Alberta, Canada, T2G 3C4, 111 pp.

Cullen, S., Wijntjes, N. and Hardy, D., 2005. Irish National Seabed Survey Cruise report for Leg CE 05_04, Zone 2, Geological Survey of Ireland.

Dangermond, J., 1991. Where is the technology leading us?, GIS '91 Symposium, Forestry, Canada, Vancouver, Canada, 1-5.

Davis, J.C., 1986. Statistics and data analysis in geology. John Wiley and Sons, New York, 403 pp.

Davis, J.C. and McCullagh, M.J., 1975. Display and analysis of spatial data. J. W. Arrowsmith Ltd., Bristol, UK, 114 pp.

Dingle, R.V., Birch, G.F., Bremner, J.M., De Decker, R.H., Du Plessis, A., Engelbrecht, J.C., Fincham, M.J., Fitton, T., Flemming, B.W., Goodlad, S.W., Gentle, R.I., Martin, A.K.,

Mills, E.G., Moir, G.J., Parker, R.J., Robson, S.H., Rogers, J., Salmon, D.A., Siesser, W.G., Simpson, E.S.W., Summerhayes, C.P., Westall, F., Winter, A. and Woodborne, M.W., 1987. Deep-sea sedimentary environments around southern Africa (South East Atlantic and South West Indian Oceans). Annals South African Museum, 98(1): 1-27.

Dingle, R.V., Goodlad, S.W. and Martin, A.K., 1978. Bathymetry and stratigraphy of the northern Natal Valley (South West Indian Ocean): A preliminary account. Marine Geology.(28): 89-106.

Durbha, S.S., King, R.L., Shah, V.P. and Younan, N.H., 2008. A framework for semantic reconciliation of disparate earth observation thematic data. Computers And GeoSciences, 2009(35): 761-773.

Elema, I. and de Jong, K., 1999. The law of the sea in the north sea, Proceedings of the international conference on technical aspects of maritime boundary delineation and delimitation. International Hydrographic Bureau, International Hydrographic Bureau, Monaco, 151-163.

ESRI, 2007. ESRI ArcGIS 9.2 Online Manual.

Fasshauer, G. and Schumaker, L., 1998. Scattered data fitting on the sphere. In: M. Daehlen, T. Lyche and L.L. Schumaker (Editors), Mathematical methods for curves and surfaces II. Vanderbilt University Press, 117-166.

Flowerdew, R., 1991. Spatial data integration. In: D.J. Maguire, M.F. Goodchild and D.W. Rhind (Editors), Geographical information systems: Principles and applications. Longman, London, 375-387.

Fowler, C. and Treml, E., 2001. Building the marine cadastral information for the United States - a case study. International Journal of Computers, Environment and Urban Systems, 25(4-5): 493-507.

Foxgrover, A.C., Higgins, S.A., Ingraca, M.K., Jaffe, B.J. and Smith, R.E., 2004. Deposition, erosion and bathymetry change in south San Francisco Bay from 1858 to 1983, US Geological Survey Pacific Science Centre and Survey Water Resources Division, Menlo Park, California, USA, 25 pp.

Franke, R. and Nielson, G., 1980. Smooth interpolation of large sets of scattered data. International Journal for Numerical Methods in Engineering., 15(2): 1691-1704.

GEBCO Task Group, 1997. Centenary Edition of the GEBCO Digital Atlas: USER GUIDE TO THE GEBCO ONE MINUTE GRID, 41 pp.

GEBCO Task Group, 2003. User Guide to the Centenary Edition of the GEBCO Digital Atlas

and its data sets. In: M.T. Jones (Editor), GEBCO Sub-Committee on Digital Bathymetry. GEBCO Task Group, 141 pp.

Golden Software, I., 2002. Surfer 8 Users Guide. Golden Software, Inc., Colorado, 640 pp.

Goodenough, D.G., 1988. Thematic mapper and SPOT integration with a Geographic Information System. Photogrammetric Engineering and Remote Sensing, 54(2): 167-176.

Goodlad, S.W., 1978. The bathymetry of the Natal Valley off Natal and Zululand coasts (Southern Africa). Joint GSO/UCT Marine Geoscience Unit Technical Report.(10): 96-104.

Goodlad, S.W., 1986. Tectonic and sedimentary history of the mid-Natal Valley (South West Indian Ocean). Joint GSO/UCT Marine Geoscience Unit Bulletin(15): 414 pp.

Goodwille, A.M., 2004. Concepts behind the GEBCO Global Bathymetric Grid, Lamont Doherty Earth Observatory, 16 pp.

Green, A.N., Goff, J.A. and Uken, R., 2007. Geomorphological evidence for upslope canyon-forming processes on the northern KwaZulu-Natal shelf, SW Indian Ocean, South Africa. Geo-Marine Letters, 27(6): 399-409.

Green, A.N., Ovechkina, M. and Uken, R., 2008. Nannofosil age constraints for the northern KwaZulu-Natal shelf-edge wedge: Implications for continental margin dynamics, South Africa, SW Indian Ocean. Continental Shelf Research, 28(2008): 2442-2449.

Green, A.N. and Uken, R., 2008. Submarine land sliding and canyon evolution of the northern KwaZulu-Natal continental shelf, South Africa, South West Indian Ocean. Marine Geology, 254: 152-170.

Green, A.N., Uken, R., Ramsay, P.J., Leuci, R. and Perritt, S., 2009. Potential sites for suitable coelacanth habitat using bathymetric data from the western Indian Ocean. South African Journal of Science, 105: 151-158.

Greene, H. G., Yoklavitch, M. M., Starr, R. M., O'Connel, V. M., Wakefield, W. W., Sullivan, D. E., 1999. A classification scheme for deep seafloor habitats. Oceanolica Acta, 1999(22): 663-678.

Guptill, S.C., 1996. The risks and rewards of GIS technology. South African Journal of Geo-Information, 17(1): 3-9.

Guy, N.R., 2000. The Relevance of Non-Legal Technical and Scientific Concepts in The Interpretation and Application of the Law of the Sea. PhD Thesis, University of Cape Town, Cape Town, 375 pp.

Hardy, R.L., 1971. Multiquadratic equations of topography and other irregular surfaces. Journal of Geophysical Resources, 76: 1905-1915.

Hengl, T., Heuvelink, G.B.M. and Rossiter, D.G., 2007. About Regression-Kriging: From equations to case studies. Computers and Geosciences, 33: 1301-1315.

Hobday, D.K., 1982. The southeast African margin. In: The ocean basins and margins.(6: The Indian Ocean.): 149-183.

Hughes Clarke, J.E., 2003a. The effect of fine scale seabed morphology and texture on the fidelity of SWATH bathymetric sounding data. University of New Brunswick, New Brunswick, 14 pp.

Hughes Clarke, J.E., 2003b. A reassessment of vessel coordinate systems: what is it we are really aligning, US Hydrographic Conference 2003. University of New Brunswick, Biloxi, MS, 12 pp.

Hughes Clarke, J.E., 2005. Lecture Notes GGE 3353, University of New Brunswick, New Brunswick, Canada.

Hughes Clarke, J.E., Mayer, L.A. and Wells, D.E., 1996. Shallow-water imaging multi-beam sonars: a new tool for investigating seafloor processes in the coastal zone on the continental shelf. Marine Geophysical Researches, 18(6): 607-629.

Huvenne, V.A.I., Hühnerbach, V., Blondel, P.H., Gómez Sichi, O. and Le Bas, T.P., 2007. Detailed mapping of shallow-water environments using image texture analysis on side scan sonar and multi-beam backscatter imagery, In: Proceedings of the 2nd underwater acoustic measurements conference 2007 (on CDROM), Heraklion, Greece, 879-886.

International Hydrographic Organisation (IHO), 2005a. International Hydrographic Organisation (IHO) Manual on Hydrography Chapter 2. In: I.H.B. (IHB) (Editor), M-13 Chapter 2. International Hydrographic Bureau (IHB), Monaco, 555 pp.

International Hydrographic Organisation (IHO), 2005b. International Hydrographic Organisation (IHO) Manual on Hydrography Chapter 3. In: I.H.B. (IHB) (Editor), M-13 Chapter 3. International Hydrographic Bureau (IHB), Monaco, 555 pp.

Johnson, D.A. and Damuth, J.E., 1979. Deep thermohaline flow and current-controlled sedimentation in the Almirante Passage: Western Indian Ocean. Marine Geology, 33(1-2): 1-44.

Jones, E.W.J., 1999. Marine Geophysics. In: E.W.J. Jones (Editor), Marine Geophysics. John Wiley and Sons, Chichester, 466 pp.

Kampfer, A., 2007. South African Navy Tide Tables. South African Navy Publications Unit, Cape Town, 260 pp.

Kennet, J.P., 1982. Marine Geology, 813 pp.

Kolla, V., Eittreim, S., Sullivan, L., Kostecki, J. and Burckle, L.H., 1980. Current-controlled abyssal microtopography and sedimentation in Mozambique Basin, South West Indian Ocean. Marine Geology, 34(3-4): 171-206.

Kolla, V., Sullivan, L., Streeter, S.S. and Langseth, M.G., 1976. Spreading of Antarctic Bottom Water and its effects on the floor of the Indian Ocean inferred from bottom-water potential temperature, turbidity and sea-floor photography. Marine Geology, 21(3): 171-189.

Kostylev, V. E., Todd, B. J., Fader, G. B. J., Courtney, R. C., Cameron, G. D. M., Pickrill, R. A., 2001. Benthic habitat mapping on the Scotian Shelf based on multibeam bathymetry, surficial geology and sea floor photographs. Marine Ecological Progress Series, 2001(219): 121-137.

Larsen, P.L., 1996. Learning to speak 'metadata'. GIS Europe, 5(7): 20-22.

Lawson, C.L., 1972. Generation of a triangular grid with application to contour plotting, Technical reference 299, Section 914, Jet Propulsion Lab, California Institute of Technology, Pasadena, California.

Le Bas, T.P. and Huvenne, V.A.I., 2008. Acquisition and processing of backscatter data for habitat mapping - Comparison of multi-beam and sidescan systems. Applied Acoustics: 10 pp. (In Press).

Le Gonidec, Y., Lamarche, G. and Wright, I.C., 2003. Inhomogeneous substrate analysis using EM300 backscatter imagery. Marine Geophysical Researches, 24(3-4): 305-321.

Le Pichon, X., 1960. The deep-water circulation in the South West Indian Ocean. Journal of Geophysical Research, 65: 4061-4074.

Leuci, R., Young, P.M. and Smith, A.M., 2004. A GIS Project Concerning Regional Seafloor Geology and Bathymetry of The Continental Shelf off Richards Bay and Thukela. 2004-0228, Marine Geoscience Unit - Council for Geoscience and Alan Smith Consulting, Durban, South Africa, 65 pp.

Lord, K.B., Dillon, P.J., Hückstedt, H.A. and Lombard, D., 1996. Regional geophysical sampling programme preliminary results: seabed prospecting for CaCO3 reserves, Richards Bay, Bellville, 7535, Cape Town, South Africa, 24 pp.

Lunetta, R.S., Congalton, R.G., Fenstermaker, L.K., Jensen, J.R., McGwire, K.C., Tinney, L.R.,

1991. Remote sensing and geographic information system data integration: Error sources and research issues. Photogrammetric engineering and remote sensing, American society for photogrammetry and remote sensing, 57(6): 677-867.

Lutjeharms, J.R.E., 2006. The Agulhas Current. Springer-Verlag, Berlin and Heidelberg, Berlin, 329 pp.

Marks, K.M. and Smith, W.H.F., 2006. An evaluation of publicly available global bathymetry grids. Marine Geological Researches, 27: 19-34.

Marsh, I. and Brown, C., 2008. Neural network classification of multi-beam backscatter and bathymetry data from Stanton Bank (Area IV). Applied Acoustics: 8 pp. (In Press).

Martin, A.K., 1978. The bathymetry of the Natal Valley (South West Indian Ocean) off the Mozambique and Tongaland coasts. Joint GSO/UCT Marine Geoscience Unit Technical Report.(10): 105-112.

Martin, A.K., 1984. Plate tectonic status and sedimentary basin in-fill of the Natal Valley (South West Indian Ocean). Joint GSO/UCT Marine Geoscience Unit Bulletin.(14): 209 pp.

Martin, A.K. and Flemming, B.W., 1988. Physiography, structure and geological evolution of the Natal continental shelf. In: E.H. Schumann (Editor), Coastal Ocean Studies off Natal, South Africa. Lecture Notes on Coastal and Estuarine Studies. Springer, 26, pp. 11-46.

McQuillin, R. and Ardus, D.A., 1977. Exploring the Geology of Shelf Seas. Graham and Trottman Limited, London, UK, 234 pp.

Merwade, V., Cook, A. and Coonrod, J., 2008. GIS techniques for creating river terrain models for hydrodynamic modelling and flood inundation mapping. Environmental Modelling and Software, 23: 1300-1311.

Miller, W.R., 2000. Durban Bight Geophysical Survey Cruise Report Nr. 1. 2000-0058, Council for Geoscience - Marine Geoscience Unit, Durban, South Africa, 24 pp.

Miller, W.R. and Ramsay, P.J., 2002. South African Coelacanth Conservation and Genome Resource Programme - Multi-beam Geophysical Mapping of Coelacanth Habitats. 2002-003, South African Institute for Aquatic Biodiversity, Durban, South Africa, 43 pp.

Moir, G.J., 1974. Bathymetry of the upper continental margin between Cape Recife (34° S) and Ponto Do Ouro (27° S) South Africa. Joint GSO/UCT Marine Geoscience Technical Report.(7): 68-78.

Monahan, D. and Mayer, L., 1999. An examination of publicly available bathymetric datasets using digital mapping tools to determine their applicability to Article 76 of UNCLOS. In:

I.H. Bureau (Editor), Proceedings of the international conference on technical aspects of maritime boundary delineation and delimitation. International Hydrographic Bureau, International Hydrographic Bureau, Monaco, 183-190.

Monahan, D. and Nichols, S., 1999. Fuzzy boundaries in a sea of uncertainty: Canada's offshore boundaries. In: O. The Coastal Cadastre-Onland (Editor), Proceedings of the New Zealand's Institute of Surveyors Annual Meeting, Bay of Islands, New Zealand, 33-43.

Müller, R.D., Eagles, S., Hogarth, P. and Hughes, M., 2007. Automated textural image analysis of seabed backscatter mosaics: a comparison of four methodologies. In: B.J. Todd and H.G. Greene (Editors), Mapping the seafloor for habitat characterization, Geological Association of Canada, St. John's, Newfoundland, 43-61.

Müller, R.D., Overkov, N.C., Royer, J.Y. and Keene, J.B., 1997. Seabed classification of the south Tasman rise from Simrad EM12 backscatter data using artificial neural networks. Australian Journal of Earth Sciences, 44(5): 689-700.

Ng' ang' a, S., Sutherland, M., Cockburn, S. and Nichols, S., 2004. Toward a 3D marine cadastre in support of good ocean governance: a review of the technical framework requirements. International Journal of Computers, Environment and Urban Systems, 28(2004): 443-470.

Nichols, S., Monahan, D. and Sutherland, M., 2000. Good governance of Canada' offshore and coastal zone: towards and understanding of the marine boundary issues. Geomatica, 54(4): 415-424.

Okabe, A., Boots, B. and Sugihara, K., 1992. Spatial Tessellations. John Wiley and Sons, Chichester, UK, 532 pp.

Podobnikar, T., Stancic, Z. and Ostir, K., 2000. Data Integration for the DTM Production, ISPRS WG VI/3 and IV/3 Meeting: Bridging the Gap. Scientific Research Centre of the Slovenian Academy of Science and Arts, Ljubljana, 7 pp.

Preston-Whyte, R.A. and Tyson, P.D., 2004. The Atmosphere and Weather of southern Africa Oxford University Press, Cape Town, 396 pp.

Preston, J., 2008. Automated acoustic seabed classification of multi-beam images of Stanton Banks. Applied Acoustics: 11 pp. (In Press).

Ramsay, P.J., 1991. Sedimentology, Coral Reef Zonation, and Late Pleistocene Coastline Models of the Sodwana Bay Continental Shelf, Northern Zululand. PhD Thesis, University of Natal, Durban, 202 pp.

Ramsay, P.J., 1996. Quaternary marine geology of the Sodwana Bay continental shelf, northern KwaZulu-Natal. Council for Geoscience Bulletin.(117): 86 pp.

Ramsay, P.J., 2000. Marine Geology of the Shelf between Leven Point and Ntabende Hill, Northern KwaZulu-Natal. 2000-0103, Marine Geoscience Unit - University of KwaZulu-Natal, Durban, South Africa, 25 pp.

Ramsay, P.J. and Miller, W.R., 2006. Marine geophysical technology used to define coelacanth habitats on the KwaZulu-Natal shelf, South Africa. South African Journal of Science, 102(9 and 10): 427-434.

Ramsay, P. J., Schleyer, M. H., Leuci, R., Muller, G. A., Celliers, L., Harris, J. M., Green, A. N., 2006. The Development of an Expert Marine Geographical Information System to Provide and Environmental and Economic Decision Support System for Proposed Tourism Developments within and around the iSimangaliso (Greater St. Lucia) Wetland National Park World Heritage Site. (Innovation Fund Project 24401): 94 pp.

Reitsma, F., Laxton, J., Ballard, S., Kuhn, W. and Abdelmoty, A., 2008. Semantics, ontologies and eScience for geosciences. Computers And GeoSciences, 2009(35): 706-709.

Remy, N., Boucher, A. and Wu, J., 2008. Applied Geostatistics with SGeMS: A users guide. Cambridge University Press, New York, 312 pp.

RESON Inc., 2002. Navisound 400/200 Operators Guide, Goleta, Ca, 93117, USA, 100 pp.

RESON Inc., 2006a. RESON SeaBat 7125 High-Resolution Multi-beam Echo-sounder System Brochure, 1 pg.

RESON Inc., 2006b. RESON SeaBat 8111 Multi-beam Echo-sounder System Brochure, 1 pg.

Richardson, A.G., 2005. The Marine Geology of the Durban Bight. MSc Thesis, University of KwaZulu-Natal, Durban, 110 pp.

Ridd, M.K., 1991. Spatial and temporal sensing issues related to the integration of GIS and remote sensing. In: J.L. Star (Editor), Proceedings: The integration of remote sensing and geographic information systems. American society for photogrammetry and remote sensing, Bethesda, MA.

Sandwell, D.T. and Smith, W.H.F., 2000. Satellite Altimetry and Earth Sciences: Chapter 12 - Bathymetric Estimation. International Geophysics Series. Academic Press, San Diego, CA, 92101, USA, 463 pp.

Sandwell, D.T. et al., 2006. Bathymetry from space: Rationale and requirements for a new high-resolution altimetric mission. Comptes Rendus Geoscience, 338(2006): 1049-1062.

Scott, L.E.P., 2006. A Geographic Information System for the African Coelacanth Ecosystem Programme. South African Journal of Science, 102(9 and 10): 475-478.

Shepard, F.P., 1963. Submarine Geology. Harper and Row, New York, 557 pp.

Sinclair, D.A., 1998. Using GIS as an Interactive marine mineral resources model for assessing economic viability - Algoa Bay as a case study. Masters Thesis in GIS, Dissertation Thesis, University of Stellenbosch, Stellenbosch, Western Cape, South Africa, 116 pp.

Smith, W.H.F. and Sandwell, D.T., 1997. Global Sea Floor Topography from Satellite Altimetry and Ship Depth Soundings. Science, 277(5334): 1956-1962.

South African Navy Hydrographic Office, 1911. Admiralty Fair Chart 34: Port Durnford to Thukela River. In: S.A.N.H. Office (Editor), Cape Town, 1 pg.

South African Navy Hydrographic Office, 1981a. Fair Chart 165: Durban Harbour Approaches. In: S.A.N.H. Office (Editor), Cape Town, 1 pg.

South African Navy Hydrographic Office, 1981b. Fair Chart 166: Richards Bay Sheet 1 - Northern Sheet. In: S.A.N.H. Office (Editor), Cape Town, 1 pg.

South African Navy Hydrographic Office, 1981c. Fair Chart 167: Richards Bay Sheet 2 - Southern Sheet. In: S.A.N.H. Office (Editor), Cape Town, 1 pg.

South African Navy Hydrographic Office, 1981d. Fair Chart 168: Richards Bay - South East Sheet. In: S.A.N.H. Office (Editor), Cape Town, 1 pg.

South African Navy Hydrographic Office, 1992. Fair Chart 200: Jesser Point to Pont Du Ouro - Southern Sheet. In: S.A.N.H. Office (Editor), Cape Town.

South African Navy Hydrographic Office, 1993a. Fair Chart 202: M.V. Petingo Wreck Investigation. In: S.A.N.H. Office (Editor), Cape Town, 1 pg.

South African Navy Hydrographic Office, 1993b. Fair Chart 204: Cape St. Lucia to Jesser Point - Northern Sheet. In: S.A.N.H. Office (Editor), Cape Town, 1 pg.

South African Navy Hydrographic Office, 1993c. Fair Chart 205: Cape St. Lucia to Jesser Point - Southern Sheet. In: S.A.N.H. Office (Editor), Cape Town, 1 pg.

South African Navy Hydrographic Office, 1995a. Index of Charts and Completed Surveys. SA Navy, Cape Town, 1 pg.

South African Navy Hydrographic Office, 1995b. SAN Chart data. In: S.A.N.H. Office (Editor), Cape Town, 1 pg.

Swan, A.R.H. and Sandilands, M., 1995. Introduction to geological data analysis. Blackwell Science Ltd., Oxford, 446 pp.

Sydow, C.J., 1988. Stratigraphic control of slumping and canyon development on the Zululand

continental margin, east coast, South Africa. Honours Thesis, University of Cape Town, Cape Town, 58 pp. (Unpublished).

United Nations, 1983. The Law of the Sea: United Nations Convention on Law of the Sea, with Index and Final Act of the Third Nations Convention on the Law of the Sea. UN Publication Sales No. 93, 16, 224 pp.

United Nations Editorial Committee, 1999. Scientific and Technical Guidelines of the Commission on the Limits of the Continental Shelf. In: U.N.E. Committee (Editor), Commission on the Limits of the Continental Shelf. United Nations, New York, pp. 64.

United Nations Editorial Committee, 2009. United Nations Convention on Law of The Sea, 202 pp.

Van de Poll, R., Halim, M., D'arcy, M., Harding, J., Macnab, R., Monahan, D., 1999. Integrated procedures for determining the outer limit of the juridicial continental shelf beyond 200 nautical miles. In: I.H. Bureau (Editor), Proceedings of the international conference on technical aspects of maritime boundary delineation and delimitation. International Hydrographic Bureau, International Hydrographic Bureau, Monaco, 235-246.

Van Deursen, W.P.A., Burrough, P.A., Heuvelink, G.B.M. and Roo., D., 1991. The development of intelligent GIS. In: J.L. Starr (Editor), Proceedings: The integration of remote sensing and geographic information systems. American society for photogrammetry and remote sensing, Bethesda, MA.

Vasquez, M.E., 2007. Tuning the CARIS implementation of CUBE for Patagonian Waters. Scientific Thesis, University of New Brunswick, New Brunswick, Canada, 121 pp.

Wadge, G., 1992. Geological applications of GIS, Conference report: Journal of the Geological Society, 672 pp.

Weinstein, M. P., Baird, R. C., Conover, D. O., Gross, M., Kreulartz, J., Loomis, D. K., 2007. Managing coastal resources in the 21st century. Ecological Society of America, 5(1): 43-48.

Westall, F., 1984. Current-controlled sedimentation in the Agulhas Passage, South West Indian Ocean. Joint GSO/UCT Marine Geoscience Unit Bulletin(12): 276 pp.

Wyrtki, K., Bennet, E.B. and Rochford, D.J., 1971. Oceanographic atlas of the international Indian Ocean expedition, Washington D.C., 531 pp.

Yongshe, L. and Journel, A.G., 2008. A package for geostatistical integration of coarse and fine scale data. Journal of Computer and Geosciences, 35(3): 527-547.

Zakrzewska, B., 2004. Map Projections in South Africa, Johannesburg, 20 pp.

Zhou, Q., 1989. A method for integrating remote sensing and geographic information systems. Photogrammetric Engineering and Remote Sensing, 55(5): 591-596.

Zhou, X. and Chen, Y., 2005. Seafloor classification of multi-beam sonar data using neural network approach. Marine Geodesy, 28(2): 201-206.

APPENDIX 2 A – NETTLETON'S METHOD

1. All available bathymetric soundings are gridded using a 2-minute Mercator grid that matches the gravity anomaly grid. To avoid seams, all work is done on a global grid between latitudes of +72° and -72°. Coastline points from GMT provide the zero-depth estimates. A finite-difference, minimum-curvature routine is used to interpolate the global grid [Smith and Wessel, 1990]. This gridding programme requires at least 256 MB of computer memory.

2. Separate the grid into low-pass and high-pass components using a Gaussian filter (0.5 gain at 160 km). Filtering and downward continuation are performed with a multiple-strip, 2-D FFT that spans 0° to 360° longitude to avoid Greenwich edge effects.

3. Form high-pass filtered gravity using the same Gaussian filter.

4. Downward continue the high-pass filtered gravity to the low-pass filtered bathymetry assuming Laplace's equation is appropriate. A depth-dependent Wiener filter is used to stabilize the downward continuation.

5. Accumulate high-pass filtered soundings and corresponding high-pass filtered/downward-continued gravity into small (160 km) overlapping areas and perform a robust regression analysis. In sediment-free areas, the topography/gravity transfer function should be flat and equal to:

$$\tfrac{1}{2}\,\pi\,G\,\delta\,\rho$$

so in the space domain, a linear regression is appropriate. This works well on young seafloor but not on old seafloor where sediment cover destroys the correlation between topography and gravity. In these cases we assume the seafloor is flat and set the topography/gravity ratio to zero. Finally there are intermediate cases where topographic depressions will be sediment filled while the highs protrude above the sediments so the topography/gravity relationship is non-linear. It is these partially sediment filled areas that make the bathymetric problem difficult and inherently non-linear. Continental margins and shelves pose similar problems.

6. Regional topography/gravity ratio estimates are gridded and multiplied by the high-pass filtered/downward-continued gravity to form high-pass filtered predicted bathymetry.

7. The total predicted bathymetry is equal to the sum of the high-pass filtered predicted bathymetry and the low-pass filtered bathymetry.

8. Finally, the pixels constrained by ship soundings or coastline data are reset to the measured values and the finite-difference, minimum curvature routine is used to perturb the predicted values toward the measured values. Measured depths are flagged so they can be extracted separately. This final step dramatically increases the accuracy and resolution of the bathymetric grid in well surveyed areas so it agrees with the best hand-contoured bathymetric charts.

APPENDIX 3 A – SURVEY BLOCK INFORMATION

APPENDIX 3 B – DEPTH MEASURING INSTRUMENT INFORMATION

APPENDIX 3 C – POSITIONING INSTRUMENT INFORMATION

APPENDIX 3 D – PROCESSED BATHYMETRIC DATA INFORMATION

APPENDIX 3 E – ETOPO5 SOURCES

ETOPO5 was generated from a digital data base of land and sea-floor elevations on a 5-minute latitude/longitude grid. The resolution of the gridded data varies from true 5-minute for the ocean floors, the USA., Europe, Japan, and Australia to 1° in data-deficient parts of Asia, south America, northern Canada, and Africa.

Ocean data sources are as follows:

- US Naval Oceanographic Office; USA, W. Europe, Japan/Korea

- US Defence Mapping Agency; Australia

- Bureau of Mineral Resources, Australia; New Zealand

- Department of Industrial and Scientific Research, New Zealand

The balance of world land masses:

- US Navy Fleet Numerical Oceanographic Centre

These various databases were originally assembled in 1988 into the worldwide 5-minute grid by Margo Edwards, then at Washington University, St. Louis, MO.

APPENDIX 3 F – GEBCO SHEET G.08 SOURCES (GEBCO ANNEXURE K.8: GREATER INDIAN OCEAN)

BATHYMETRY (compiled September 2002)

(Note: a subset of this sheet was released as GEBCO sheet 97.1 in the 1997 release of the GEBCO Digital Atlas covering the area of the Indian Ocean south of 31° S and extending from 10° W in the south Atlantic to 140° E south of Australia. This area has been further updated and the sheet now extends to cover the whole of the Indian Ocean from Asia down to Antarctica, extending eastwards to 170° E in the south-west Pacific and westwards to 12° W in the south-east Atlantic. The area covered is approximately a quarter of the world's oceans)

- Author: Dr. Robert L. Fisher, Scripps Institution of Oceanography, La Jolla, California, USA

- Digitised by: Pauline Weatherall, British Oceanographic Data Centre

- Sheet Limits: 31° N to 72° S; 12° W to 170° E (see below for detailed coverage)

- Scale: Contours compiled and digitised on Mercator sheets at a scale of 4 inches per degree longitude (i.e. approximately 1:1 000 000)

- Horizontal Datum: WGS84

- Contour Units: Bathymetric depth in corrected metres

- Contours present: Standard GEBCO depths of 200 m, 500 m and at 500 m intervals thereafter down to 7 000 m. Locally the 100 m contour is also present.

- Coastline Source: SCAR Coastline of Antarctica south of 60° S (version 3.0; Full resolution

- at a scale of 1:1 000 000 or better). NIMA World Vector Shoreline north of 60° S. (Scale of 1:1 000 000)

Geographic Coverage:

- SE Atlantic from 24° S to 72° S; 12° W to 20° E with an extension to 20° W between 56° S to 60° S. south of 65° S and west of 2° E, the bathymetry is provided by GEBCO sheet G.07 and the two sheets are merged at this boundary.

- Indian Ocean from 20° E to 147° E, from Asia down to Antarctica (including the Gulf of Aden). The north-east boundary with the south China and Eastern Archipelagic Seas is along a line taken between 9° N, 99° E; 0° N, 105° E; 0° N, 115° E; 4° N, 115° E; 4° N, 136° E; and then southwards to the coast of Australia.

- SW Pacific from 24° S to 72° S; 147° E to 170° E but restricted in the north-east where it abuts, and is merged with, GEBCO sheet G.09 – in this region the eastern limit is as follows: 24° - 31° S, 158.6° E; 31° - 47° S, 157° E; 47°- 54° S, 165° E; 54° -57.5° S, 163.5° E.

PREPARATION OF GEBCO SHEET G.08

The compilation and hand contouring of all echo-sounding data used in the construction of Sheet G.08 was carried out by Dr. Robert L. Fisher of the Scripps Institution of Oceanography (SIO) as part of the International Indian Ocean Data Compilation Project (IODCP), a collaborative venture between scientists at SIO and L'Ecole et Observatoire de Physique du Globe, Strasbourg, France. The project's aim is to produce a detailed tectonic chart for the entire Indian Ocean and the contiguous southern Ocean between 5° W to 166° E. It will include the compilation and interpretation of all available bathymetric, magnetic and satellite-derived gravity data from Africa-Asia-Australia south to Antarctica. The basic "source document" used for the bathymetric contouring was the 1950-1995 compilation of echo-sounding data maintained by Dr. Fisher at SIO on a set of 240 or so hard copy oceanic scale (4 inches to 1° longitude, Mercator projection) plotting sheets. These were augmented in very large degree by further soundings contributed by academic and government agency sources (as listed below).

These sources contributed data either as hard copy plotting sheets (typically 1:1 000 000 scale Mercator plots) or as digital files of cruise navigation and soundings accompanied by standard velocity correction notations. The digital files were plotted out for Dr. Fisher by Virginia Wells and Uta Albright at the SCRIPPS Institution for Oceanography's (SIO's) Geological Data

Centre. During the compilation, the soundings were compared and checked for recording errors and, for pre-satellite-navigated tracks, slight track adjustments were made as necessary to minimize crossover discrepancies. A compilation of track lines, corrected for digitising errors and omitting segments without soundings, was compiled concurrently on a parallel set of hard copy plotting sheets at the same scale.

The sounding data were hand contoured by geological interpretation by Dr. Fisher sheet by sheet, employing multiple cruise sounding overlays as required for legibility and clarity. In contouring, the standard GEBCO contour levels were followed i.e. 500 m intervals, plus the 200 m contour and, occasionally, on wide shelves, the 100 m contour. The contoured depths are in "corrected metres" using Carter's Tables (NP 139, "Echo-Sounding Correction Tables", 3rd Edition, D.J.T. Carter, Hydrographic Department, Taunton, 1980). None of the contouring was taken from existing nautical or scientific publications or manuscripts; rather, all was done by hand from 1987 to 2002 by Dr. Fisher from his collection of soundings sheets.

In constructing the contours, the echo-sounding based interpretation was compared with large-scale portrayals of satellite altimetry "topography". Such gravity-based portrayals were constructed from a data file available at SIO (Sandwell, D.T. and W.H.F. Smith, "Marine Gravity Anomalies from GEOSAT and ERS-1 Altimetry", (version 7.2, Aug. 1996), Journal of Geophysical Research, vol.102, p.10 039-10 054). These comparisons at large scale helped eliminate spurious structural trends or major misconnections in regions contoured from sparse shipboard coverage. However, depth contour levels are based entirely on sounding data; gravity indications affected only the general shape of features detectable from existing soundings. The hand contoured sheets at a scale of 4 inches per 1° longitude and their corresponding track line plotting were duplicated at SIO and sent to the British Oceanographic Data Centre (BODC) at the Proudman Oceanographic Laboratory, Birkenhead, UK - a total of some 250 pairs of sheets. The contours and track lines were digitised by Pauline Weatherall at BODC employing raster scanning techniques and subsequent vectorisation and labelling using Laser-Scan's VTRAK system.

Careful control was exercised in the geographic registration of the material which was checked at one degree intervals of both latitude and longitude across the full area of each sheet. Both contours and track lines were digitised with registration accuracy within the line thickness of the source material. For the area between 10° W and 20° E, the contours were hand digitised by

Karen Walters and Jon Anderson at SIO and the files transmitted to BODC for quality control. Miss Weatherall was responsible for edge matching the digitised contours across sheet boundaries so as to provide a seamless data set. She was also responsible for incorporating a digital coastline into the data set using the Defence Mapping Agency's World Vector Shoreline (north of 60° S) and the Scientific Committee on Antarctic Research's coastline of Antarctica (south of 60° S). Careful checks were made to ensure that the bathymetric contours were consistent with the coastlines, particularly around islands.

The contouring and digitizing work was undertaken over a period of more than 10 years – as new sounding data continued to be acquired over this period, the bathymetry was updated as and when appropriate. As a result of this, over 600 sections of update charts were delivered to BODC for digitising during the project, in addition to the 250 'first version' sheets. The work was completed in September 2002.

DATA SOURCES USED FOR GEBCO SHEET G.08

During the compilation of data for GEBCO Sheet G.08, the "oceanic scale" (4 inches per 1° longitude, Mercator projection) sounding compilation sheets maintained at SIO were augmented by shipboard data from the following sources (individuals responsible for contributing the data are named in parenthesis):

Principal sources: collector sheets

1.1 GEBCO Collected Soundings Sheets (1:1 000 000 scale, Mercator) maintained by Volunteering Hydrographic Offices with geographic responsibilities within the region:

- U.K. Hydrographic Department, Taunton: complete collection, including southern Ocean, updated to 1988-1989: (Nigel Gooding, Brian Harper)

- South Africa Hydrographic Office, Tokai, Cape: complete collection variously updated to 1981-1983: (C.G.H. Wagenfeld, D.B. MacPherson)

- Hydrographic Office, Royal Australian Navy, Garden Island and Wollongong, NSW: 57 sheets, variously updated to 1971-1989: (Mark A. Bolger)

USNOO Bay St. Louis, Mississippi: USNS Wilkes, 1977-1979, 1981-82 operations (Francis Marchant, Luther Little)

Principal sources: digital files

Government agencies:

- Australian Antarctic Division, Kingston, Tasmania: R/V Aurora Australis 1990's sub-Antarctic cruises: (Henk Brolsma, Lee Belbin, Ursula Ryan)

- Australian Geological Survey Organisation (formerly Bureau of Mineral Resources), Canberra:

  o   979-1995 tracks and soundings of geophysical survey ships in the Australian EEZ, on Kerguelen Plateau and the Antarctic margin: (Chris Johnston, Millard Coffin)

  o   SOJOURN 7 and TASMANTE cruises: (Neville Exon, Peter Hill)

- Australian CSIRO Division of Oceanography, Hobart, Tasmania: R/V Franklin 1987-1998 tracks and soundings on continental margins, EEZ and near Christmas Island: (Bernadette Heaney, Data Librarian and Terry Byrne)

- Geological Survey of Japan, Marine Geophysics Section, Marine Geology Department: bathymetric data collected during JNOC (Japan National Oil Corporation) survey cruises off Antarctica, R/V Hakurei Maru 1980-1995: (Takemi Ishihara, JGS)

- Japanese (JARE, ANTAC) and Soviet (R/V Ob, 1957-58) research vessel soundings off Antarctica (received via US National Geophysical Data Centre, Boulder, Colorado)

- South African Hydrographic Office, Tokai, Cape: throughout S.A. GEBCO Area of Responsibility, 1990-1998: (Sidney Osborne, B.D. Law, Tony Pharaoh)

Laboratories and academic institutions:

- Alfred-Wegener-Institut für Polar- und Meeresforschung, Bremerhaven: R/V Polarstern pre-1998 soundings in the sub-Antarctic between 10° W and 40° E: (Hans Werner Schenke)

- L'Ecole et Observatoire de Physique du Globe de Strasbourg: track and soundings of R/V Marion Dufresne and R/V L'Atalante in central and eastern Indian Ocean, 1980-1998: (Marc Munschy, Marc Schaming, Roland Schlich, Marie-Odile Boulanger)

- Institut Universitaire European de la Mer, Universite de Bretagne Occidentale, Plouzane: 1998 MAGOFOND 2 cruise of R/V Marion Dufresne: (Jerome Dyment); R/V Marion Dufresne 110 and R/V Atalante TASMANTE 1994 cruises: (J.-Y. Royer)

- Laboratoire de Geophysique Marine, Institut de Physique du Globe de Paris, Paris VI: R/V Marion Dufresne and R/V L'Atalante 1982-1995 sounding data in the western and east-central Indian Ocean: (Philippe Patriat, Jacques Segoufin)

- R/V Melville (SIO) soundings in the South East Indian Ocean, 1994-1995: contributions from Lamont-Doherty Earth Observatory, New York: (Christopher Small, James Cochran, Carl Brenner); Oregon State University: (David Christie); University of Washington: (Jean-Christophe Sempere)

- Geological Data Center, Scripps Institution of Oceanography, La Jolla, California: "Alliance exotique" (IODCP) files, 1987-2001: (Virginia Wells)

3. Secondary sources: digital files

- Bullard Laboratories, University of Cambridge, UK: 1986-1987 cruises of RRS Charles Darwin, RRS Shackleton: (Carol Williams)

- Bundesamt fur Seeschiffahrt und Hydrographie, Hamburg: 1997 tracks and soundings being compiled for IOC's International Bathymetric Chart of the Western Indian Ocean: (Hartmut Kluger)

- Hydrographic Office, Taunton, UK: (Gordon Taylor)

- National Institute of Water and Atmospheric Research Ltd, Wellington New Zealand: 1997: partial tracks of 15 NIWA cruises between 166° E and 170° E: (Ian Wright)

- Netherlands Institute for Sea Research, Texel: R/V Tyro 1992-1993 cruise, Arabian Sea: (C.N. van Bergen Henegouw)

- Ocean Research Institute, Tokyo: 1999 tracks and soundings from ORI's FUJI and INDOYO cruises: (Kensaku Tamaki, Hiromi Fujimoto, Tomohiro Yamaashi) also (Catherine Mevel, Laboratoire de Petrologie, Mineralogie, Metallogenie, Paris VI)

- southampton Oceanography Centre, southampton, UK: RRS Discovery cruises 199, 200, 207, 208 South West Indian Ocean: (Martin Saunders, Peter Hunter)

- University of Texas Institute of Geophysics, Austin: tracks and soundings of Australia's R/V Rig Seismic (1994) and of R/V Maurice Ewing (1996), Macquarie Ridge Complex: (Millard Coffin, Christina Massell)

- Woods Hole Oceanographic Institution, Massachusetts: 1987 RRS Charles Darwin Durban-Fremantle cruise: (John Toole)

- National Geophysical Data Centre, Boulder, Colorado: Acquisition updates 1995-1998

APPENDIX 4 A – CONFIGURATION OF GOLDEN SOFTWARE ® SURFER 8 ® SURFACE FUNCTION

The surface function in Golden Software ® Surfer 8 ® has these user configurable components according to the tabs from left to right:
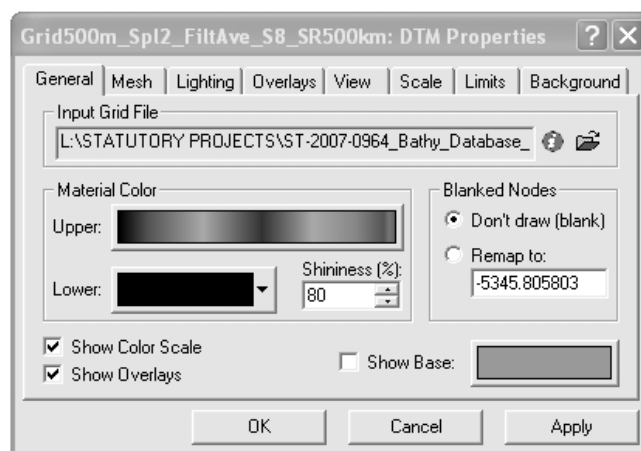
The colour ramp (material colour) selection for the surface and its gradation adjustment and subsequent saving as a user defined colour ramp is possible. A block base and sides of the surface can also be added and configured along with the addition of a colour scale to relate depth values to the map surface colours.
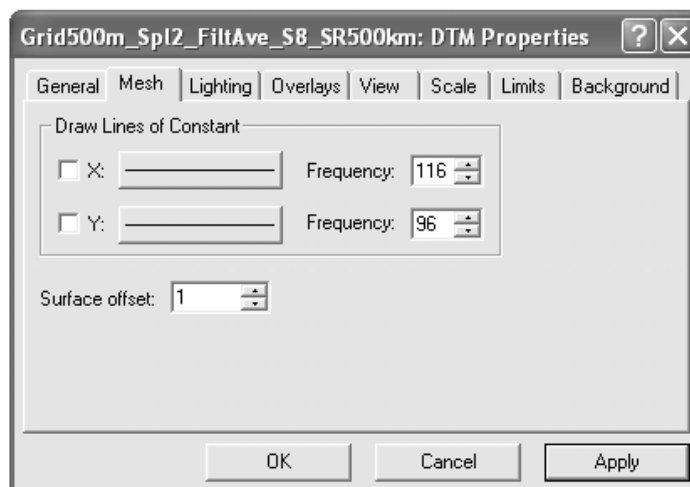
The addition of surface mesh lines are possible but were not necessary.
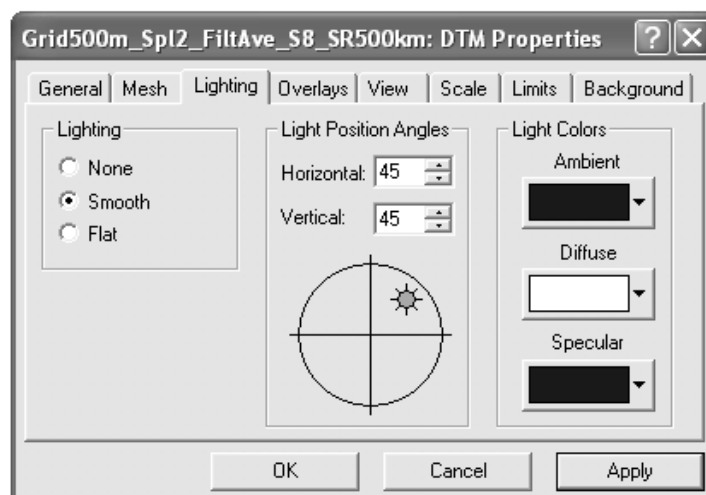
Light source settings determine the appearance of the colours of the surface.
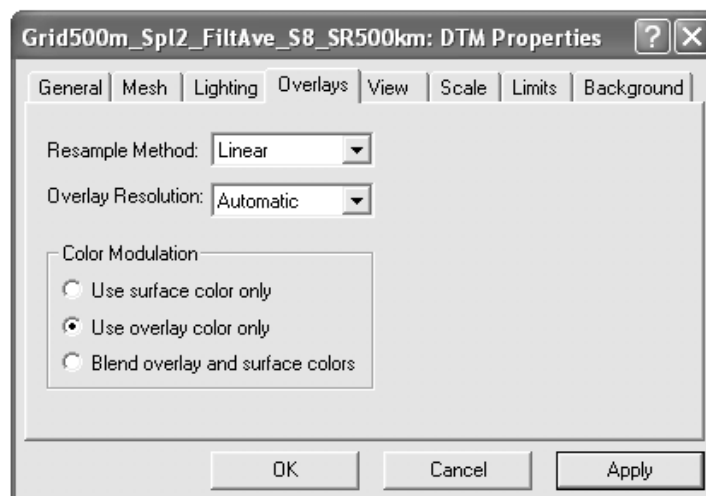
Colour blending based on one or a combination of the grid derived surface
or an added overlay surface can be selected.
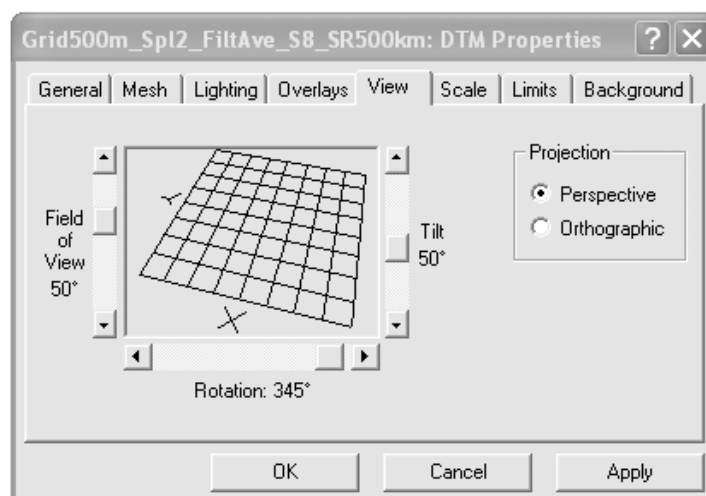
The View (map orientation) in the X, Y and Z axes can also be determined to
allow for optimal viewing.
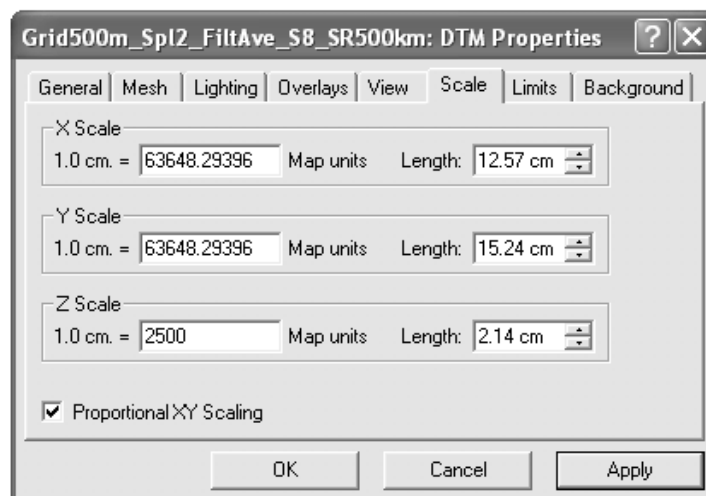
The map scales in the X, Y and Z axes can also be set.
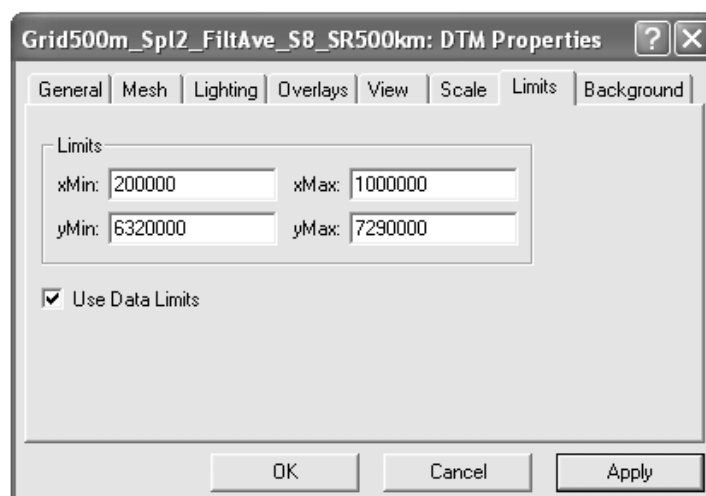
Adjustment of the map limits can be user specified or make use of the data limits.
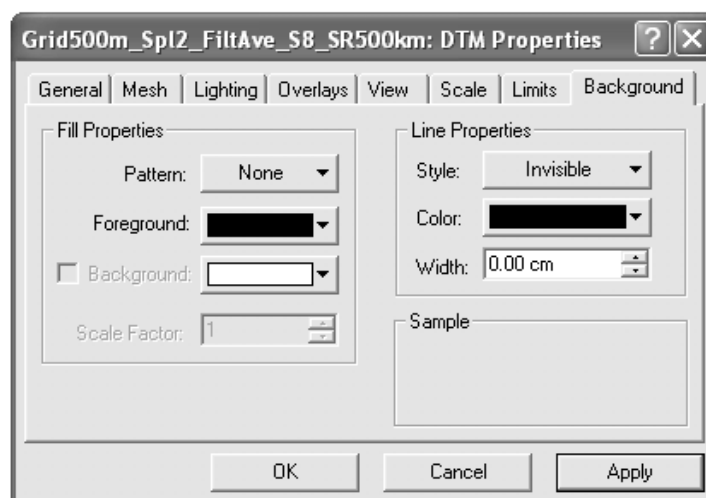
The addition of foreground and background colours to blend with the surface colour can be selected and line properties can be selected.

APPENDIX 5 A – MICROSOFT ® ACCESS ® FIELDS AND DATA

Table indicating the Microsoft ® Access ® supported data types, storage sizes and numerical ranges:

Data Type	Storage size (bytes)	Numerical Range
Byte	1 byte	0 to 255
Boolean	2 bytes	True or False
Integer	2 bytes	-32,768 to 32,767
Long (long integer)	4 bytes	-2,147,483,648 to 2,147,483,647
Single (single-precision floating-point)	4 bytes	-3.402823E38 to -1.401298E-45 for negative values; 1.401298E-45 to 3.402823E38 for positive values
Double (double-precision floating-point)	8 bytes	-1.79769313486231E308 to -4.94065645841247E-324 for negative values; 4.94065645841247E-324 to 1.79769313486232E308 for positive values
Currency (scaled integer)	8 bytes	-922,337,203,685,477.5808 to 922,337,203,685,477.5807
Decimal	14 bytes	+/-79,228,162,514,264,337,593,543,950,335 with no decimal point; +/-7.9228162514264337593543950335 with 28 places to the right of the decimal; smallest non-zero number is +/-0.0000000000000000000000000001
Date	8 bytes	January 1, 100 to December 31, 9999
Object	4 bytes	Any Object reference
String (variable-length)	10 bytes + string length	0 to approximately 2 billion
String (fixed-length)	Length of string	1 to approximately 65,400
Variant (with numbers)	16 bytes	Any numeric value up to the range of a Double
Variant (with characters)	22 bytes + string length	Same range as for variable-length String
User-defined (using Type)	Number required by elements	The range of each element is the same as the range of its data type.

Note: Arrays of any data type require 20 bytes of memory plus 4 bytes for each array dimension plus the number of bytes occupied by the data itself. The memory occupied by the data can be calculated by multiplying the number of data elements by the size of each element. For example, the data in a single-dimension array consisting of 4 integer data elements of 2 bytes each occupies 8 bytes. The 8 bytes required for the data plus the 24 bytes of overhead brings the total memory requirement for the array to 32 bytes.

A variant containing an array requires 12 bytes more than the array alone.

Note: Use the "StrConv" function to convert one type of string data to another.

Data Type Comparisons

The Microsoft ® Jet ® database engine recognizes several overlapping sets of data types. In Microsoft ® Access ®, there are four different contexts in which you may need to specify a data type: in the table design view, in the query parameters dialog box, in Visual Basic ®, and in the SQL ® view in a query.

The following table compares the five sets of data types that correspond to each context. The first column lists the type property settings available in table design view and the five field size property settings for the number data type. The second column lists the corresponding query parameter data types available for designing parameter queries in the query parameters dialog box. The third column lists the corresponding Visual Basic ® data types. The fourth column lists "DAO" field object's data type. The fifth column lists the corresponding Microsoft ® Jet ® database engine's SQL ® data types along with their valid synonyms.

Table fields	Query parameters	Visual Basic ®	DAO Data Type property constants	Microsoft ® Jet ® database engine SQL ® and synonyms
Not supported	Binary	*Not supported*	adBinary	BINARY (See Notes) (Synonym: VARBINARY)
Yes/No	Yes/No	Boolean	adBoolean	BOOLEAN (Synonyms: BIT, LOGICAL, LOGICAL1, YESNO)
Number (FieldSize = Byte)	Byte	Byte	adUnsignedTinyInt	BYTE (Synonym: INTEGER1)
AutoNumber (FieldSize= Long Integer)	Long Integer	Long	adInteger	COUNTER (Synonym: AUTOINCREMENT)
Currency	Currency	Currency	adCurrency	CURRENCY (Synonym: MONEY)
Date/Time	Date/Time	Date	adDate	DATETIME (Synonyms: DATE, TIME, TIMESTAMP)
Number (FieldSize =	Double	Double	adDouble	DOUBLE (Synonyms: FLOAT, FLOAT8, IEEE

Double)				DOUBLE, NUMBER, NUMERIC)
AutoNumber /GUID (FieldSize = Replication ID)	Replication ID	*Not supported*	adGUID	GUID
Number (FieldSize = Long Integer)	Long Integer	Long	adInteger	LONG (See Notes) (Synonyms: INT, INTEGER, INTEGER4)
OLE Object	OLE Object	String	adLongVarBinary	LONGBINARY (Synonyms: GENERAL, OLEOBJECT)
Memo	Memo	String	adLongVarWChar	LONGTEXT (Synonyms: LONGCHAR, MEMO, NOTE)
Number (FieldSize = Single)	Single	Single	adSingle	SINGLE (Synonyms: FLOAT4, IEEESINGLE, REAL)
Number (FieldSize = Integer)	Integer	Integer	adSmallInt	SHORT (See Notes) (Synonyms: INTEGER2, SMALLINT)
Text	Text	String	adVarWChar	TEXT (Synonyms: ALPHANUMERIC, CHAR, CHARACTER, STRING, VARCHAR)
Hyperlink	Memo	String	adLongVarWChar	LONGTEXT (Synonyms: LONGCHAR, MEMO, NOTE)
Not supported	Value	Variant	adVariant	VALUE (See Notes)

Notes:

- Microsoft ® Access ® doesn't use the "Binary" data type. It is recognized only for use in queries on linked tables from other database products that support the "Binary" data type.

- The "Integer" data type in the Microsoft ® Jet ® database engine's SQL ® format doesn't correspond to the "Integer" data type for table fields, query parameters, or Visual Basic ®. Instead, the SQL ® "Integer" data type corresponds to a "Long Integer" data type for table fields and query parameters and to a "Long" data type in Visual Basic ®.

- The "Value" reserved word doesn't represent a data type defined by the Microsoft ® Jet ® database engine. However, in Microsoft ® Access ® or SQL ® queries, the "Value" reserved word can be considered a valid synonym for the Visual Basic ® "Variant" data type.

- If you are setting the data type for a "DAO" object in Visual Basic ® code, you must set the object's type property.

APPENDIX 5 B – GOLDEN SOFTWARE ® SURFER 8 ® GRID INFORMATION FOR INTEGRATED GIS DATASET CONTOUR MAP

500 m grid node separation

Data Source

X Column:	A
Y Column:	B
Z Column:	C

Data Counts

Active Data:	3978584
Original Data:	4007970
Excluded Data:	0
Deleted Duplicates:	44795
Retained Duplicates:	15409
Artificial Data:	15409
Superseded Data:	0

Univariate Statistics

_____
_____

	X	Y	Z
Minimum:	199990.075025	6322890.46238	-5346
25%-tile:	463004.18	6909520.49	-347.16
Median:	470641.7	6952647.56	-82.67
75%-tile:	475915.94	6961327.54	-31.91
Maximum:	939295.871252	7286681.20869	0
Midrange:	569642.9731385	6804785.835535	-2673
Range:	739305.796227	963790.74631	5346
Interquartile Range:	12911.76	51807.05	315.25
Median Abs. Deviation:	6274.19	24187.91	67.89
Mean:	442706.1296812	6897990.3379836	-206.19197853844
Trim Mean (10%):	447346.16901365	6905883.1404883	-179.33712045822
Standard Deviation:	65850.134398216	111173.87047255	286.62718992213
Variance:	4336240200.2631	12359629475.848	82155.146002658

Coef. of Variation:	-1
Coef. of Skewness:	-6.6374433182091

─────

Inter-Variable Correlation

	X	Y	Z
X:	1.000	0.876	-0.384
Y:		1.000	-0.046
Z:			1.000

Inter-Variable Covariance

	X	Y	Z
X:	4336240200.2631	6413056214.834	-7240956.2974829
Y:		12359629475.848	-1450824.0240212
Z:			82155.146002658

Planar Regression: Z = AX+BY+C

Fitted Parameters

─────

	A	B	C

─────

Parameter Value:	-0.0064322705314668		0.0032201360775549
Standard Error:	3.166988927079E-006		
	1.8758602713836E-006		11.731406938265

─────

Inter-Parameter Correlations

	A	B	C
A:	1.000	0.876	0.847
B:		1.000	0.998
C:			1.000

ANOVA Table

Source	df	Sum of Squares	Mean Square	F
Regression:	2	166718341397.89	83359170698.943	
	2.071E+006			
Residual:	3978581	160142808005.79	40251.237314458	
Total:	3978583	326861149403.68		

Coefficient of Multiple Determination (R^2): 0.5100586034836

Nearest Neighbor Statistics

	Separation	|Delta Z|
Minimum:	0.034928498252362	0
25%-tile:	2.8546453369238	0.049999999999997
Median:	9.8800202428999	0.25999999999999
75%-tile:	9.9700200598996	0.99
Maximum:	21383.016907282	2094
Midrange:	10691.52591789	1047
Range:	21382.981978784	2094
Interquartile Range:	7.1153747229758	0.94
Median Abs. Deviation:	0.090024892143312	0.24999999999999
Mean:	30.503805669874	1.4045072229229
Trim Mean (10%):	7.2759029164126	0.65537777384735
Standard Deviation:	268.03843069618	7.1863918190126
Variance:	71844.600330072	51.644227376372
Coef. of Variation:	8.7870488553793	5.1166641949031
Coef. of Skewness:	17.328671097401	41.04142717403
Root Mean Square:	269.76857209566	7.3223539873205
Mean Square:	72775.082490532	53.616867915628

Complete Spatial Randomness

Lambda:	5.5836947534507E-006
Clark and Evans:	0.144160027149
Skellam:	10158106.809361

Exclusion Filtering

Exclusion Filter String: Not In Use

Duplicate Filtering

Duplicate Points to Keep: Average
X Duplicate Tolerance: 0.088
Y Duplicate Tolerance: 0.11

Deleted Duplicates: 44795
Retained Duplicates: 15409
Artificial Data: 15409

X	Y	Z	ID	Status
200003.66	6514989.5	-53	Artificial	Retained
200003.66	6514989.5	-54	3978113	Deleted
200003.66	6514989.5	-52	3977257	Deleted
200022.82	6514324.1	-69	Artificial	Retained
200022.82	6514324.1	-70	3967651	Deleted
200022.82	6514324.1	-68	3966777	Deleted
200034.18	6507331.2	-108	Artificial	Retained
200034.18	6507331.2	-108	3965406	Deleted
200034.18	6507331.2	-108	3965405	Deleted
200101.92	6514881.4	-58	Artificial	Retained
200101.92	6514881.4	-60	3979871	Deleted
200101.92	6514881.4	-58	3979395	Deleted
200101.92	6514881.4	-56	3978818	Deleted
200149.81	6513217.7	-87	Artificial	Retained
200149.81	6513217.7	-86	3961927	Deleted
200149.81	6513217.7	-88	3961387	Deleted
200162.58	6512774.1	-97	Artificial	Retained
200162.58	6512774.1	-102	3965832	Deleted
200162.58	6512774.1	-92	3960415	Deleted
200193.8	6514995	-57	Artificial	Retained
200193.8	6514995	-58	3979394	Deleted
200193.8	6514995	-56	3978817	Deleted
200206.56	6514551.4	-67	Artificial	Retained
200206.56	6514551.4	-68	3966778	Deleted

200206.56	6514551.4	-66	3966652	Deleted
200282.49	6515219.6	-54.666667	Artificial	Retained
200282.49	6515219.6	-56	3978816	Deleted
200282.49	6515219.6	-54	3978111	Deleted
200282.49	6515219.6	-54	3978110	Deleted
200388.61	6508229.5	-104	Artificial	Retained
200388.61	6508229.5	-104	3965592	Deleted
200388.61	6508229.5	-104	3965591	Deleted
200388.61	6508229.5	-104	3965583	Deleted
200435.7	6509895.9	-104	Artificial	Retained
200435.7	6509895.9	-104	3965557	Deleted
200435.7	6509895.9	-104	3965556	Deleted
200458.05	6509119.5	-104	Artificial	Retained
200458.05	6509119.5	-104	3965576	Deleted
200458.05	6509119.5	-104	3965575	Deleted
200469.45	6515335.9	-57	Artificial	Retained
200469.45	6515335.9	-58	3979392	Deleted
200469.45	6515335.9	-56	3978815	Deleted
200494.95	6514448.7	-75	Artificial	Retained
200494.95	6514448.7	-76	3968789	Deleted
200494.95	6514448.7	-74	3968212	Deleted
200524.33	6510120.4	-102	Artificial	Retained
200524.33	6510120.4	-102	3965728	Deleted
200524.33	6510120.4	-102	3965727	Deleted
200529.47	6516558.7	-37	Artificial	Retained
200529.47	6516558.7	-36	3974590	Deleted
200529.47	6516558.7	-38	3957614	Deleted
200553.07	6509122.2	-104	Artificial	Retained
200553.07	6509122.2	-104	3965574	Deleted
200553.07	6509122.2	-104	3965573	Deleted
200556.26	6509011.3	-104	Artificial	Retained
200556.26	6509011.3	-104	3965581	Deleted
200556.26	6509011.3	-104	3965580	Deleted
200556.26	6509011.3	-104	3965579	Deleted
200556.26	6509011.3	-104	3965578	Deleted
200643.67	6515896	-49	Artificial	Retained
200643.67	6515896	-50	3976454	Deleted
200643.67	6515896	-48	3975648	Deleted

200647.4	6512455	-94	Artificial	Retained
200647.4	6512455	-94	3959810	Deleted
200647.4	6512455	-94	3959809	Deleted
200648.09	6509125	-104	Artificial	Retained
200648.09	6509125	-104	3965582	Deleted
200648.09	6509125	-104	3965572	Deleted
200648.09	6509125	-104	3965571	Deleted
200656.41	6515452.3	-57	Artificial	Retained
200656.41	6515452.3	-58	3979391	Deleted
200656.41	6515452.3	-56	3978814	Deleted
200711.19	6510236.8	-102	Artificial	Retained
200711.19	6510236.8	-102	3965724	Deleted
200711.19	6510236.8	-102	3965723	Deleted
200714.38	6510125.9	-102	Artificial	Retained
200714.38	6510125.9	-102	3965732	Deleted
200714.38	6510125.9	-102	3965731	Deleted
200714.38	6510125.9	-102	3965730	Deleted
200714.38	6510125.9	-102	3965722	Deleted
200735.56	6516009.6	-49	Artificial	Retained
200735.56	6516009.6	-50	3976453	Deleted
200735.56	6516009.6	-48	3975647	Deleted
200741.93	6515787.8	-53	Artificial	Retained
200741.93	6515787.8	-54	3978105	Deleted
200741.93	6515787.8	-52	3977252	Deleted
200748.3	6515566	-57	Artificial	Retained
200748.3	6515566	-58	3979390	Deleted
200748.3	6515566	-56	3978813	Deleted
200761.03	6515122.3	-68	Artificial	Retained
200761.03	6515122.3	-68	3966782	Deleted
200761.03	6515122.3	-68	3966781	Deleted
200776.96	6514567.8	-79	Artificial	Retained
200776.96	6514567.8	-80	3962901	Deleted
200776.96	6514567.8	-78	3955090	Deleted
200796.07	6513902.3	-89	Artificial	Retained
200796.07	6513902.3	-88	3961383	Deleted
200796.07	6513902.3	-90	3960674	Deleted
200815.79	6509906.8	-104	Artificial	Retained

200815.79	6509906.8	-104	3965562	Deleted

More...

_____

Breakline Filtering

Breakline Filtering: Not In Use

Gridding Rules

Gridding Method: Kriging
Kriging Type: Point

Polynomial Drift Order: 0
Kriging std. deviation grid: no

Semi-Variogram Model
Component Type: Linear
Anisotropy Angle: 0
Anisotropy Ratio: 1
Variogram Slope: 1

Search Parameters
Search Ellipse Radius #1: 500000
Search Ellipse Radius #2: 500000
Search Ellipse Angle: 0

Number of Search Sectors: 8
Maximum Data Per Sector: 8
Maximum Empty Sectors: 6

Minimum Data: 8
Maximum Data: 64

Output Grid Information

Grid   File   Name:
D:\KZN\Grid500m\FiltAveS8SR500km\NearShore_HighRes_Dingl
e1978_SatAlt_CoastZero_WGS84_UTM36S.grd
Grid Size: 1941 rows x 1601 columns
Total Nodes: 3107541
Filled Nodes: 3107541
Blanked Nodes: 0

Grid Geometry

X Minimum: 200000
X Maximum: 1000000

X Spacing: 500

Y Minimum: 6320000
Y Maximum: 7290000
Y Spacing: 500

Grid Statistics

Z Minimum: -5345.750088884
Z 25%-tile: -3036.9531070641
Z Median: -1915.7919844897
Z 75%-tile: -189.10367909503
Z Maximum: 210.00685393176

Z Midrange: -2567.8716174761
Z Range: 5555.7569428158
Z Interquartile Range: 2847.8494279691
Z Median Abs. Deviation: 1232.4400384581

Z Mean: -1937.4785684942
Z Trim Mean (10%):   -1881.1832857165
Z Standard Deviation: 1530.8498564775
Z Variance: 2343501.2830772

Z Coef. of Variation: -1
Z Coef. of Skewness: -0.22975258938564

Z Root Mean Square: 2469.2761057563
Z Mean Square: 6097324.4864591